Atomic Energy Control Board
P.O. Box 1046
Ottawa, Canada
K1P 5S9

Commission de contrôle de l'énergie atomique
C.P. 1046
Ottawa, Canada
K1P 5S9

INFO-0371

# CALIBRATION AND VALIDATION OF FEMWATER/FEMWASTE

by

D.W. Lafleur and K.G. Raven
Intera Technologies Ltd.

A research report prepared for the
Atomic Energy Control Board
Ottawa, Canada

Project No. 5.121.1

March 1990

Canada

Research report

91-06287/

# CALIBRATION AND VALIDATION OF FEMWATER/FEMWASTE

A report by D.W. Lafleur and K.G. Raven, Intera Technologies Ltd., Ottawa, Ontario under contract to the Atomic Energy Control Board

---

## ABSTRACT

The purpose of this study was to evaluate the ability of the FEMWATER/FEMWASTE computer models to simulate groundwater and contaminant transport at Canadian uranium mine tailings sites. The study involved development and calibration of simulation models for the Nordic tailings area, Elliot Lake, Ontario, using historical data. Prediction of pH and radium 226 concentrations were then made and compared to recently collected field data. The models poorly predicted most regions of the current groundwater contaminant plumes. This was attributed to the simplistic treatment of geochemical processes within the model, uncertainty regarding source term configuration, the two-dimensional nature of the flow model and the uncertainties of the geochemical results. Three-dimensional flow models coupled to multi-component geochemical models may be more suitable to assessing migration of contaminated groundwater at uranium mine tailings sites.

## RÉSUMÉ

La présente étude a pour but d'évaluer la capacité des modèles informatisés FEMWATER/FEMWASTE pour simuler la migration des eaux souterraines et des contaminants dans les aires de résidus de mines d'uranium. L'étude comprenait la mise au point et l'étalonnage de modèles de simulation pour l'aire de résidus Nordic, à Elliot Lake, en Ontario, à l'aide de données existantes. Les valeurs de pH et les concentrations de radium 226 prédites par les modèles ont été comparées aux valeurs récemment mesurées sur le terrain. Les qualités prédictives des modèles sont médiocres pour la plupart des régions des panaches actuels de contaminants dans les eaux souterraines. Ceci s'explique par le traitement simpliste des processus géochimiques dans le modèle, par les incertitudes concernant la configuration du terme source, par la nature bidimensionnelle du modèle de débit et par l'incertitude des mesures géochimiques. Il serait peut-être plus valable de se servir de modèles de débit tridimensionnels couplés à des modèles géochimiques à plusieurs éléments pour évaluer la migration des eaux souterraines contaminées dans les aires de résidus des mines d'uranium.

---

DISCLAIMER

The Atomic Energy Control Board is not responsible for the accuracy of the statements made or opinions expressed in this publication, and neither the Board nor the author assumes liability with respect to any damage or loss incurred as a result of the use made of the information contained in this publication.

# TABLE OF CONTENTS


| | | Page |
|---|---|---|
| ABSTRACT | | i |
| LIST OF FIGURES | | iv |
| LIST OF TABLES | | vii |
| 1. | INTRODUCTION | 1 |
| 1.1 | Background | 1 |
| 1.2 | Study Objectives | 1 |
| 1.3 | Scope of Work | 2 |
| 2. | INSTALLATION AND VERIFICATION | 3 |
| 2.1 | Program Description | 3 |
| 2.2 | Installation | 5 |
| 2.3 | Verification Tests | 7 |
| 2.3.1 | FEMWATER | 7 |
| 2.3.2 | FEMWASTE | 7 |
| 2.3.2.1 | Instantaneous Point Source Problem | 8 |
| 2.3.2.2 | Continuous Source Problem | 12 |
| 3. | REVIEW OF EXISTING DATA (PRE-1985) | 16 |
| 3.1 | History and Physiography of Site | 16 |
| 3.2 | Summary of Previous Investigations | 20 |
| 3.3 | Site Instrumentation | 24 |
| 3.4 | Geologic Setting | 27 |
| 3.5 | Physical Hydrogeologic Data | 28 |
| 3.5.1 | Hydraulic Conductivity | 28 |
| 3.5.2 | Hydraulic Head and Groundwater Flow | 33 |
| 3.6 | Geochemical Data | 39 |
| 3.6.1 | Groundwater Analysis | 39 |
| 3.6.2 | Analyses of Aquifer Materials | 47 |
| 4. | PRELIMINARY MODEL | 50 |
| 4.1 | Approach | 50 |
| 4.2 | Conceptual Model | 50 |
| 4.2.1 | Groundwater Flow System | 52 |
| 4.2.2 | Source Term | 54 |
| 4.2.3 | Transport Properties | 55 |
| 4.3 | Numerical Model | 59 |
| 4.3.1 | Finite Element Mesh | 59 |
| 4.3.2 | Simulation Runs | 61 |
| 4.3.2.1 | Flow | 61 |
| 4.3.2.2 | Transport | 62 |

## TABLE OF CONTENTS


| | | Page |
|---|---|---|
| 4.4 | Conclusions and Recommendations Based on Preliminary Modeling | 70 |
| 5. | RESULTS OF JUNE 1989 SITE INVESTIGATION | 72 |
| 5.1 | Scope | 72 |
| 5.2 | Piezometer Rejuvenation | 73 |
| 5.3 | Piezometric Measurements | 75 |
| 5.4 | Hydraulic Conductivity Tests | 78 |
| 5.5 | Tracer Tests | 81 |
| 6. | FINAL MODEL | 84 |
| 6.1 | Changes to Preliminary Model | 84 |
| 6.2 | Numerical Model | 85 |
| 6.2.1 | Mesh | 85 |
| 6.2.2 | Simulation Runs | 87 |
| 6.2.2.1 | Flow Calibration | 87 |
| 6.2.2.2 | Transport Calibration | 93 |
| 6.2.2.3 | Transport Predictions | 105 |
| 7. | ACCURACY OF MODEL | 110 |
| 7.1 | Description of September 1989 Groundwater Sampling | 110 |
| 7.2 | Comparison of Predicted and Measured Data | 114 |
| 7.2.1 | pH | 114 |
| 7.2.2 | Ra226 | 116 |
| 8. | RECOMMENDATIONS AND CONCLUSIONS | 120 |
| REFERENCES | | 124 |
| APPENDIX A | Water Level Data | |
| APPENDIX B | Chemical Analyses and Predictions | |

## LIST OF FIGURES


| | | Page |
|---|---|---|
| Figure 2.1 | Concentration Profile (3.6 days) for Instantaneous Point Source - Analytic Solution (Sauty, 1980) and FEMWASTE Solution | 10 |
| Figure 2.2 | Relative Error for Instantaneous Point Source Test Case | 11 |
| Figure 2.3 | Concentration Profile (4.0 days) for Continuous Column Injection - Analytic Solution (Ogata and Banks, 1961) and FEMWASTE Solution | 15 |
| Figure 2.4 | Relative Error for Continuous Column Injection Test Case | 16 |
| Figure 3.1 | Location Map for Nordic Tailings Area (Cherry et al., 1980) | 18 |
| Figure 3.2 | Plan of Nordic Tailings Impoundments (Cherry et al., 1980) | 19 |
| Figure 3.3 | Piezometer Locations - Nordic Tailings Areas (after Morin, 1985) | 22 |
| Figure 3.4 | Typical Piezometer Configuration | 26 |
| Figure 3.5 | Representative Grain Size Distribution of Sand Aquifer (Morin, 1983) | 29 |
| Figure 3.6 | Geologic Cross-Section of Plume Centreline Seepage Area 4 (Morin, 1983) | 30 |
| Figure 3.7 | Geologic Cross-Section of Plume Centreline Seepage Area A (Blair et al., 1980) | 31 |
| Figure 3.8 | Water Table Map for Seepage Area A (Based on May, 1980 and June, 1981 data from Morin, 1983) | 36 |
| Figure 3.9 | Piezometric Contours Along Plume Centreline Seepage Area A (Based on May, 1980 and June, 1981 data from Morin, 1983) | 37 |
| Figure 3.10 | pH Concentration Contours along Plume Centreline Seepage Area A (from Morin, 1983; 1985) | 43 |
| Figure 3.11 | Ra-226 Concentration Contours along Plume Centreline Seepage Area A (from Morin, 1983; 1985) | 45 |
| Figure 3.12 | $Cl^-$ Concentration Contours along Plume Centreline Seepage Area A (from Morin 1983; 1985) | 46 |
| Figure 3.13 | Representative Concentrations in Tailings (Dubrovsky, 1986) | 48 |

## LIST OF FIGURES (cont'd)


| | | Page |
|---|---|---|
| Figure 4.1 | Preliminary Conceptual Model of the Hydrogeologic Regime at the Nordic Main Tailings Area | 53 |
| Figure 4.2 | Acid flux as a function of Depth in the Tailings (Senes, 1986) | 56 |
| Figure 4.3 | Finite Element Mesh used in Preliminary Model | 60 |
| Figure 4.4 | Piezometric Contours (a) Observed (b) Simulation 1 (c) Simulation 2 | 63 |
| Figure 4.5 | Hydraulic Conductivity Distribution (a) Simulation 1 and (b) Simulation 2 | 64 |
| Figure 4.6 | Concentration Profiles at 25 Years Using:<br>(1) Flow Simulation 1<br>(2) Flow Simulation 2<br>(3) Flow Simulation 3 | 66 |
| Figure 4.7 | Concentration Profiles at 25 Years Using Flow System for Simulation 1:<br>(1) Constant source, $\alpha$ = 5 m<br>(4) Triangular source distribution, $\alpha$ = 5 m<br>(5) Constant source, $\alpha$ = 2.5 m | 68 |
| Figure 4.8 | Concentration Profiles at 25 Years Using Flow System for Simulation 1:<br>(1) Areal extent of source 2 m<br>(6) Areal extent of source 20 m | 69 |
| Figure 5.1 | Location of Monitoring Instrumentation (June, 1989) | 74 |
| Figure 5.2 | Water Table and Piezometric Cross-Section for June, 1989 | 76 |
| Figure 5.3 | Piezometric Surfaces (masl) for June, 1989 | 77 |
| Figure 6.1 | Numerical Mesh used in Final Model | 86 |
| Figure 6.2 | Piezometric Contours along Plume Centreline | 89 |
| Figure 6.3 | Concentration Profiles for Various Source Widths | 96 |
| Figure 6.4 | Concentration Contours for Various kd | 98 |

## LIST OF FIGURES (cont'd)


| | | Page |
|---|---|---|
| Figure 6.5 | Concentration Contours for Various $\alpha_L$ | 99 |
| Figure 6.6 | pH Contours | 102 |
| Figure 6.7 | Correlation plots for model calibrated and measured pH for 1983 and 1984 | 113 |
| Figure 6.8 | Simulated Ra226 Contours (pCi/L) | 114 |
| Figure 6.9 | Correlation plots for model calibrated and measured Ra 226 for 1983 and 1984 (pCi/L) | 106 |
| Figure 6.10 | pH Contours<br>(a) Prediction 1989<br>(b) Prediction 1995<br>(c) Sensitivity Run 1989 | 108 |
| Figure 6.11 | Simulated Ra226 Contours (pCi/L)<br>(a) Prediction 1989<br>(b) Prediction 1995<br>(c) Sensitivity Run 1989 | 109 |
| Figure 7.1 | Measured pH Concentrations | 111 |
| Figure 7.2 | Measured Ra226 Concentrations (pCi/L) | 113 |
| Figure 7.3 | Comparison of Measured - Simulated pH | 115 |
| Figure 7.4 | Correlation plots for predicted and measured pH and Ra 226 for 1989 | 117 |
| Figure 7.5 | Comparison of Measured Simulated Ra226 (pCi/L)<br>(a) Measured<br>(b) Predicted<br>(c) Sensitivity Analyses | 118 |

## LIST OF TABLES


| | | Page |
|---|---|---|
| Table 2.1 | Values of Physical Parameters for Instantaneous Problem | 9 |
| Table 2.2 | Values of Physical Parameters for Continuous Column Injection | 14 |
| Table 3.1 | Water Table in Elevation in Area A in Meters Above Sea Level (Morin, 1983) | 35 |
| Table 3.2 | Summary of Chemical Analyses of Seepage from the Nordic Tailings (Morin, 1983) | 40 |
| Table 5.1 | Summary of Hydraulic Conductivity Measurements | 80 |

# 1. INTRODUCTION

## 1.1 BACKGROUND

The mining and milling of uranium ore in northern Ontario has resulted in the creation of numerous mine tailings impoundments adjacent to the milling sites. The tailings at some of these sites, such as those in the Elliot Lake district, contain a high percentage (8%) of pyrite ($FeS_2$). Upon exposure to the atmosphere the pyrite undergoes oxidation resulting in the creation of free $Fe^{+2}$, $SO_4^{-2}$ and $H^+$. The oxidation process therefore, results in a significant lowering of the pH of the pore water in the tailings. This acidic pore water (pH of 2 to 4) causes the leaching of trace substances (Pb, Th, Ra, U) within the tailings to occur. As a result of these processes the groundwater in the vicinity of many of these impoundments has become (or is becoming increasingly) contaminated with low pH waters containing significant concentrations of hazardous materials.

The Atomic Energy Control Board (AECB) is considering using a computer model UTAP (Uranium Tailings Assessment Program) to evaluate the health risks posed to man by such tailings. UTAP is a systems model designed to evaluate the migration of contaminants through a variety of pathways.

One such pathway is the saturated/unsaturated groundwater pathway. UTAP, like most systems models, simplistically models the groundwater system. To ensure that the results provided by these simple groundwater models are accurate it is necessary to select input parameters carefully. In order to evaluate these parameters accurately, a more sophisticated groundwater flow and transport code is frequently used. A previous study (Water and Earth Science Associates Ltd. (WESAL), 1987) evaluated available finite element saturated/unsaturated models and concluded that the FEMWATER/FEMWASTE models most closely met AECB's needs for accurate parameter evaluation.

## 1.2 STUDY OBJECTIVES

The overall objectives of the current study are to assess the suitability of the FEMWATER/FEMWASTE programs for simulation and prediction of contaminant distributions in groundwater flow systems at uranium mine tailings

sites. This objective was to be achieved through the calibration and validation of the FEMWATER/FEMWASTE programs to a well documented field site.

Verification or the assurance that the program algorithms have been coded correctly was not considered to be a significant part of this study, having been assumed to have been completed in the earlier study (WESAL, 1987). Verification was initially intended only to ensure that installation had not inadvertently altered the codes.

## 1.3 SCOPE OF WORK

In order to validate the FEMWATER/FEMWASTE models a specific site must be selected. For this study the Nordic tailings areas were selected and the ability of the models to simulate the migration of three contaminants $Cl^-$, $Ra^{226}$ and pH were suggested. The original request for proposal (RFP) identified eleven major tasks to be undertaken as part of the proposed study. Briefly these tasks were:

- Task 1: Gather and compile existing information;
- Task 2: Determine best estimates and uncertainty of input variables;
- Task 3: Install and verify FEMWATER/FEMWASTE;
- Task 4: Develop preliminary model and identify additional data requirements;
- Task 5: Obtain additional data;
- Task 6: Perform best estimate prediction run;
- Task 7: Obtain 1989 field data;
- Task 8: Compare predicted and observed data;
- Task 9: Install software on AECB computer;
- Task 10: Document findings;
- Task 11: Seminar.

This report documents the methods and results of Tasks 1 to 10.

# 2. INSTALLATION AND VERIFICATION

## 2.1 PROGRAM DESCRIPTION

The FEMWATER/FEMWASTE suite of computer models were developed to simulate groundwater flow and trace contaminant transport in unsaturated porous media. Although the programs can be used independently of each other they are complementary in nature with the dependent output variables (i.e., velocity and saturation) of the flow model (FEMWATER) being used as input for the transport model (FEMWASTE). Both models use the same numerical technique, a galerkin finite-element method employing either triangular or quadrilateral elements, to solve the respective partial differential equations describing partially saturated flow or transport. Both models are two-dimensional in nature and can be used to model either an areal plane or a cross-section. A wide variety of boundary condition options are available including conventional prescribed head, flux and pressure gradient, distributed and point source fluxes and rainfall/seepage conditions. The flow system is assumed isothermal and can either be steady state or transient. The transport equation describes the convection-dispersion of a trace, sorbing and non-conservative (i.e., decaying) constituent. A Freundlich isotherm is used to represent sorption.

The FEMWATER/FEMWASTE programs were developed at Oak Ridge National Laboratories (ORNL) by G.T. Yeh and D.S. Ward by modifying two existing unsaturated groundwater flow and transport codes. These existing codes had been previously developed at ORNL by J.O. Duguid and M. Reeves and have subsequently become known as the Reeves-Duguid (flow model) and the Duguid-Reeves (transport model) models (Reeves and Duguid, 1975). The original version of FEMWATER (Yeh and Ward, 1980) consisted of modifications to the following areas of the Reeves-Duguid model:

1. method of computing velocity magnitudes;
2. calculation of mass balance;
3. algorithm used in evaluating non-linear terms;
4. variable array dimensioning;

5. compressed storage arrays;
6. numerical weighting and lumping schemes.

The original version of FEMWASTE (Yeh and Ward, 1981) modified the following aspects of the Duguid-Reeves model:

1. mass balance computation;
2. addition of alternate weighting schemes;
3. retardation (making the retardation factor, R, a function of saturation, S).

In recent years the programs have undergone some additional modifications/development resulting in the creation of additional versions of codes. These versions have included FEMWATER-1 (Yeh, 1983) and the version supplied to AECB by Water and Earth Science Associates Ltd. (1987). The programs used as part of this study are a slightly different version of these two earlier FEMWATER/FEMWASTE codes. The version used in the current study was supplied to INTERA by AECB and contained no unique version identifier (such as a version or quality assurance number or date) which makes the task of differentiating from previous or subsequent versions difficult. The "current" version of the codes does contain some new or unique features which distinguish them from the original programs. Both the FEMWATER and FEMWASTE codes contained the following additional features:

1. Automatic mesh generation;
2. A new matrix inversion technique (point iterative);
3. Additional boundary condition types.

These changes necessitated the change of data input format. This is significant from the standpoint that it prohibits the use of unmodified data sets for comparison testing with alternate (earlier) versions.

It should also be pointed out that the version used as part of this study was a relatively recent version. The documentation consisted solely of a draft copy of the input guide. No documentation describing the theory or mathematical implementation of these new features was available to INTERA.

## 2.2 INSTALLATION

The current version of the FEMWATER/FEMWASTE programs consists of three source code modules comprising FEMWATER (3873 lines), FEMWASTE (4124 lines) and FEMUTILITY (363 lines). The FEMUTILITY module contains subroutines which are common to both FEMWATER and FEMWASTE such as generic input routines and tabular interpolation routines.

The codes were installed on both an IBM-AT micro-computer and a VAX-II micro-computer. The codes were first installed on the IBM-AT and were compiled using Microsoft's Fortran Version 4.1 compiler. In order to enable compilation, the source code for both FEMWATER and FEMWASTE was broken down into their individual routines. Both FEMWASTE and FEMUTILITY were free of fatal compilation errors. Such was not the case for FEMWATER which recorded seven fatal errors. Six of these errors were associated with common blocks of varying size (i.e., different number of variables in different subroutines). The seventh error was associated with a varying number of arguments in a subroutine CALL statement. Once these errors were corrected FEMWATER also compiled on the IBM-AT.

Having obtained executable files for FEMWATER/FEMWASTE the next step was to run test data sets to verify the correctness of programs and test for the presence of execution errors. The selection and results of the verification test problems are described in detail in the following section (2.3). This section (2.2) deals solely with execution errors encountered while attempting to run the test cases.

An execution error was encountered when trying to use the point iterative solver for FEMWASTE. In this particular case the error, an arithmetic overflow error caused by a division by zero, was fatal resulting in termination of the program. It was discovered that this error was caused by a failure to pass the variable IPNTS (which controls the solution method) to the subroutine BC. This problem was corrected by including the labelled common OPTN in the subroutine.

Another problem was detected in the calculation of material balances. In both FEMWATER and FEMWASTE values of material in place are not preserved over subsequent time steps. The error is due to the fact that these values are assigned to local variables in a subroutine (the variable QSOS (in FEMWATER) in the subroutine SFLOW and the variables QR, QD, QL, QLKW, QLKS, QDH and SOURCE in the same FEMWASTE routine) and are not retained after the subroutine is exited. These variables correspond to water in place, dissolved constituent, sorbed constituent, loss due to decay for dissolved and sorbed constituents, change due to consolidation and source rate. At the beginning of these routines the values are reassigned to other local variables and subsequently used to evaluate the change of material in place. However because these variables are only defined as local variables there can be no guarantee that the correct values will be preserved. This problem occurred because the program was written using Fortran 66 and has not been updated to the current Fortran standard. This problem can be circumvented by including "SAVE" statements in those subroutines where local variable values must be preserved. We have included such statements in all subroutines of the program. By doing this we also found that we eliminated a sporadic problem with the direct solution routine.

On a precautionary note, we found that several boundary conditions are unconventional in definition. Neuman flux boundaries, for example, are based solely on pressure head gradients as opposed to the more universally accepted total head gradient definition. The same appears to be true for the Neuman component of the rainfall-seepage boundary conditions. This results in the addition of a flux which is orders of magnitude larger than that specified for a typical saturated system.

Because of the problems encountered during the installation of FEMWATER/FEMWASTE, we would urge caution when using additional program options that have not been previously tested.

## 2.3 VERIFICATION TESTS

### 2.3.1 FEMWATER

The literature does not abound with analytical solutions to partially saturated groundwater flow problems. The major reason for this is the complex relationships that are typically used to describe relative permeability and capillary pressure. In the application at hand, the unsaturated zone is of little interest. No data describing flow (or transport) in the unsaturated zone has been collected. To use FEMWATER to model flow in the capillary fringe cannot be justified based on available data.

With this in mind, and given the ease with which simple saturated systems can be verified, it was decided only limited effort should be expended to verify the partially saturated aspects of the model. A previous version of FEMWATER had been verified by WESAL (1987) using a quasi-analytical solution to a problem originally proposed by Philip (unreferenced) and evaluated by Haverkamp et al. (1977). Unfortunately, WESAL (1987) provided neither the analytical solution nor the data points at which it was evaluated. Our verification test case consisted of reproducing the WESAL (1987) output for their specified test case conditions. Results from our simulation were virtually identical to the results described by WESAL (1987).

### 2.3.2 FEMWASTE

Two test problems were run as part of the verification cases for FEMWASTE. The first of these test problems was provided by the AECB and consisted of an instantaneous point injection of tracer in a two-dimensional uniform and steady velocity field. A second verification problem corresponding to a continuous injection of tracer in a one-dimensional steady flow field was

also run. Exact analytic solutions are available for both of these problems. Sauty (1980) presented a solution to the instantaneous point source problem, while Ogata and Banks (1961) presented a solution to the continuous column injection problem.

#### 2.3.2.1 Instantaneous Point Source Problem

The AECB provided INTERA with sample input and sample output data sets for a specific application of the instantaneous point source problem. The physical data describing this specific problem is presented in Table 2.1. The mesh used by AECB to simulate this problem consisted of 70 elements in the flow direction and 41 elements in the transverse direction and comprised a total of 781 nodes. Each element was 2 m by 1 m with the long side oriented parallel to the direction of flow. The results of the AECB numerical simulation and the analytic solution of Sauty (1980) are presented graphically in Figure 2.1 as a plot of concentration versus distance for a specific point in time (t = 3.6 days). An identical concentration profile was obtained from an INTERA simulation using a similar data set on the IBM-AT. The INTERA data set was identical to that of the AECB with the exception of the mesh. Due to memory restrictions a smaller grid composed of 320 elements (32 by 10) was employed. No discernable difference existed between the AECB and the INTERA simulations and based on Figure 2.1 both simulations appear to give acceptable fits to the analytic solution. However consider Figure 2.2 which shows a semi-logarithmic plot of the relative percent error for the same profiles on the upgradient and downgradient limbs of the concentration profile. In this Figure percent error is defined as the percent difference between the numerical and analytic solutions relative to the analytic solution. From this Figure it can be seen that in certain areas the deviation from the analytic solution is significant especially at low concentrations on the upgradient limb of the concentration profile. In many applications the deviation from the analytic solution at concentrations less than two orders of magnitude of the peak concentration would not be of concern. However, given the need to simulate pH over the range of 3 to 7 or four orders of magnitude the need for such accuracy becomes evident. For example at relative concentrations of $10^{-3}$ on the downgradient limb, equivalent to pH of 4

Table 2.1 Values of Physical Parameters for Instantaneous Problem

| Parameter | Value |
|---|---|
| Darcy velocity, V | 2 m/d |
| Porosity $\phi$ | 0.35 |
| Longitudinal dispersivity, $\alpha_L$ | 4 m |
| Transverse dispersivity, $\alpha_T$ | 1 m |
| Retardation coefficient, R | 1 |
| Decay constant, $\lambda$ | 0.0/d |
| Saturation, S | 1.0 |
| Solute mass per unit aquifer thickness, m | 3500 mg/m |

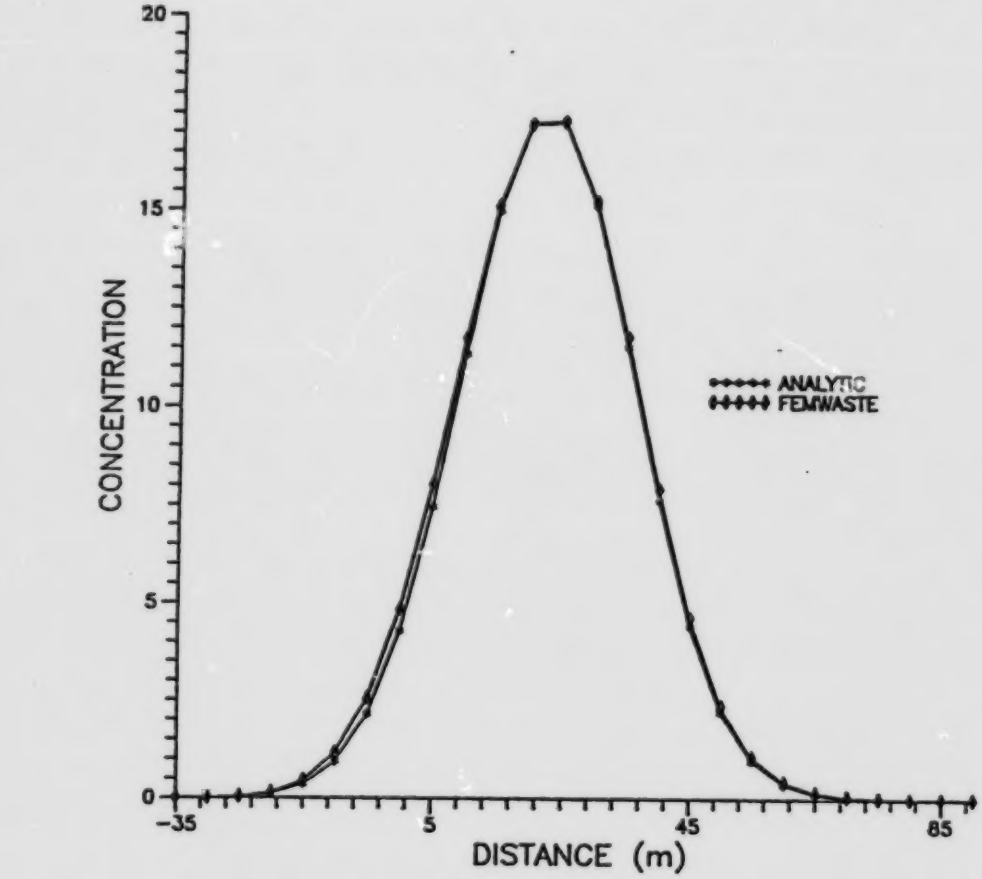


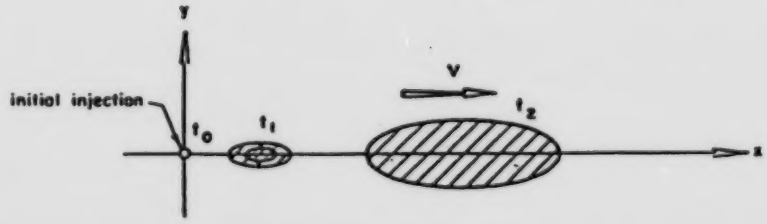


| | |
|---|---|
| Drawn by | Date |
| Checked by | Date |
| Revisions | Date |
| | |

Concentration Profile (3.6 days) for Instantaneous Point Source - Analytic Solution (Sauty 1980) and FEMWASTE Solution

INTERA Technologies

Figure 2.1

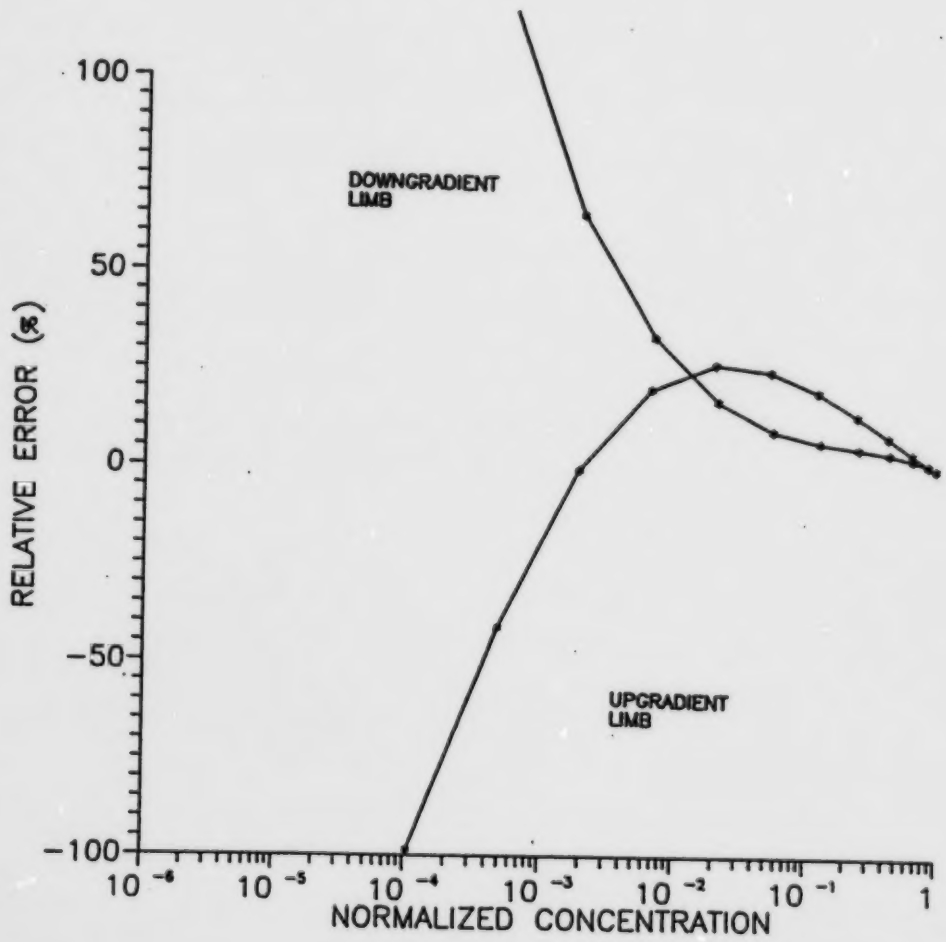


| | |
|---|---|
| Drawn by | Date |
| Checked by | Date |
| Revisions | Date |
| | |

Relative Error for Instantaneous Point Source Test Case

INTERA Technologies

Figure 2.2

from a starting pH of 7, the error is close to 100% or a factor of 2 in proton concentration. This corresponds to an uncertainty of pH equal to 0.3 pH units. As field pH measurements are usually made to ± .02 units this numerical error may be significant.

A number of additional simulations were made in an effort to improve the accuracy of these results. These simulations involved trying alternate weighting schemes (the original solution used a Crank Nicholson or central time difference and upstream weighting scheme), refining the grid to reduce the effect of numerical dispersion, using a smaller time step (to reduce the impact of numerical overshoot), reducing the time over which the pulse was introduced and trying various mass lumping options. These modifications were employed both individually and in various combinations. Unfortunately it was found that none of these changes significantly improved the accuracy of the solution. Upon closer examination of the discrepancy it was found that the model tended to over-predict concentrations on the down-gradient side of the peak concentration while under-predicting concentrations on the upgradient side. At this time it occurred to us that the spatial weighting scheme employed in the model may be the source of the error. FEMWASTE has the capability of using either a galerkin or upstream weighting scheme. The upstream weighting scheme (after Christie et al., 1976) is preferred over the galerkin weighting scheme for problems which contain a strong convective component and is typically more stable and more accurate. However a problem arises in this particular instantaneous point source example. The problem is associated with the upgradient side of the plume in which dispersion is acting in the opposite direction to the convection. Since both transport components are evaluated on the upper convective side this approach will inherently under-estimate the upstream dispersion. The overprediction of the downgradient side will occur as a consequence of the upstream underprediction.

#### 2.3.2.2 Continuous Source Problem

To verify the assumed source of the inaccuracy in FEMWASTE it was decided to run an additional problem where upstream dispersion was not

significant. A two-dimensional problem should ideally be used for such a simulation since this will provide a test of the transverse dispersive components of the model. Unfortunately such two-dimensional problems are difficult to evaluate analytically. The Cleary (1978) analytic solution used by WESAL (1987) in their verification of FEMWASTE is such a solution. Unfortunately neither the analytic solution nor its evaluation for the specific test problem were provided to the AECB. As an alternative, a similar one dimensional problem, i.e., continuous injection of tracer into a column, to which an analytic solution is available (Ogata and Banks, 1961) was used. This problem was run using the physical properties outlined in Table 2.2. The mesh employed in the numerical model consisted of 320 elements (a total of 363 nodes) each being 1 m x 1 m. The comparison between the numerical solution and the analytic solution is depicted in Figures 2.3 and 2.4. Figure 2.3 presents a plot of the numerical and analytic solutions. Figure 2.4 plots the relative error as previously defined versus concentration. It can be seen that the deviation between the two is only significant at concentrations six orders of magnitude smaller than the peak or input concentrations.

These results confirm the reason for the inability of the FEMWASTE code to accurately solve the Sauty (i.e., instantaneous point source) problem, i.e., the use of an upwind weighting scheme to solve a problem in which dispersive and convective terms act in opposite directions. The question must now be asked as to how or if this limitation affects the use of the model for the Nordic tailings site. It is difficult to provide a conclusive answer to such a question since the magnitude of any error will be highly dependent on both the geometry and the physical properties of the problem. It may likely be that the Nordic tailings will continue to release contaminants over a significant time period and for this reason its behaviour should more closely resemble a continuous injection problem than an instantaneous point source and therefore the error may not be significant. However, the error is also a function of the relative values of convective and dispersive fluxes and therefore will likely be greater for retarded species than non-retarded species.

Table 2.2 Values of Physical Parameters for Continuous Column Injection

| Parameter | Value |
|---|---|
| Darcy velocity, V | 2 m/d |
| Porosity $\phi$ | 0.35 |
| Longitudinal dispersivity, $\alpha_L$ | 4 m |
| Retardation coefficient, R | 1 |
| Decay constant, $\lambda$ | 0.0/d |
| Saturation, S | 1.0 |
| Solute input concentration | 1.0 |

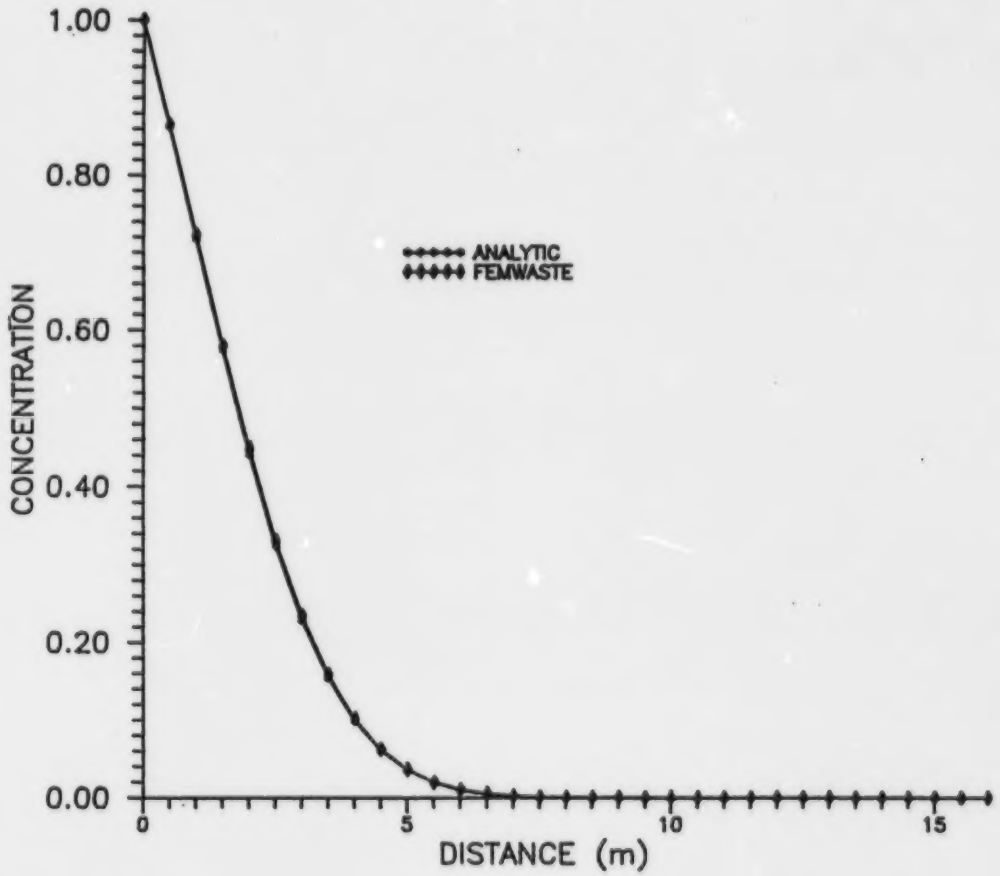


| | |
|---|---|
| Drawn by | Date |
| Checked by | Date |
| Revisions | Date |
| | |

Concentration Profile (4.0 days) for Continuous Column Injection - Analytic Solution (Ogata and Banks, 1961) and FEMWASTE Solution

INTERA Technologies

Figure 2.3

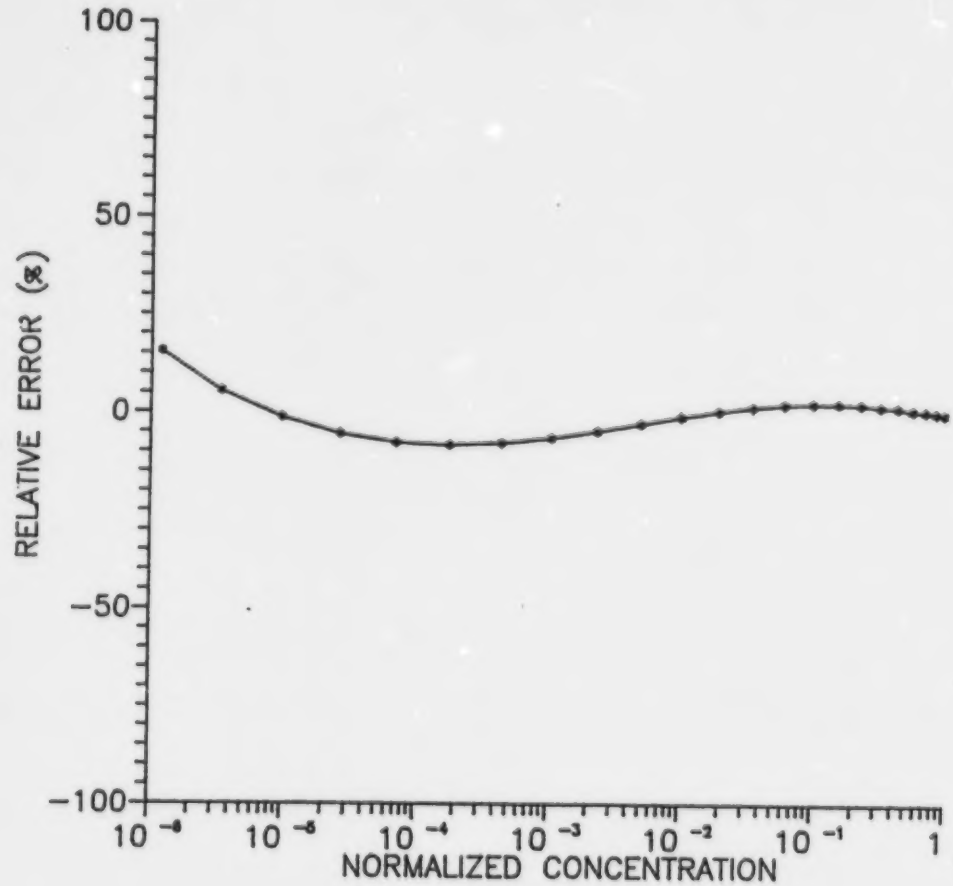


| | |
|---|---|
| Drawn by | Date |
| Checked by | Date |
| Revisions | Date |
| | |

Relative Error for Continuous Column Injection Test Case

INTERA Technologies

Figure 2.4

# 3. REVIEW OF EXISTING DATA (PRE-1985)

## 3.1 HISTORY AND PHYSIOGRAPHY OF THE SITE

The Nordic mine is located approximately 4 km east of the town of Elliot Lake (see Figure 3.1). The mine operated from 1957 to 1968 with a milling rate ranging from 2,500 to 3,300 tonnes per day. An estimated 12.3 million tonnes were milled over the operational period (Blair et al., 1980).

The milling process consisted of grinding the ore until 50% percent was finer than a 200 mesh followed by acid digestion using dilute sulphuric acid. Uranium was removed from this solution through the use of ion exchange columns. The sorbed uranium was subsequently removed by using a nitric acid solution and precipitated using ammonium. The process effluent water together with the digested ore was neutralized with limestone and lime before being discharged to the tailings ponds.

The Nordic tailings were deposited on a discontinuous layer of peat formed in a spruce bog that had previously occupied the area. The peat layer overlies a glacial fluvial sand aquifer which in turn is underlain by a layer of glacial till and bedrock (Morin, 1983).

The Nordic mine used two separate tailings impoundments over its operational period. The first area to be used is now known as the Nordic West Arm. The history of the tailings deposition is well described in Cherry et al. (1980) and the subsequent discussion is abstracted from this reference. Tailings were first discharged in 1957 and were contained by constructing a tailings dam "A" (see Figure 3.2) at the west end of the impoundment. Initially tailings were discharged so that clear effluent flowed to Westner Lake. With time, tailings dam "B" was constructed and the effluent discharge point was moved to the west end of the impoundment. Tailings were initially discharged in the middle of the impoundment and subsequently moved westward towards dam "B". There is only limited information available describing the construction of the Nordic tailings

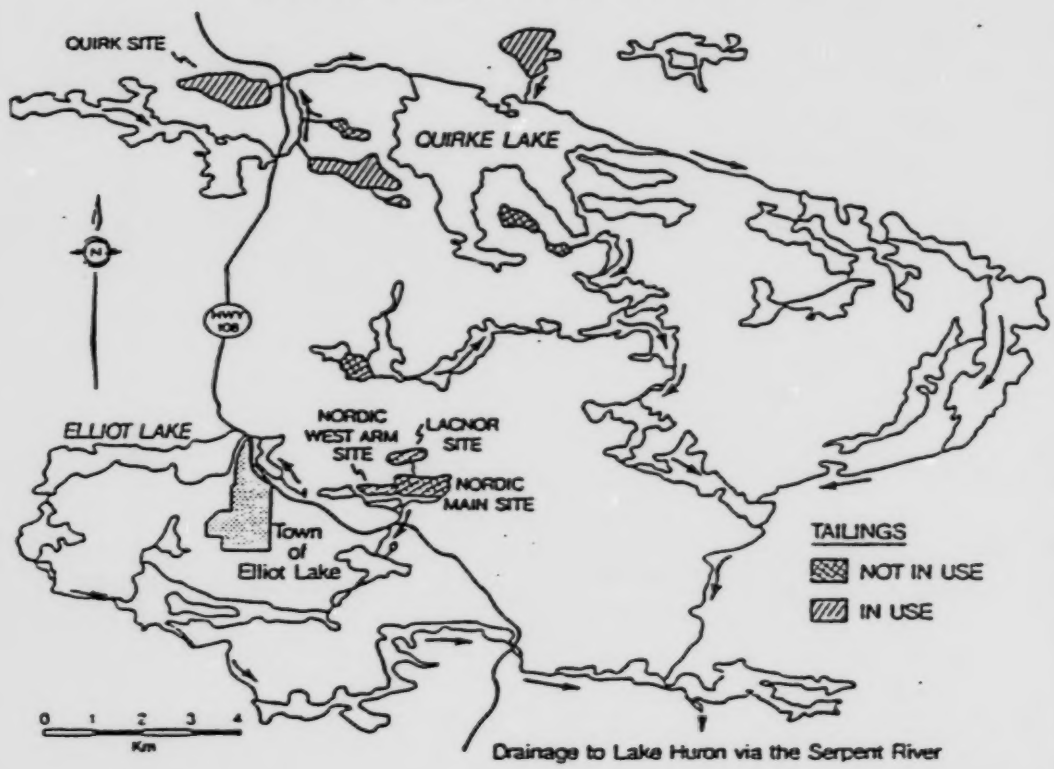


| | |
|---|---|
| Drawn by | Date |
| Checked by | Date |
| Revisions | Date |
| | |

Location Map for Nordic Tailings Area
(Cherry et al., 1980)

INTERA Technologies

Figure 3.1

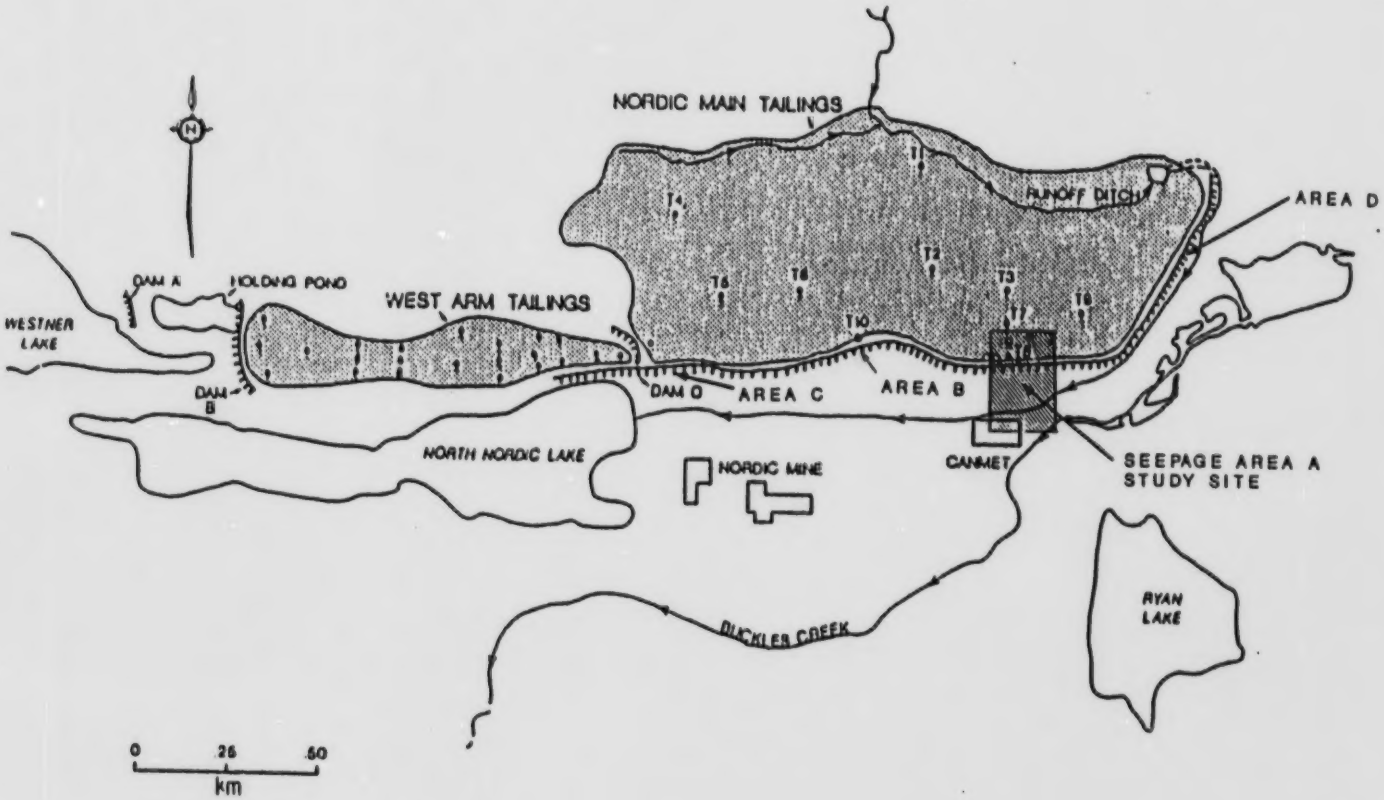


| | | |
|---|---|---|
| INTERA Technologies | Plan of Nordic Tailings Impoundments (Cherry et al., 1980) | Figure 3.2 |

dams, including dam "C". Consequently, the material used in the construction of dam "C" and the existence of peat under the dam are highly uncertain. However it has been established that no drains were installed under the dam (A. Vivyurka, Rio Algom Ltd., personal communication, 1989) and that the bulk of the dam was likely constructed with rock fill.

The Nordic Main impoundment was created by raising dam "C" in 1960. At this time, discharges to the West Arm area were discontinued and were moved to the southwest corner of the Main tailings area. Tailings were spigotted into the impoundment from the crest of the dam extending northward and eastward. The tailings deposit consisted of broad low angle alluvial fans with particle size likely decreasing with increasing distance from the spigot point. Dam "C" was progressively raised over the period from 1960 to 1964. The impoundment was filled to capacity and became inactive with the closure of the mine in 1968. The eastern portion of the tailings area contained some ponded water until it was subsequently drained in 1970-1971.

Over the following years a number of attempts were made to seed the tailings. In 1975 the surface of the tailings was first treated with lime and crushed limestone (Blair et al., 1980). After several subsequent attempts, a dense grass cover was finally established by 1980.

The surface of the tailings is currently described as dry, vegetated and accessible by vehicle (Blair et al., 1980). The tailings slope gently to the north. Runoff is collected primarily by a ditch which traverses the northern edge of the impoundment.

The instrumented site used in this study for calibration and validation of the FEMWATER/FEMWASTE computer programs is shown in Figure 3.2. The site is located in Seepage Area "A" down gradient from tailings dam "C" in the vicinity of the former CANMET buildings.

## 3.2 SUMMARY OF PREVIOUS INVESTIGATIONS

Over the years the Nordic tailings areas have been the subject of numerous hydrogeologic, hydrogeochemical and environmental impact studies. The vast majority of these studies have been conducted independently of one another and have typically examined different areas or have had different objectives.

The first reported investigations were conducted by Moffet and Tellier (1978) who investigated the geochemical nature of porewater contained in the Nordic West Arm tailings area. Following this study, a number of investigations were conducted by researchers associated with the University of Waterloo. The first of these were conducted by Blair et al. (1980) on the Nordic Main tailings area in 1979. They installed a network of piezometers in both the tailings (nested piezometers at three sites) and the surrounding sand aquifer (multi-level piezometers at nineteen sites, M-1 to M-19) the locations of which are shown in Figure 3.3. Hydraulic heads were measured and samples of groundwater collected and analyzed for major contaminants. The following field season (1980), a number of additional multi-level piezometers (M-20 to M-34 and WW-1) were installed in the sand aquifer as described in Morin (1983). The following field season three additional piezometers (M-35 to M-37) were installed in the sand aquifer beneath the tailings. As part of his research, Morin measured water levels and collected samples for analyses of major contaminants and ions in 1980, 1981 and 1982. Measurements of calcium carbonate within the sand aquifer were also made as part of this study.

Morin (1983) identified a total of four seepage areas, known as A through D, at the Nordic main tailings area. Area B was instrumented with four single narrow diameter piezometers and Area C was not instrumented. Area D was instrumented with two multilevel piezometers. Area A was determined to have the most distinct low pH plume and consequently most investigative effort was concentrated on this area.

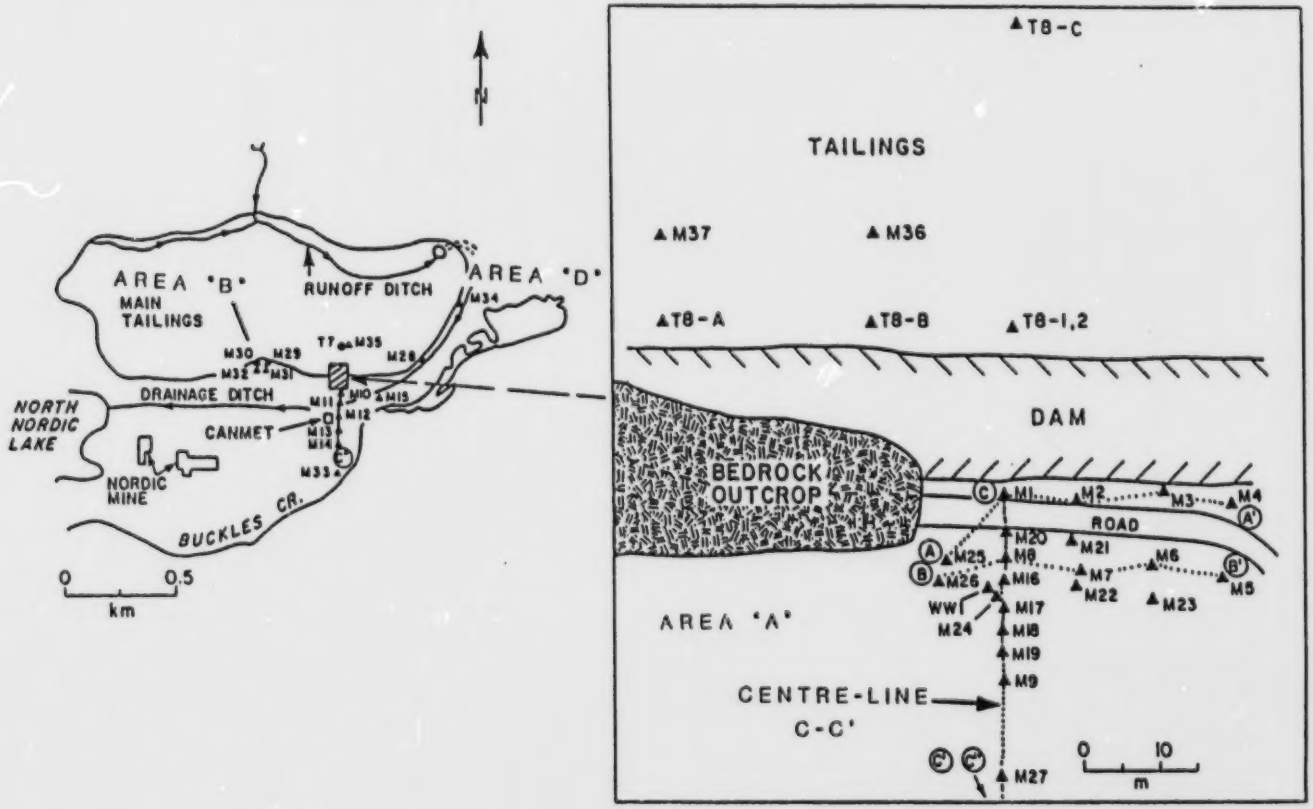


| INTERA Technologies | Piezometer Locations - Nordic Tailings Areas (after Morin, 1985) | Figure 3.3 |
|---|---|---|

Although Morin's study (as described in Morin, 1983; Morin et al., 1982) concentrated on the movement of tailings contaminants within the sand aquifer, because of difficulties in defining the source term he interacted with N. Dubrovsky who, as part of another University of Waterloo research team, was studying the oxidation of pyrite within the tailings (Dubrovsky, 1986; Dubrovsky et al., 1985). The exact number and locations of all piezometers installed by Dubrovsky is uncertain. By 1982 (see Dubrovsky et al., 1985) the numbering of the piezometers in the Nordic Main tailings area had increased to T-10 although data was only reported by Dubrovsky (1986) for the first seven. Some additional information was reported on piezometer T-8 by Morin (1983). In addition an unspecified number of piezometers were installed in the West Arm area. During the 1982 field season two additional piezometers were installed as well as three bundle piezometers. The bundle piezometers were actually installed through the tailings into the underlying aquifer, although some of the upper screens of M-35, M-36 and M-37 also intersect the mine tailings. As part of his work, Dubrovsky (1986) collected samples of tailings porewater and cores of tailings solids. Grain size and carbonate mineral content were among the tests conducted on these latter samples. Porewater samples were analyzed for major contaminants and ions.

Additional investigations were conducted by Morin in 1984 for CANMET (Morin, 1985). This study involved collecting and analyzing an additional round of geochemical samples. This sampling was performed in mid-November unlike previous sampling which was conducted during summer months. This fact has been suggested as an explanation for some of the discrepancies noted in the resulting chemical analyses.

A significant amount of additional work has been based on the interpretation of the data collected up to 1984. Publications by Cherry et al. (1984), Morin and Cherry (1986), Morin and Cherry (1988), Morin et al. (1988a,b) fall into this category. Most of these studies present little in the way of new site specific data and are, for the most part, interpretations based on pre-1985 data.

Another relevant study was conducted by Blowes and Gillham (1988) on the eastern portion of the Nordic West Arm. This study was undertaken in an effort to establish the relative contribution of groundwater versus runoff to total streamflow. The study was based on a simple mass-balance approach using $Cl^-$ and the environmental isotope $^{18}O$ as tracers.

Two additional studies conducted at the Nordic site bear mentioning. These studies conducted by Golder and Senes (1987) and Senes (1988) assessed seepage control alternatives and predicted future water quality of Lake Westner. Although these studies do not present substantial new data they are useful since they provide estimates of the acid generating potential of the Nordic tailings.

Additional data has been, and is continuing to be, collected on the site by various parties including Rio Algom. Some of this information has been obtained for use in the current study.

## 3.3 EXISTING SITE INSTRUMENTATION

Because of the investigations that have been conducted at the Nordic tailings areas, a significant quantity of monitoring instrumentation has been installed (and remains) on site. The vast majority of this instrumentation is associated with investigations conducted by University of Waterloo researchers (Blair et al., 1980; Morin, 1983) and is of similar construction.

In the glaciofluvial sand aquifer 37 multi-level bundle piezometers were installed. These piezometers consisted of up to 12 individual 9 mm diameter polyethylene tubes fastened to a central 15 mm diameter PVC pipe. Each tube was of a different length (to allow for different monitoring intervals) and had a 0.1 m polyethylene piezometer screen at the bottom. Piezometer tips were typically located at 0.5 m intervals over the first 4 m increasing to 2 m below this depth. Of the 37 multi-level assemblies installed, three (M-35 to M-37) were installed through the tailings themselves, four (M-29 to M-32) were installed at seepage area B, 10 were scattered about at various strategic locations and the remainder were concentrated in the immediate vicinity of

seepage area A. These piezometers were installed by inserting the assembly through the centre of a hollow-stem auger. By knocking out the center auger plug the augers could be removed allowing the host material to collapse around the assembly.

Additional steel drivepoint piezometers (at least 5) were installed by Rio Algom some time prior to 1982. Little information is known about these piezometers aside from their location and depth of monitoring points.

The majority of the single piezometers that were installed in the tailings were part of a network of piezometer nests. These piezometers (as described by Dubrovsky, 1986) were a modified Casagrande drive point type consisting of a solid PVC drive point connected to a 15 cm length of perforated pipe which in turn was connected to solid riser pipe using a female coupling and a caulking sealant (Blair et al., 1980). These piezometers were installed by augering to within one meter of the desired depth and then driving the piezometer the remaining distance. Initially (1979-80) ten piezometer nests were installed by Dubrovsky (1986) in the Nordic Main tailings area and 24 were installed in the West Arm. In 1982, an additional number of piezometers were installed in the Nordic tailings. These new installations, also installed by Dubrovsky, included both piezometer nests and multi-level bundle piezometers. However, little information is provided by Dubrovsky (1986) regarding the location, nature and number of these additional installations.

Figure 3.3 presents a plan of the Nordic site showing the location and designation of all known piezometer instrumentation for the sand aquifer. This figure together with the tailings piezometer locations of Figure 3.2 show the location of all piezometers at the Nordic site. Figure 3.4 presents a schematic of typical piezometer nest and bundle piezometer construction (from Dubrovsky, 1986).

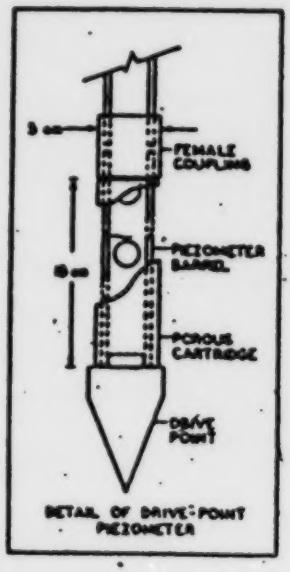


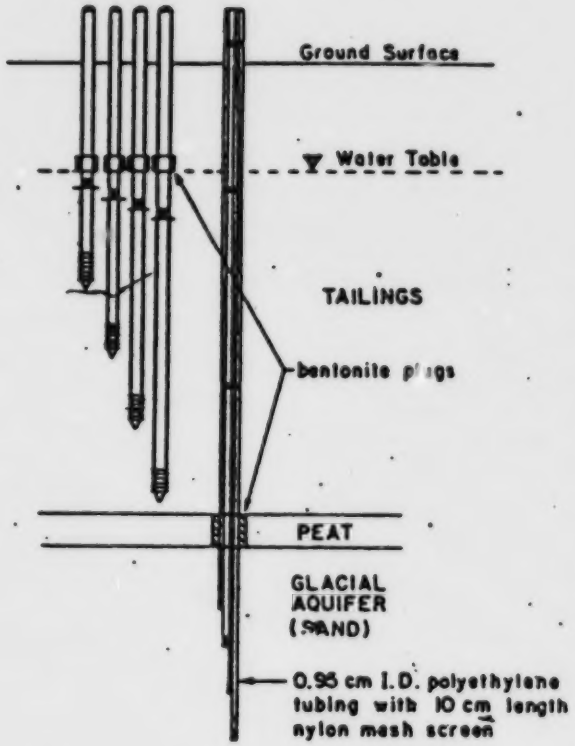


| | | |
|---|---|---|
| Drawn by | Date | Typical Piezometer Configuration |
| Checked by | Date | |
| Revisions | Date | |
| | | |
| INTERA Technologies | | Figure 3.4 |

## 3.4 GEOLOGIC SETTING

The Nordic tailings impoundments are located in a glaciated valley that is oriented primarily east-west between bedrock outcrops. The bedrock is a metasedimentary deposit which strikes east-west and dips to the north. During the Pleistocene period, glaciers moved through this region depositing a layer of sand and gravel till over the top of bedrock. During the glacier's retreat meltwaters eroded some of this till while subsequently forming fluvial deposits of sand and gravels. Throughout much of the valley the glacial fluvial sands are overlain by a layer of black peat, 0.5 to 1.0 m in thickness which was formed by a spruce bog that formerly existed in the area. Dubrovsky (1986) reports that the peat layer was removed along the east and southeast edges of the Nordic Main impoundment prior to tailings deposition. He further states that the peat may also be absent from areas that were topographic highs.

Borehole logs for the piezometers installed at the Nordic Main area (Dubrovsky, 1986; Morin, 1983; Blair et al., 1980) indicate that the tailings are approximately 10 m thick (varying between 7 and 14 m). The peat layer (where found) was subject to poor core recovery and hence its thickness is uncertain. The maximum likely thickness is probably 2.4 m based on core recovery (and lack there of) for piezometer M-20. Generally however the peat layer is between 0.5 and 1.0 m in thickness. In the vicinity of piezometers M-16 to M-27 the peat layer is overlain by a sand and cobble fill. This fill layer varies in thickness from less than 1.0 m (0.9 in the vicinity of M-22) to approximately 4.0 m (in the vicinity of M-27) and probably averages 1.5 m. The sand that underlies the peat varies from a fine sand to a coarse sand with pebbles. The thickness of this layer varies as a function of proximity to bedrock outcrops. In the vicinity of M-20, for example, the sand is only about 4.6 m thick. Over most of the area for which borehole logs are available it would appear that the sand averages about 10 m in thickness.

Morin (1983) further classified the sand into an upper and lower layer. The upper layer is described as a dark tan, medium grained sand varying in thickness from 4 to 8 m. The lower layer of the sand is described as light

grey, very fine grained sand ranging between 3 and 8 m in thickness. Morin (1983) indicated that grain size analyses show the lower sand contains some silt beds. Morin (1983) also indicated that although no direct evidence was contained in recovered cores, a thin silt layer may separate the upper and lower sands. Typical grain size analyses of the upper and lower sand are presented in Figure 3.5 (after Morin, 1983). Figure 3.6 presents a geologic section along the plume centre-line in seepage area A (after Morin, 1983).

A similar but slightly different geologic interpretation for the same section was presented by Blair et al. (1980). In their interpretation (see Figure 3.7) no distinction is made between an upper and lower sand and a low permeability silt layer is shown in the vicinity of piezometer M-1 at a depth approximately equal to the contact between Morin's upper and lower sand. Blair et al. (1980) also included a low permeability peat layer that subcrops in the area of monitoring wells M-16 and M-17. The existence of both the silt layer and the peat layer were proposed by Blair et al. (1989), based on drilling observations, to reconcile the available hydraulic head measurements.

The implications of this difference in geologic interpretation are discussed more fully in the following sections.

## 3.5 PHYSICAL HYDROGEOLOGIC DATA

The available physical hydrogeologic data for the study area primarily includes estimates of hydraulic conductivity and water level data. The hydrogeologic units of interest consist of the tailings, the underlying discontinuous peat layer, the sand aquifer and the underlying glacial till. The following sections describe the available data (i.e., prior to this study) for these hydrostratigraphic units.

### 3.5.1 Hydraulic Conductivity

The hydraulic conductivity of the tailings has been investigated by several researchers (Blair et al, 1980; Blowes and Gillham, 1988).

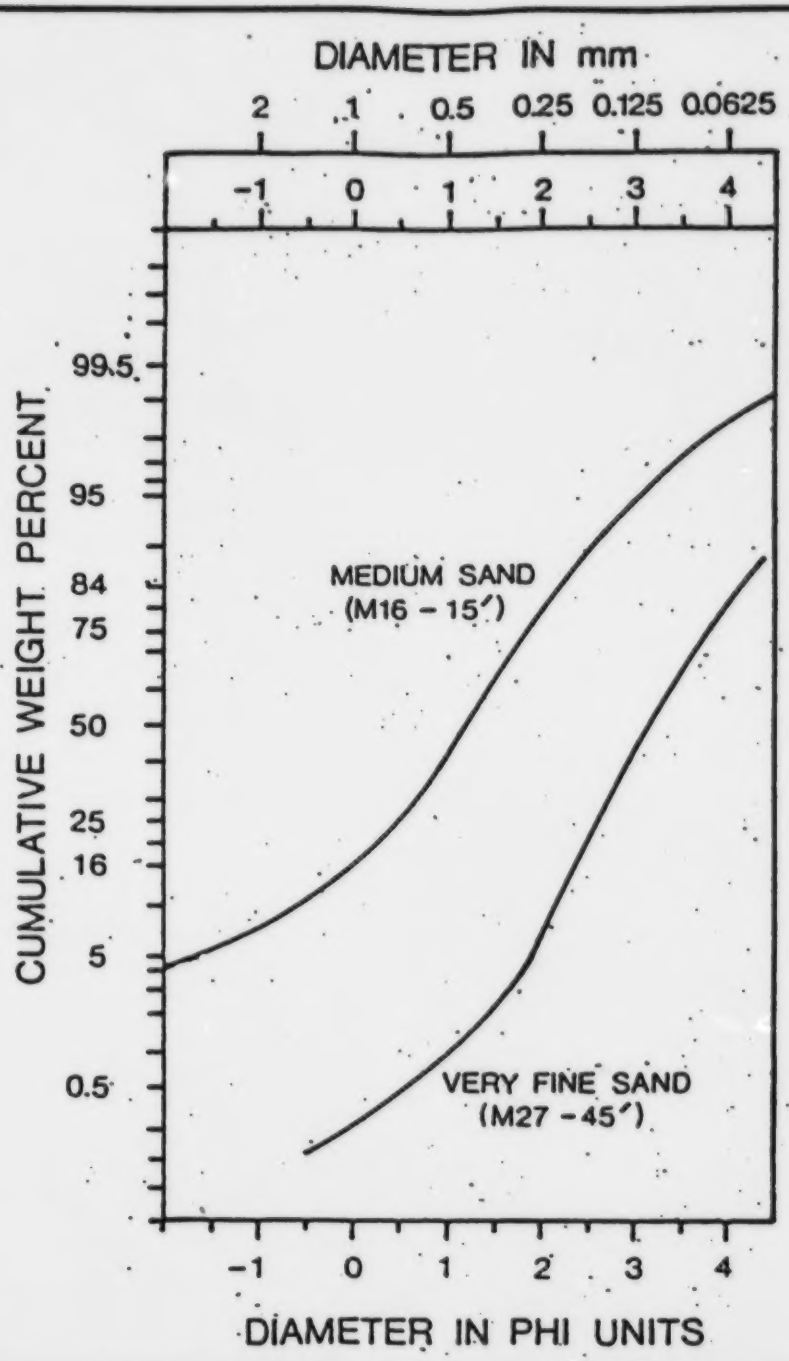


| | |
|---|---|
| Drawn by | Date |
| Checked by | Date |
| Revisions | Date |
| | |

Representative Grain Size Distribution of Sand Aquifer (Morin, 1983)

INTERA Technologies

Figure 3.5

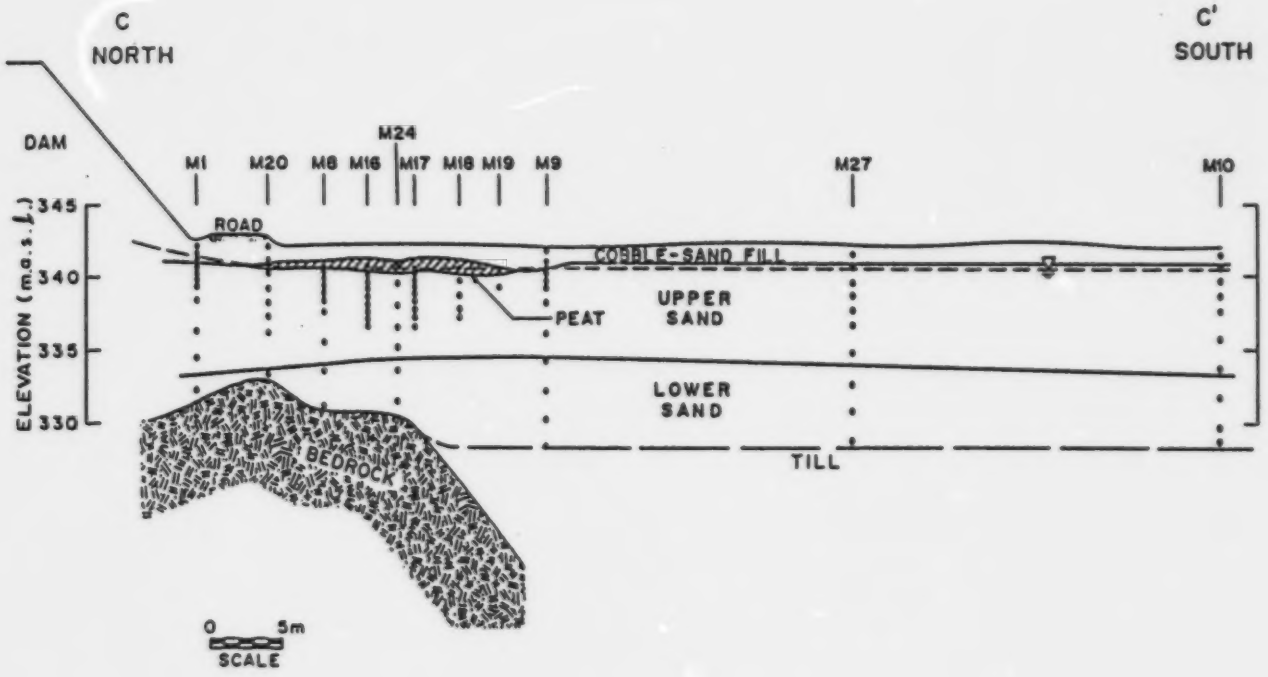


| INTERA Technologies | Geologic Cross-Section of Plume Centreline Seepage Area A (Morin, 1983) | Figure 3.6 |
|---|---|---|

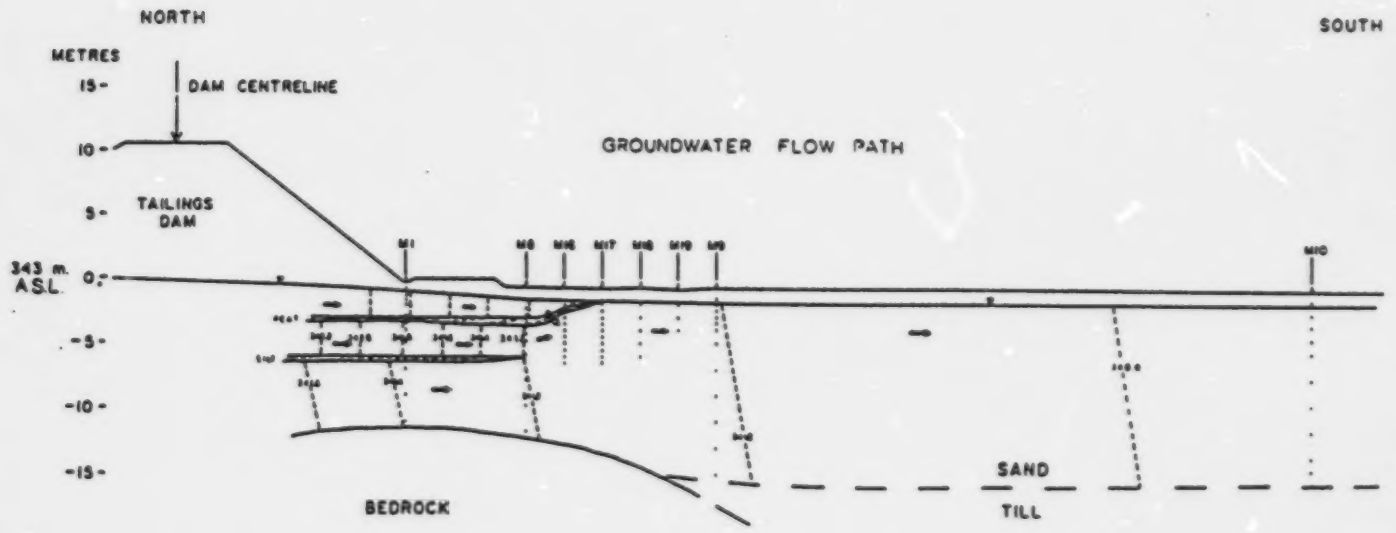


| | | |
|---|---|---|
| INTERA Technologies | Geologic Cross-Section of Plume Centreline Seepage Area A (Blair et al., 1980) | Figure 3.7 |

The following summarizes these findings:

1. A range of $1.0 \times 10^{-6}$ to $3.1 \times 10^{-8}$ m/s based on rising head tests conducted in three piezometers in the tailings (Blair et al., 1980);

2. Results of a pumping test conducted in the West Arm by Wardrop Assoc. Ltd. yielded a value of $1.0 \times 10^{-7}$ m/s (Blair et al., 1980);

3. Vertical hydraulic conductivity measured by constant head permeameters on an unspecified number of relatively undisturbed cores averaged $2.6 \times 10^{-7}$ m/s (Blowes and Gillham, 1988);

Reported values for the hydraulic conductivity of the sand aquifer are summarized below:

1. Permeameter tests conducted on an unspecified number of disturbed samples yielded a range of $1.7 \times 10^{-5}$ to $2.1 \times 10^{-4}$ m/s (Blair et al., 1980);

2. A pump test conducted in the West Arm tailings by Wardrop Assoc. Ltd. yielded values ranging from $1.2 \times 10^{-4}$ to $2.2 \times 10^{-4}$ m/s (Blair et al., 1980);

3. Average values of $1.2 \times 10^{-4}$ m/s and $5.3 \times 10^{-5}$ m/s, were reported for the "upper" and "lower" sands by Morin (1983). The values were estimated using an empirical relationship to relate grain size and hydraulic conductivity. Averages were based on four samples in the upper sand and two samples in the lower sand.

4. Interpretation of a borehole dilution test (Morin, 1983) indicated an interstitial velocity which was judged (Morin, 1983) to be comparable to that calculated using hydraulic conductivities and gradients.

5. Two dimensional finite element modeling conducted by Matanga (as reported by Morin (1983)) used hydraulic conductivities of 1.5 x $10^{-4}$ m/s for the "upper" sand and 6.0 x $10^{-5}$ m/s for the "lower" sand.

Hydraulic conductivity values for both the peat layer and the glacial till were not measured directly at the site. A value of 4 x $10^{-9}$ m/s was estimated for the peat layer by Blair et al. (1980) based on measured gradients across the layer and inferred flux rates. The hydraulic conductivity of the till unit was estimated by Blair et al. (1980) to be of the order of 1 x $10^{-8}$ m/s based on tests conducted in the vicinity of the site.

The significance of hydraulic conductivity anisotropy at the Nordic site was not extensively addressed. Morin (1983) suggested a value of 10:1 for horizontal to vertical hydraulic conductivity was representative for the sand aquifer based in part on the computer modeling of Matanga. Blowes and Gillham (1988) reported that despite the observed layering, the tailings did not possess strong anisotropy.

### 3.5.2 Hydraulic Head and Groundwater Flow

In spite of the apparent abundance of monitoring points and the significant number of investigations, there is no complete water level survey including all monitoring points at one time for the study area. For the vast majority of investigations, water levels were only measured sporadically-typically only once during a field season. In addition, water levels were usually only measured for those piezometers of immediate interest to individual researchers. The result is a series of piezometric measurements for distinct sets of piezometers at different times. For example, Dubrovsky (1986) presents water levels on June 21 and July 28, 1980 and June 13, 1981 for piezometers T-1 and T-10. He also presents water levels for piezometers T-1 to T-3, T-7 and T-8 as well as several bundle piezometers for August 3 and August 16, 1983. Blair et al. (1980) report only a single value for each piezometer, however, they do indicate that the maximum water table fluctuation between August and December was 0.5 m.

Morin (1983) also discussed the significance of seasonal response for the sand aquifer. He indicated the magnitude of this response to be generally less than 0.2 m and that this response was uniform throughout the study area. On this basis he concluded that a steady state flow assumption was reasonable. The seasonal fluctuations of hydraulic head in the tailings has been found to be much more significant. Cherry et al. (1980) indicate a seasonal response of 0.5 and 1.5 m and Blowes and Gillham (1988) observed in excess of 0.2 m rise in the water table during a single event.

Prior to the current study, the data presented in Morin (1983) for seepage area A probably represents the best collection of water level information. Water table information for seepage area A from Morin (1983) are presented in Table 3.1. The water table is the uppermost saturated surface. The data in Table 3.1 highlight the shortage of available water level data. Using these data a water table map was constructed and is presented in Figure 3.8. The data used in constructing this map corresponded to May, 1980 and mid-June, 1981. These data were combined in an effort to extend areal coverage for use in conducting preliminary modeling only. These data were selected because the difference between overlapping points was generally small. By examining the water table map, the lack of data for various areas becomes apparent. For example, no points exist either east or west of the plume centreline between piezometers M-10 and M-18. As a result flow directions in this area are subject to high uncertainty. The implications of this are discussed in more detail below.

A cross-section of hydraulic heads using Morin (1983) data was prepared (Figure 3.9) for the "plume centre-line" using the hypothesized source location at T-8-B (Morin, 1983) as the upstream boundary. A number of interesting observations can be made regarding this section. First, high hydraulic gradients are apparent in the region between M-1 and M-18. These gradients are generally greatest in the upper sand unit. The orientation of piezometric contours in this direction would indicate flow is both horizontal and vertically downward. Morin

Table 3.1 Water Table in Elevation Area A in Meters Above Sea Level (Morin, 1983)

| Piez | Oct-Nov 1979 | May 1980 | Early-June 1981 | Mid-June 1981 | Early-July 1982 |
|---|---|---|---|---|---|
| M1 | 342.07 | 341.93 | 341.83 | 341.91 | 341.68 |
| M2 | 341.66 | 341.68 | 341.59 | 341.67 | 341.29 |
| M3 | 341.78 | 341.84 | 341.68 | 341.72 | 341.54 |
| M4 | 341.78 | 341.80 | 341.65 | 341.70 | 341.52 |
| M5 | | 341.73 | 341.56 | | 341.44 |
| M6 | 341.63 | 341.65 | 341.51 | 341.53 | 341.34 |
| M7 | | 341.19 | 341.15 | 341.09 | 340.95 |
| M8 | 341.66 | 341.43 | 341.33 | 341.37 | 340.91 |
| M9 | 341.06 | 340.98 | | | 340.77 |
| M10 | | 340.72 | | | |
| M12 | | 340.08 | | | |
| M13 | | 339.65 | | | |
| M14 | | 339.26 | | | |
| M15 | | 340.59 | | | |
| M16 | 341.40 | 341.36 | | | |
| M17 | 341.19 | 341.05 | | | |
| M18 | 341.11 | 341.02 | | | 340.79 |
| M19 | 340.95 | 341.00 | | | 340.77 |
| M20 | | | 341.69 | | |
| M21 | | | 341.15 | | |
| M22 | | | 341.13 | 341.15 | 340.94 |
| M23 | | | 341.35 | 341.35 | 341.21 |
| M24 | | | | | 340.83 |
| M25 | | | | | 340.86 |
| M26 | | | | | 340.85 |
| M27 | | | | | 340.69 |
| T8-1 | | | | 342.10 | 342.12 |
| T8-2 | | | | 342.11 | 341.93 |
| T8-A | | | | 343.63 | 343.61 |
| T8-B | | | | 342.29 | 342.15 |
| T8-C | | | | 342.79 | |

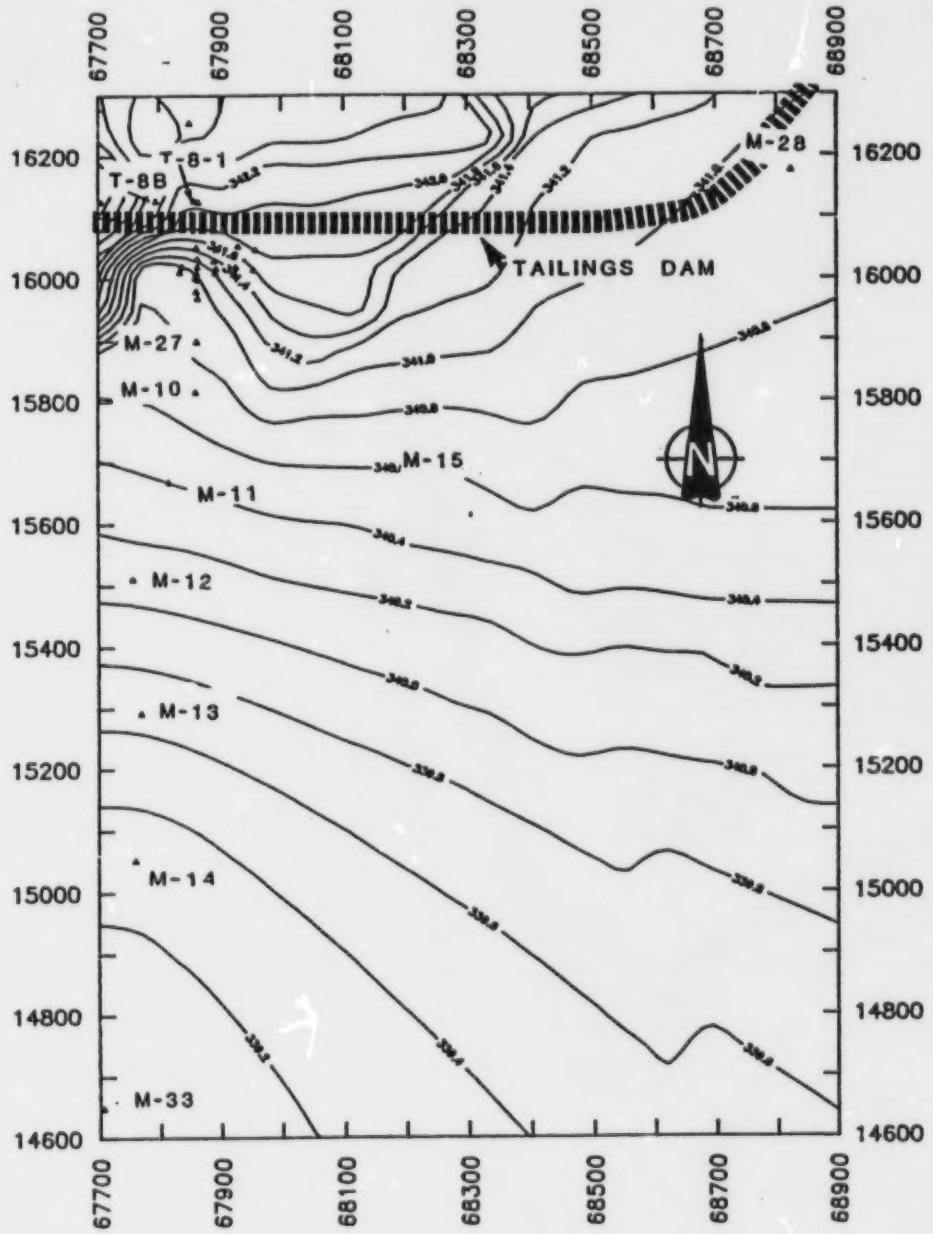


| | |
|---|---|
| Drawn by | Date |
| Checked by | Date |
| Revisions | Date |
| | |

Water Table Map for Seepage Area A (Based on May, 1980 and June, 1981 data from Morin, 1983)

INTERA Technologies

Figure 3.8

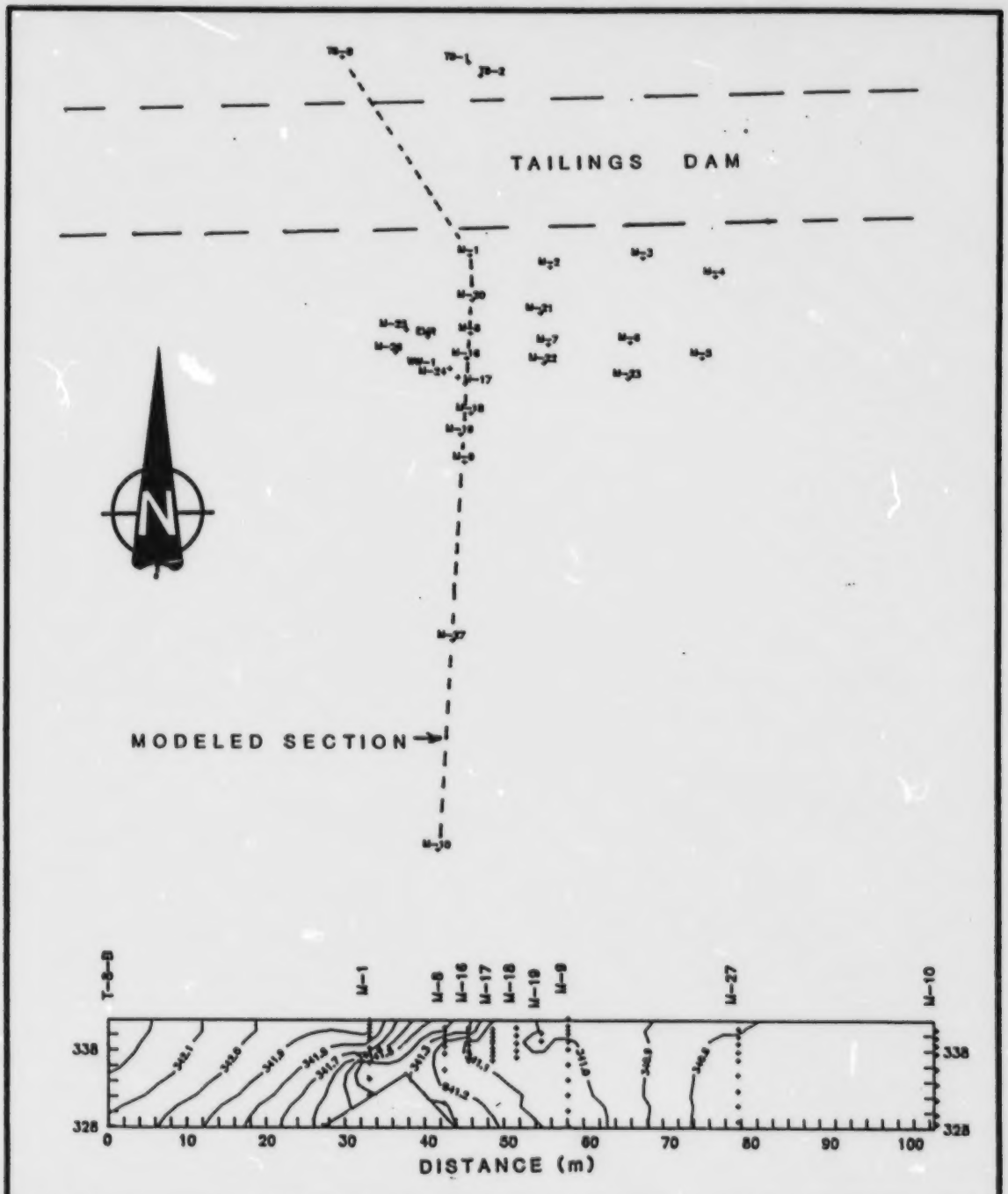


| | |
|---|---|
| Drawn by | Date |
| Checked by | Date |
| Revisions | Date |
| | |

Piezometric Contours along Plume Centreline Seepage Area A (Based on May, 1980 and June, 1981 data from Morin, 1983)

INTERA Technologies

Figure 3.9

(1983) also noticed this change in piezometric head and attributed it to a reduction in the available flow area caused by the nearby bedrock outcrop. It is also conceivable that permeability variation may account for some of this head change. For example, Blair et al. (1980) accounted for the increased hydraulic gradient between M-8 and M-18 by the presence of a low permeability peat layer that subcrops in the area of M-17.

A second observation can be made regarding the vertical gradients in this same region, specifically piezometers M-1 and M-8. In these piezometers vertical gradients change significantly at a depth of approximately 4 m. This change is in the vicinity of the contact between the "upper" and "lower" sands and is probably the basis for including a silt layer at this point in their interpretation (Blair et al., 1980).

A third observation concerns the presence of local hydraulic "sinks" (e.g., M-19, M-9) along the section. Two possible explanations for these are:

1) measurement error;

2) the section is not oriented along a single streamline but actually intersects several streamlines with flow into and out of the section.

This second possibility can only be evaluated through the use of a comprehensive plan map of hydraulic head that enables piezometric contours and streamlines to be drawn. Such a plan map and section could also be used to evaluate streamline divergence and convergence which would provide an estimate of the relative contribution of increasing/decreasing flow area to the observed head gradients. Unfortunately we feel the data for the period 1979-84 is inadequate to allow the construction of such a map.

## 3.6 GEOCHEMICAL DATA

### 3.6.1 Groundwater Analyses

The most extensively sampled piezometers at the Nordic site are those that lie along the plume "centreline" of seepage area A (see Figure 3.3). Blair et al. (1980) performed groundwater analyses for $SO_4^{-2}$, $Fe^{+2}$, Ni, Co, pH and $^{226}Ra$ for piezometers M-1, M-8, M-9, M-10 and M-16 through M-19. A more extensive sampling and analyses program was conducted by Morin (1983) during August of 1980, 1981 and 1982. pH was measured for virtually all piezometer monitoring points (for piezometers M-1 through M-34) with extensive analyses being conducted on three to four points. The extensive analyses consisted of a variety of cations and anions which included several radionuclides including three isotopes of thorium ($^{228}Th$, $^{230}Th$, $^{232}Th$), $^{210}Pb$, $^{226}Ra$, and U. Table 3.2 presents the range of concentrations representative of plume conditions (after Morin, 1983).

Morin (1985) presents the results of an additional round of sampling conducted for the plume "centreline" piezometers in seepage area A. This round of sampling and analyses was not as extensive as those previously undertaken since fewer monitoring points were sampled and fewer contaminants were considered. Typically three monitoring points were sampled - one from a relatively deep location and the two others from near the centre of the plume. pH was measured at all monitoring points. Several duplicate samples were collected from a number of points and submitted to different laboratories for comparative analyses. Duplicate samples submitted to the same laboratory provided an indication of the precision of various analyses. Not surprisingly precision varied as a function of concentration. For most major cations precision was generally 5 to 20% while chloride analyses were reported to have a significant lack of precision due to the use of unacidified samples (Morin, 1985). One laboratory, the Process Development Laboratory of Rio Algom did have acceptable precision for $Cl^-$ (under 20%). Analyses for $^{226}Ra$ showed precision of about 10% for relatively high levels and 30% for low levels. Accuracy was estimated based on interlaboratory comparison. For concentrated plume waters, major ions were found to vary by up to a factor of two, a factor of seven for minor ions and up to an order of magnitude for radionuclides and trace metals.

Table 3.2 Summary of Chemical Analyses of Seepage from the Nordic Main Tailings (from Morin, 1983)

| Parameter | Laboratory | Concentration Range in Area A (ppm unless marked) |
|---|---|---|
| Fe | 1 | 80-5390 |
| Ca | 1 | 47-500 |
| Mg | 1 | 13-519 |
| Na | 1 | 2.6-51 |
| K | 1 | 1.6-127 |
| Mn | 1 | 1-49 |
| Cu | 1 | <0.01-0.04 |
| Co | 1 | <0.01-4.90 |
| Zn | 1 | <0.01-1.00 |
| Pb | 1 | <0.1-4 |
| Ni | 1 | <0.1-4 |
| Al | 1 | <0.1-187 |
| Se | 1 | <1 |
| V | 1 | <1 |
| Cr | 1 | 0.05-0.14 |
| $SO_4$ | 2 | 305-12900 |
| Cl | 1 | 6-67 |
| $SiO_2$ | 2 | 9.1-74.1 |
| $PO_4$ | 2 | <0.04 |
| Alkalinity (as $HCO_3$) | 3 | 6-906 |
| DIC (as C) | 2 | 69.6-86.4 |
| DOC | | 2.4-6.6 |
| pH | 3 | 4.3-6.8 units |
| Eh | 3 | +110 to +410 mV |
| Electrical conductance | 3 | 1000-10000 uS/cm |
| Ra-223 | 6 | 8-83 pCi/L |
| Ra-226 | 1&4&6 | 4-162 pCi/L |
| Pb-210 | 5&6 | <10-110 pCi/L |
| Th-227 | 6 | 91-600 pCi/L |
| Th-228 | 6 | <0.5-9.7 pCi/L |
| Th-230 | 6 | <0.5-6.2 pCi/L |
| Th-232 | 6 | <0.5-1.7 pCi/L |
| Th total | 7 | 18-70 ug/L |

Table 3.2 Summary of Chemical Analyses of Seepage from the Nordic Main Tailings (from Morin, 1983)

| Parameter | Laboratory | Concentration Range in Area A (ppm unless marked) |
|---|---|---|
| Ac-227 | 6 | 72-311 pCi/L |
| U-234 | 7 | 15-205 pCi/L |
| U-238 | 7 | 4-167 pCi/L |
| U total | 1&6 | <0.2-8500 ug/L |
| $^{2}H$ | 2 | -74 to -84 °/∞ |
| $^{18}O$ | 2 | -11.9 to -11.6 °/∞ |
| $^{13}C$ | 2 | -20.8 to -19.2 °/∞ |

1 = Chemistry Laboratory, Research and Development, Rio Algoma Ltd., Elliot Lake, Ontario
2 = Geochemistry and Isotope Laboratories, University of Waterloo, Waterloo, Ontario
3 = field measurements by Kevin Morin
4 = laboratory measurements by Tjoe Lim
5 = CANMET, Ottawa, Ontario
6 = MONENCO, Analytical Laboratories, Calgary, Alberta
7 = laboratory measurement by Eric Veska

Figures 3.10, 3.11 and 3.12 present concentration profiles for pH, $^{226}Ra$ and $Cl^-$ for the plume centreline between M-1 and M-10. By examining the pH profiles (Figure 3.10) it can be seen that a general plume progression occurs over most of the subsequent profiles. There are a number of anomalous pH points (for example in the vicinity of piezometer M-17), but generally this trend is evident. An exception to this observation is found when comparing the 1983 and 1984 pH profiles. In this instance the plume experiences an apparent retrograde movement. Because the 1983 and previous samples were all collected during summer months whereas the 1984 samples were collected in mid-November, this apparent plume decrease may be due to seasonal effects present during the autumn months. Morin (1985) suggested that higher "watertable and rates of infiltration" in November 1984 caused "distortion of the plume". However, it has been suggested that the 1983 pH data were anomalous because they were collected by researchers other than those who collected the previous data. This would also indicate that there was no retrograde movement of the pH plume.

Radium profiles (in pCi/L) show a possible similar retrograde movement as is evident in Figure 3.11. Morin (1985) suggested this apparent retrograde could be due to decreasing source concentration.

Chloride profiles presented in Figure 3.12 require additional information for interpretation. Morin (1983) defined two distinct groundwaters within seepage area A. The first of these waters corresponds to recently infiltrated precipitation having a $Cl^-$ concentration of less than 20 ppm. The second groundwater described by Morin (1983) is "process water" - original slurry water which was deposited with the tailings. This water was believed to have a $Cl^-$ content of greater than 40 ppm. Comparison of 1984 profiles for $Cl^-$ with those of 1981 and 1982 indicate that a similar contour pattern continues to occur although in 1984 $Cl^-$ levels are somewhat lower. This may, as pointed out by Morin (1983), either further substantiate the additional infiltration believed experienced in November, 1984 or be the result of an analytical error.

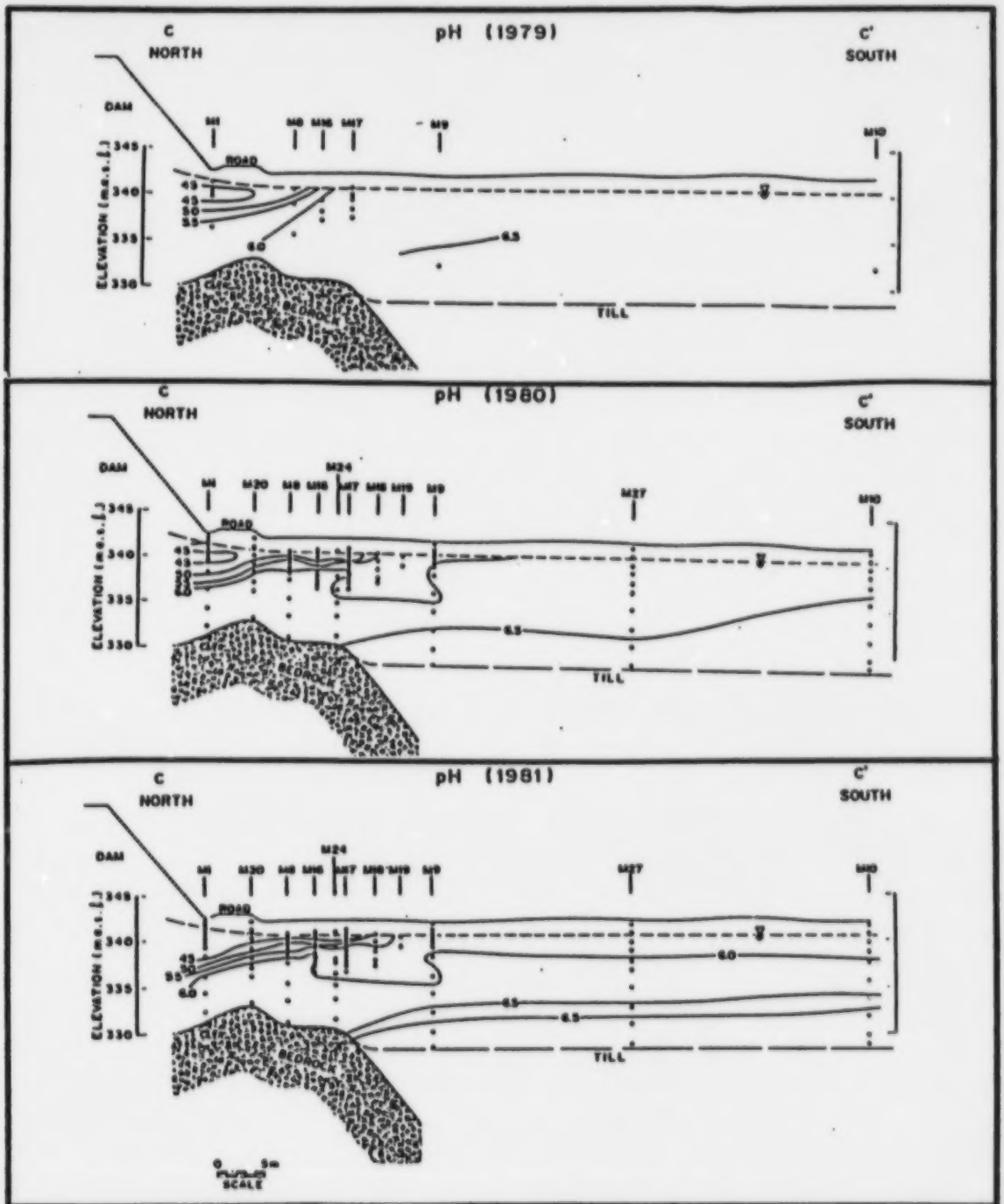


| | |
|---|---|
| Drawn by | Date |
| Checked by | Date |
| Revisions | Date |
| | |

pH Concentration Contours along Plume Centreline Seepage Area A (from Morin, 1987; 1985)

INTERA Technologies

Figure 3.10

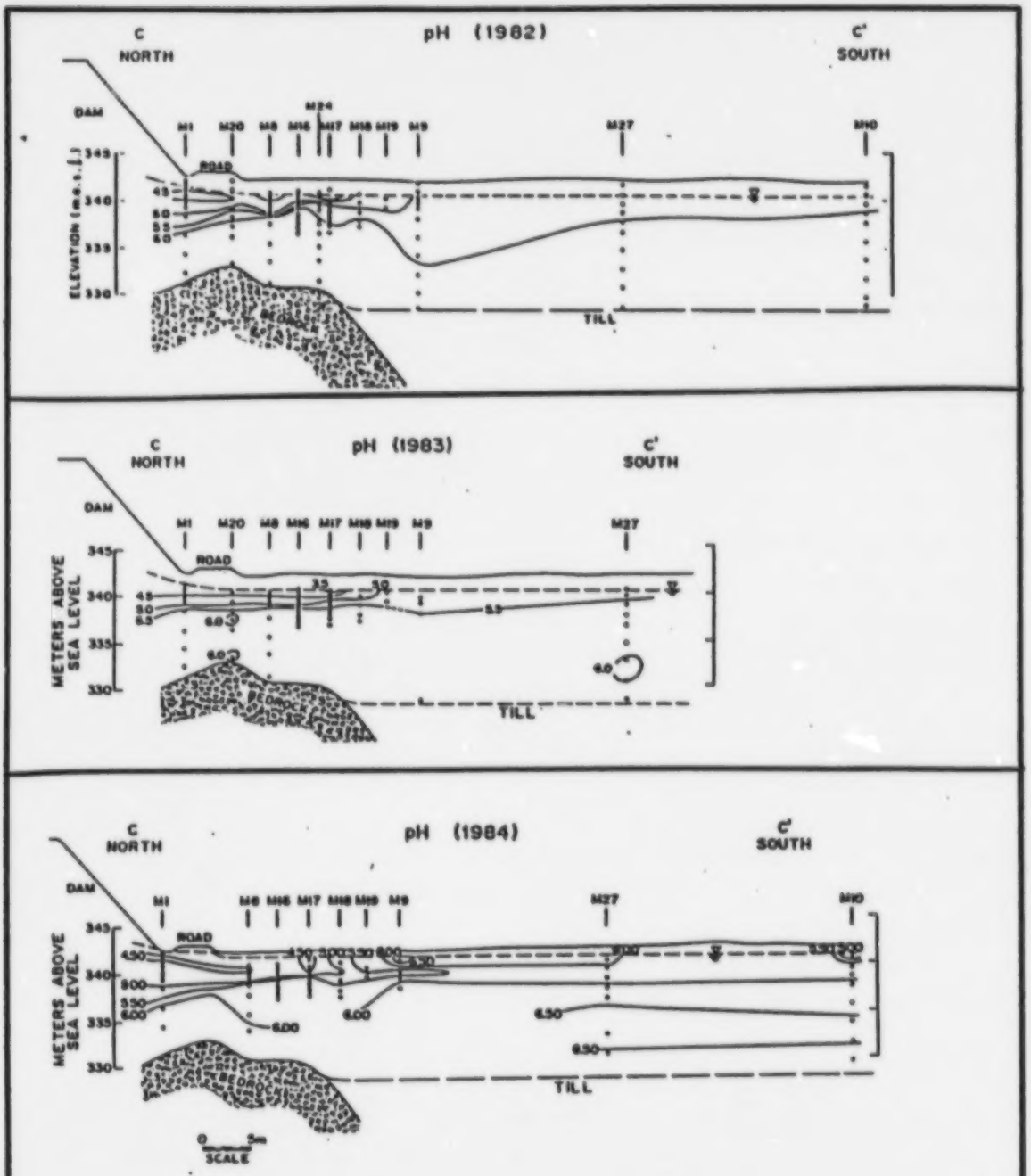


| | |
|---|---|
| Drawn by | Date |
| Checked by | Date |
| Revisions | Date |
| | |

pH Concentration Contours along Plume Centreline Seepage Area A (cont'd)

INTERA Technologies

Figure 3.10

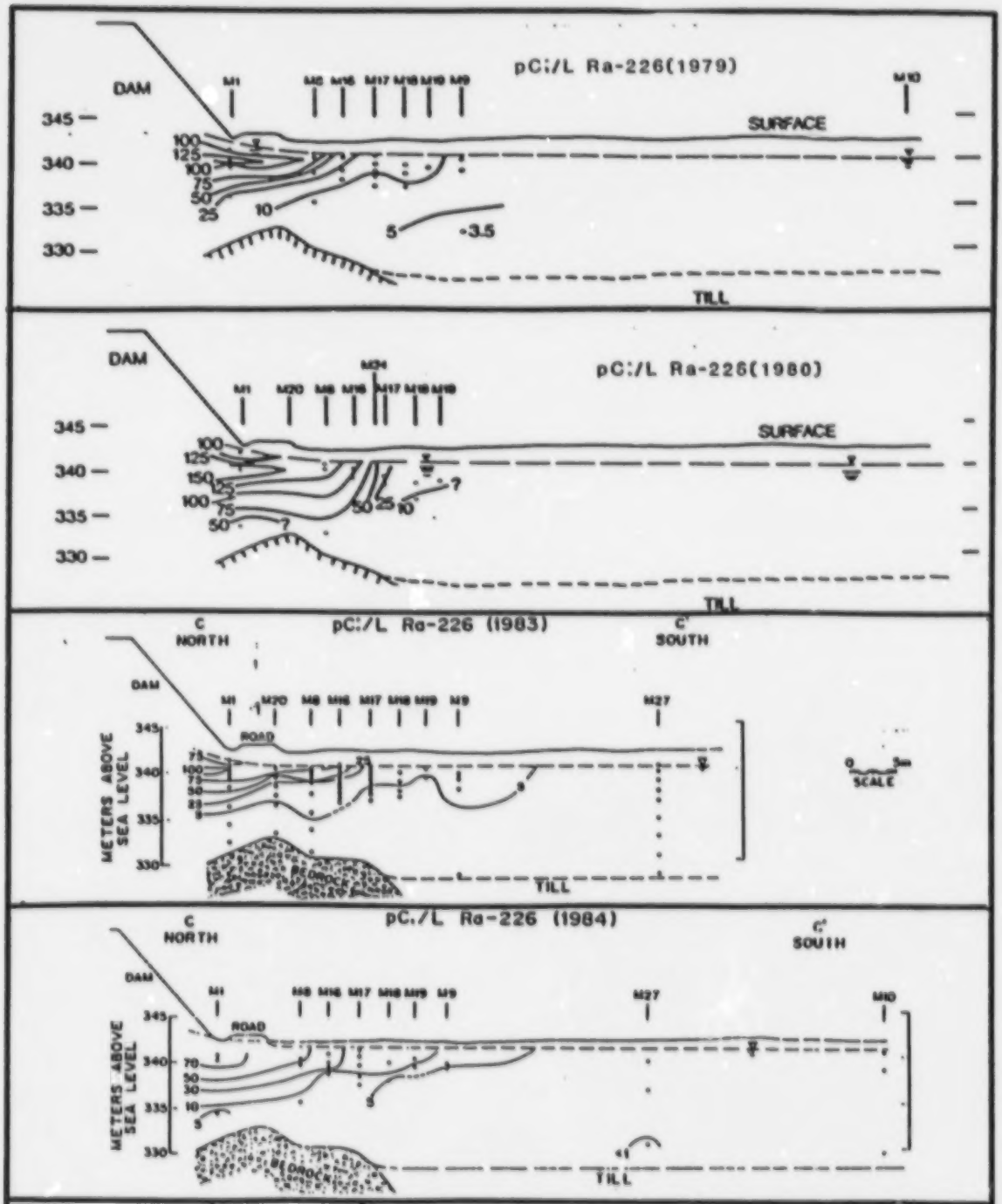


| | |
|---|---|
| Drawn by | Date |
| Checked by | Date |
| Revisions | Date |
| | |

Ra-226 Concentration Contours along Plume Centreline Seepage Area A (from Morin, 1983; 1985

INTERA Technologies

Figure 3.11

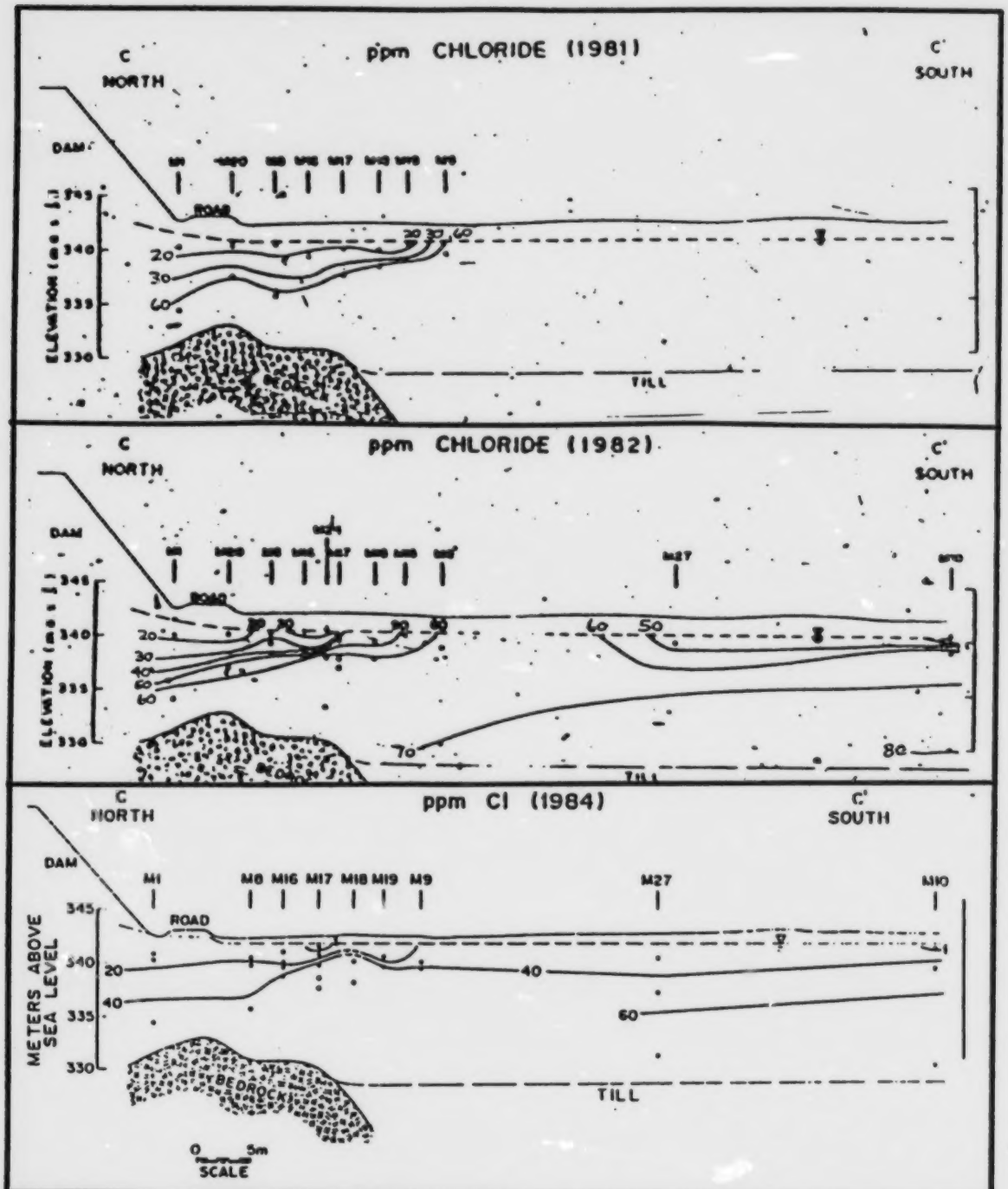


| | |
|---|---|
| Drawn by | Date |
| Checked by | Date |
| Revisions | Date |
| | |

$Cl^-$ Concentration Contours along Plume Centreline Seepage Area A (from Morin, 1983; 1985)

INTERA Technologies

Figure 3.12

In discussing the $Cl^-$ concentrations in the Nordic tailings the work performed by Blowes and Gillham (1988) on the West Arm is important. In this study $Cl^-$ was used as a tracer to enable separation of surface runoff and groundwater components in streamflow. As part of this study groundwater samples were collected at depths of 0.1 to 3.0 m in the tailings. They found that $Cl^-$ concentrations were a maximum of between 80 and 130 ppm at a depth of 0.1 m and decreased to approximately 60 ppm at a depth of 3 m. This trend was observed both in the spring and fall and was attributed to higher evaporation rates at shallow depths. It is also worth noting the $Cl^-$ concentration of all of the precipitation measured as part of this study was less than 2 ppm. This suggests that the chloride concentration data possess significant uncertainty. The implications of these findings are discussed further in Section 4 under the development of our conceptual model.

The data collected by Dubrovsky (1986) represent the most extensive and available set of groundwater analyses for the tailings. Dubrovsky performed numerous analyses for pH, $Cl^-$, $SO_4^{-2}$ and $Fe^{+2}$ but only a few analyses for $^{226}Ra$ . Generally his $Cl^-$ data supports the premise that both a low $Cl^-$ (<20 ppm) and high $Cl^-$ (>40 ppm) water exists. A number of facts should be considered when comparing Dubrovsky's (1986) data with that of Blowes and Gillham (1988). The vast majority of samples collected by Dubrovsky were taken from significantly greater depths (>3 m) than those of Blowes and Gillham (1988). At least one piezometer (coincidentally located in the West Arm) showed $Cl^-$ levels comparable to those reported by Blowes and Gillham (1988). pH levels as low as 1.47 were encountered. Samples were collected in both 1980 and 1983 for the initial piezometers (T1-T7) and, only in 1983 for the remainder. Unfortunately many of the piezometers in the vicinity of seepage area A were not installed until later, consequently only a single set of sample analyses (for 1982) are available for most of these piezometers. A typical profile is presented in Figure 3.13.

### 3.6.2 Analyses of Aquifer Materials

No discussion of the geochemistry would be complete without addressing the solid phase. Morin (1983) describes the mineralogic composition of the sand

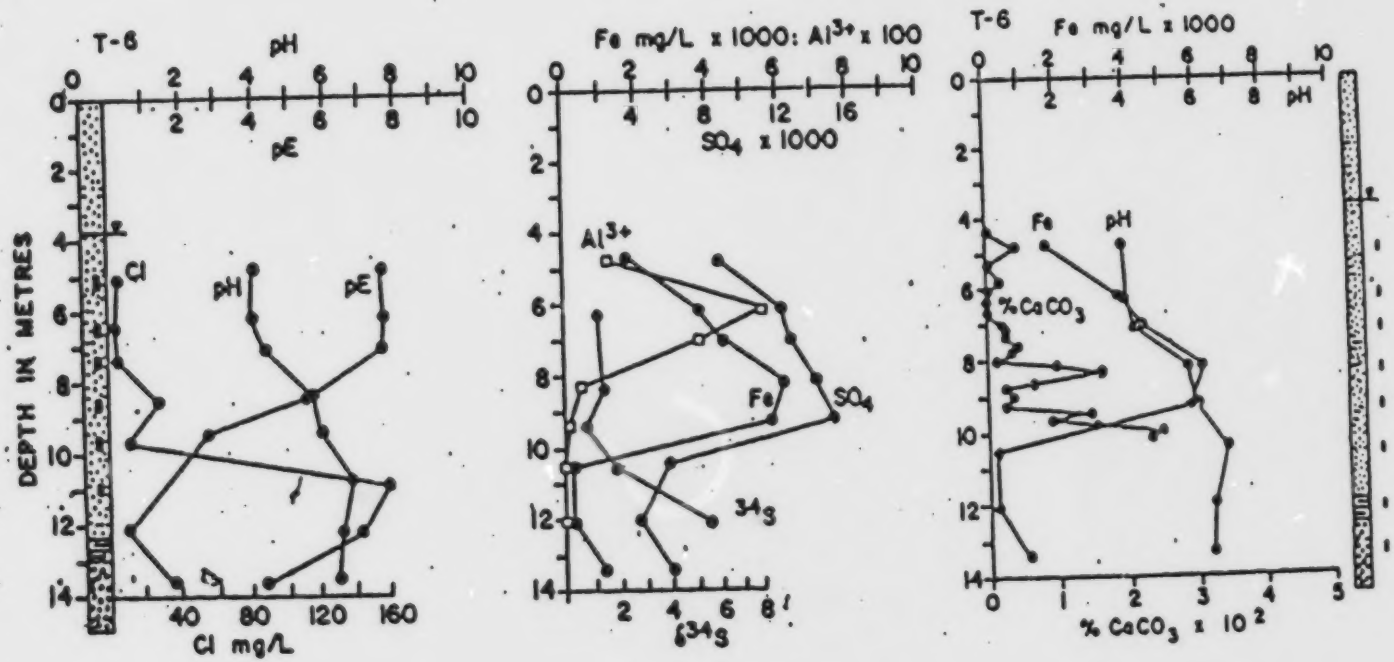


| INTERA Technologies | Representative Concentrations in Tailings (Dubrovsky, 1986) | Figure 3.13 |
|---|---|---|

aquifer in terms of his previously defined upper and lower sands. A sample of the medium grained upper sand was analyzed and found to be comprised of:

| | |
|---|---|
| Quartz | 48.7% |
| Feldspar | 20.4 |
| Altered Ca-spar (clay) | 12.0 |
| Pyroxene and Amphibole | 5.8 |
| Spinel Group | 12.1 |
| Miscellaneous | 1.0 |
| | 100.0 % |

The dominant member of the spinel group was magnetite and the miscellaneous category included apatite, hypersthene and mica minerals. The mineralogy of the fine grained lower sand was sampled and analyzed at piezometer M-27 (11 m depth):

| | |
|---|---|
| Quartz | 43.4% |
| Feldspar | 39.6 |
| Pyroxene and Amphibole | 9.2 |
| Spinel Group | 6.4 |
| Calcite | 1.4 |
| | 100.0 % |

Because of the importance of calcite in controlling the overall transport process, Morin (1983) investigated its distribution throughout the aquifer in more detail. Based on thirty-two (32) samples he concluded that the inner core was essentially devoid of calcite (<.002%) and the initial carbonate content of both the lower and upper sand was likely between 0.3 and 1.4%.

Carbonate mineral content in the tailings was measured by Dubrovsky (1986). His data show a consistent pattern for each of the sites measured - varying from less than 0.009% at depths less than 8 m to values as high as 0.056% at greater depths. This is of interest since it shows that not all of the buffering capacity within the tailings has been exhausted implying that the source term may not have stabilized.

# 4. PRELIMINARY MODEL

## 4.1 APPROACH

The sequence of tasks followed in this study included a review of existing data, preliminary modeling based on existing information, the collection of field data, final modeling (incorporating the new field data), collection of groundwater samples for chemical analyses and analyses of results. The review of existing data is described in Chapter 3. The preliminary modeling was based solely on existing information available up to 1985. The conceptualization used in this preliminary modeling has subsequently been revised for the final modeling However, for the sake of completeness, it was felt that it was worthwhile to briefly discuss the modeling conducted as part of this task, the major findings, comments from outside reviewers and suggested revisions. It should also be noted that an error exists in the location of piezometer M-18 used in the preliminary modeling and its analyses. This error was due to incorrect existing survey data. Although the position of M-18 has been corrected for the final modeling the preliminary modeling has not been revised.

## 4.2 CONCEPTUAL MODEL

The choice of a site for the preliminary model was based on the evaluation of a number of factors:

1. geologic definition - the area to be modeled should be well understood;

2. hydrogeologic properties - hydraulic conductivity and porosity should be well known for all hydrogeologic units at the site;

3. boundary conditions - the section should have identifiable and quantifiable boundary conditions;

4. historical data record - a longer and more comprehensive existing data set (e.g. hydraulic head and groundwater chemistry) will reduce uncertainty regarding mechanisms and their temporal dependence;

5. existing instrumentation - the area should be adequately instrumented.

After reviewing the available data it became readily apparent that the section defined along the plume centreline of seepage area A (i.e., referred to as C-C′ by Morin (1983)) was the best documented and instrumented site of all possible sites at the Nordic tailings area and best satisfied the criteria identified above. This does not mean that this site fully satisfied items 1 to 5 above, merely that it was the best of the available databases.

The exact region selected for the preliminary model corresponded to the area between piezometer M-10 and a point approximately 30 m north of M-1. The selection of the southern boundary coincident with M-10 was done in an effort to reduce some of the uncertainty with regards to the downgradient boundary condition. While it was recognized that using M-10 water levels as a boundary condition precludes its use as a comparison (or calibration) point it is felt that by eliminating the uncertainty associated with this edge the overall uncertainty will be reduced drastically. This fact, in conjunction with the relative abundance of other head monitoring points justifies its use. The choice of piezometer M-10 as the edge of the modeled system was also made based on the anticipated rate of plume movement.

A number of additional factors were considered in selecting the upstream model edge. These include the likely location and size of the source. In addition, the upstream boundary is approximately coincident with piezometer T8-B (for a similar rationale as to the choice of M-10). In addition Morin (1983) suggested the source was in the vicinity of T8-B.

### 4.2.1 Groundwater Flow System

The original conceptual model used as the basis for preliminary flow modeling is shown in Figure 4.1. This conceptual model was based on the available (pre 1985) data. Although subsequent data collected in the field and discussions with panel members resulted in revisions to the conceptual model, the original preliminary conceptual model is presented here for the sake of completeness.

The major points of the preliminary conceptual model included:

1. Vertical flow in the tailings is directed downwards;

2. Flow in the sand aquifer underlying the tailings is predominately horizontal;

3. The tailings are generally underlain by a low permeability peat layer. The absence of the peat layer in one or more locations has allowed tailings porewater to enter the sand aquifer.

4. Although seasonal effects may cause fluctuations in overall piezometric levels, hydraulic gradients do not change appreciably.

5. The bedrock and glacial till which forms the lowermost horizontal boundary can be assumed to be impermeable.

Based on this conceptualization of the hydrogeologic system the approach adopted to model the contaminant plume was to model only the saturated sand aquifer. For areas outside the tailings the water table is typically below or coincident with the peat layer. Hence in this region flow through the peat will be vertical and the effect of the peat layer can easily be incorporated by altering the surface recharge flux. In the tailings area groundwater flow is also vertically downward. Hence a similar approach can be used in this region. By adopting this approach, the uncertainty associated with flow/transport through

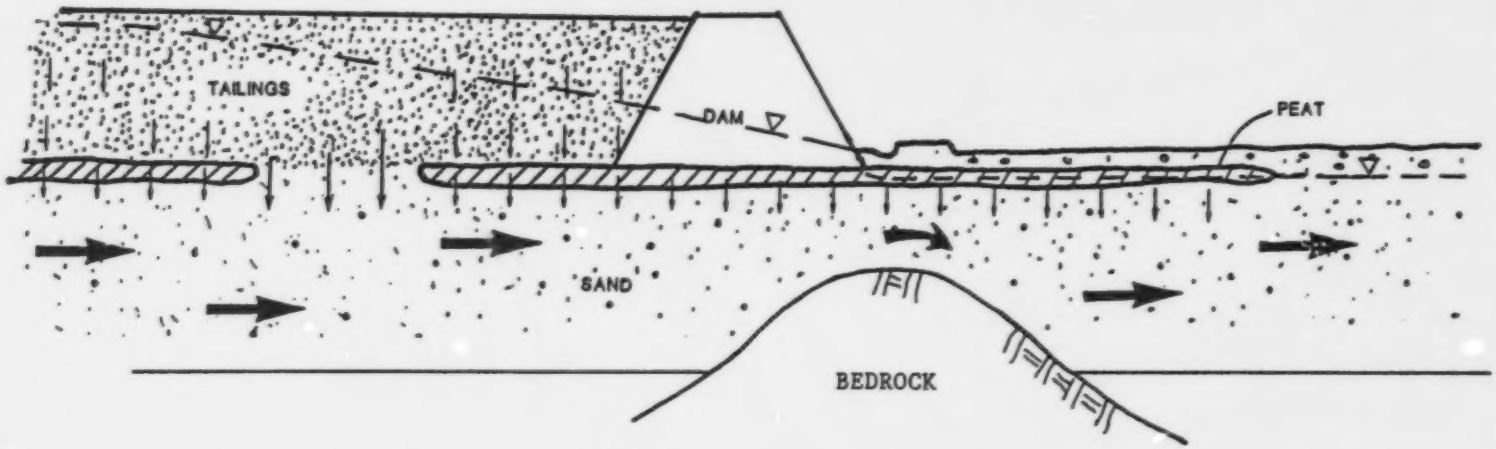


| INTERA Technologies | Preliminary Conceptual Model of the Hydrogeologic Regime at the Nordic Main Tailings Area | Figure 4.1 |
|---|---|---|

the tailings themselves will be eliminated and replaced by source terms and recharge fluxes along the top of the system. This decoupling facilitates analyses of the plume migration in the area of interest (e.g., sand aquifer) and eliminates the need to model the peat, fill or tailings areas explicitly.

Hydraulic boundary conditions for the flow system consisted of a hydraulic head of 340.72 m at M-10 and 342.29 m at T8-B. These values are mean values of measured heads. No vertical variation of the values was used. This is also consistent with available observed data. A no flow boundary was assigned to the bottom of the system corresponding to the sand-till bedrock interface. Although there is some evidence to suggest that vertical gradients exist across this interface, these gradients are small, and exhibit directional fluctuations which do not appear to correlate to observed concentration profiles.

The amount of flux entering the surface of the system was difficult to estimate. The presence of a low permeability layer located at the top of the modeled system will restrict the rate at which recharge enters the sand aquifer. Based on permeability estimates for this layer and typical gradients across it this flux can be estimated to be approximately 0.18 m/yr. An alternate approach to estimating this quantity based on the total groundwater flow through the aquifer at the southeastern and southern boundaries gave 0.3 m/yr. Infiltration fluxes of 0.2 m/yr were used in the flow system simulations in this study.

Initially hydraulic conductivity estimates for the model were selected based on Morin's (1983) representative values of $1 \times 10^{-4}$ m/s and $5 \times 10^{-5}$ m/s for the upper and lower sands, respectively. The values eventually used are based on calibration to head data. These results are discussed in detail in Section 6.2.2.1.

### 4.2.2 Source Term

Both the areal extent and the rate of contaminant flux entering into the aquifer are subject to high degrees of uncertainty. In the case of the rate of contaminant flux, the uncertainty arises from a number of factors including:

- the complex nature of the processes governing pyrite oxidation;
- the seasonal variation in parameters (such as water table elevation, temperature) that influence pyrite oxidation;
- the spatial variation in parameters (such as $Fe_2O_3$, tailings size, water table elevation, etc.) that influence pyrite oxidation.

Figure 4.2 presents a typical plot of acid generation versus time for three depths (0.2, 1.0 and 2.2 m) within the tailings. It can be seen that acid flux rates for deeper layers generally peak later and higher. This observation is due to a number of factors including availability of oxygen, presence of buffering material and vertical permeability.

Based on Figure 4.2 it is apparent that in order for low pH water to enter the sand aquifer the entire thickness of tailings (at least locally) must be oxidized. The original tailings contained between 3 and 8% pyrite and up to 0.056% carbonate. Assuming a 10 m thickness of tailings, the cumulative $H_3O^+$ generated through total oxidation would be 9,000 - 25,000 moles/$m^2$. Based on field investigations (Dubrovsky, 1986; Morin, 1983) it is evident that this condition exists at relatively few locations. Based on both the lack of such sites and the estimated streamtube diameter and mass balance calculations, Morin (1983) estimated that the areal extent of the source could range from 9 $m^2$ to 100 $m^2$ and was likely located in the vicinity of T8-B.

### 4.2.3 Transport Properties

The principal transport properties required for the FEMWASTE simulations include retardation and dispersivity coefficients. Other transport parameters, such as molecular diffusion and decay coefficient will have a negligible impact on the overall transport simulation and are generally well known.

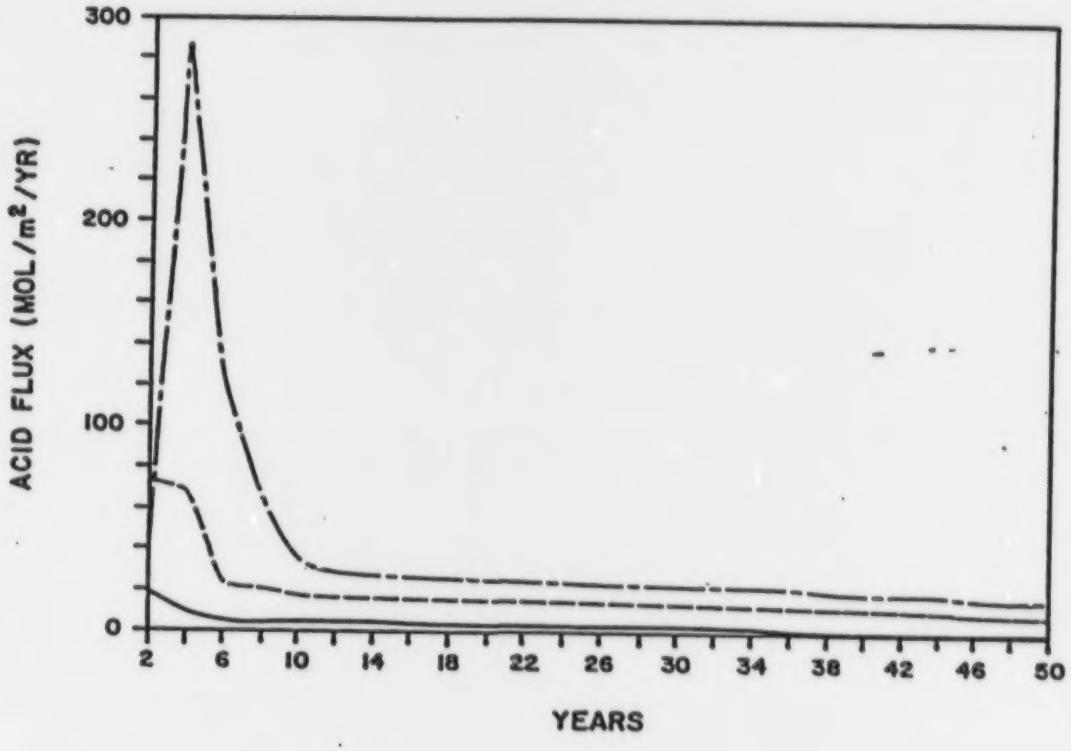


LEGEND:

——— 0.2m DEPTH
– – – – 1.0m DEPTH
——— 2.2m DEPTH

| | | |
|---|---|---|
| Drawn by | Date | Acid flux as a function of Depth in the Tailings (Senes, 1986) |
| Checked by | Date | |
| Revisions | Date | |
| | | |
| INTERA Technologies | | Figure 4.2 |

Retardation coefficients in the current study may be estimated by two methods, 1) observations of groundwater and plume migration and 2) chemical equilibrium transport models. The first method is based on direct observation. That is, the rate of plume migration is compared to the actual groundwater velocity. Some of the difficulties associated with this approach include:

1. Obtaining an accurate estimate of groundwater velocity - this may vary both temporally (e.g., seasonally) as well as spatially along the plume (e.g., diverging streamlines, varying K, );

2. Obtaining an accurate estimate of plume migration - this is especially true for slow moving plumes and laboratory analyses having poor resolution.

Cherry et al. (1984) and Morin (1983, 1985) indicate that the inner core of the plume most likely travelled at a rate of 1 to 2 m/yr. Using this value together with the results of a borehole dilution test (which gave a value of interstitial velocity of 440 m/yr) they suggested that the observed retardation factor of the inner core was 0.003. Blair et al. (1980) and Morin (1983) indicate that the groundwater velocity in the vicinity of the dam could range anywhere from 250 to 1000 m/yr. Based on this range of values "R" could range from 0.001 to 0.008.

Morin (1985) also recognized the uncertainty introduced into observed plume movements due to variability in laboratory analyses. He states "yearly comparisons of Ra-226 are complicated (partially) by ... changes in laboratories performing analyses. As a result, migration rates of the Ra-226 plume are difficult to define..". Consequently, Morin (1983, 1985) only reported retardation coefficients for the pH regions of the plume.

Morin (1983) and Cherry et al. (1984) used the second approach to estimate retardation factors. They used a chemical equilibrium transport model (ADNEUT) to predict aqueous and solid phase concentrations at various points along a streamtube. Based on best estimates of input values Morin (1983) calculated the following retardation factors for the geochemical sub-regions:

| Sub-region | pH | R (upgradient edge) |
|---|---|---|
| Inner core | 4.40 | |
| Al $(OH_3)$ | 5.02 | 0.0020 |
| Siderite | 5.27 | 0.0046 |
| Calcite | 5.73 | 0.14 |

Major deficiencies associated with this model exist primarily in the calcite sub-region, and include a significant difference between observed (0.02 - 0.06) and calculated (0.14) retardation factors.

Dispersivity ($\alpha$), the other transport parameter of concern, is also difficult to estimate since it is site specific and scale dependent. A number of researchers have proposed various relationships to describe dispersivity and its scale-dependence. Pickens and Grisak (1981) for example suggested, for unconsolidated porous media, a model of the form:

$$\alpha = a\Delta X \qquad (4.1)$$

where: $a$ = constant and $\Delta X$ = travel distance.

Given the high degree of uncertainty associated with this parameter we feel that a model such as that presented above is an adequate first approximation for dispersivity. The retarded interstitial velocity of the inner core is estimated at one to two metres per year, and the time of interest varies from 1960-1984 (25 years) the total path length could be on the order of 50 m. The constant "a" in Equation 4.1 has been found to range from 0.002 to greater than 2 (Pickens and Grisak, 1981) with most values between .05 and 0.2. Using a representative value of 0.1 yields a starting value of dispersivity of 5 m.

## 4.3 NUMERICAL MODEL

### 4.3.1 Finite Element Mesh

Based on our conceptual model a finite element mesh was discretized along the vertical section between piezometers T8-B and M-10. The mesh is presented in Figure 4.3. A total of 54 elements ranging in size from 1.15 to 2 m were used to discretize the horizontal direction for a total length of 103.0 m. The vertical direction was discretized using 10 elements varying in size from 0.2 to 4 m. The smallest elements were used to discretize the lower sand unit in the vicinity of the bedrock high. The remainder of the mesh consists of fairly uniform griding using eight 1 m thick elements underlain by a 2 m and 4 m thick elements. The top of the mesh dips to the south and represents the overall average slope of the water table.

The mesh was discretized using a number of criteria:

1. maximum adjacent element sizes (approximately 2:1);
2. aspect ratios (less than 3:1);
3. Peclet number ($2\alpha > \Delta X$);
4. hardware constraints.

Hardware constraints did not directly limit the physical size of the mesh. It must be mentioned however, that one consideration in the sizing was the anticipated execution time for a representative transport run. A typical simulation requiring on the order of 100 time steps should require execution times that are less than several hours. A turnaround time that is significantly greater than this amount (e.g., on the order of a day) would severely limit the ability to use the model effectively.

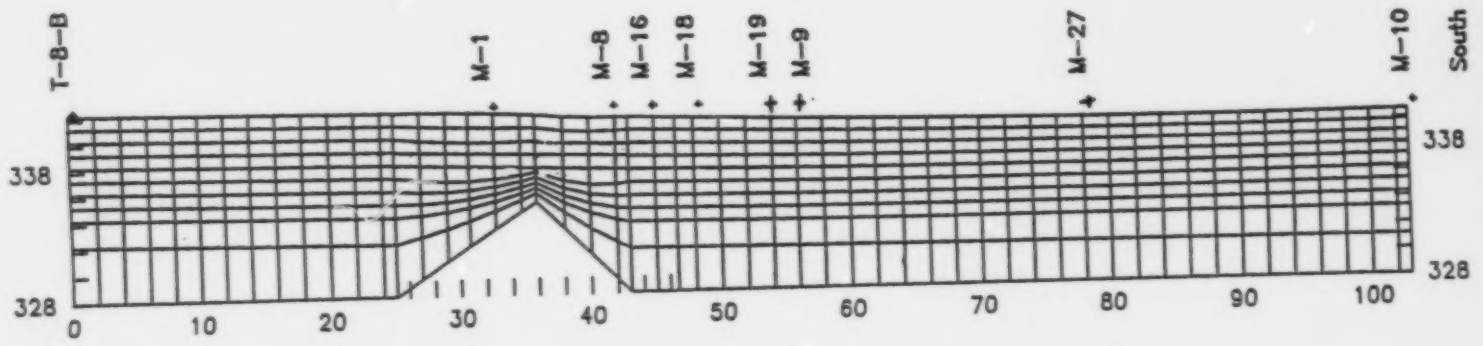


| INTERA Technologies | Finite Element Mesh used in Preliminary Model | Figure 4.3 |
|---|---|---|

### 4.3.2 Simulation Runs

#### 4.3.2.1 Flow

As part of the preliminary modelling task three separate steady state flow systems were simulated. These included:

Simulation 1. Base case simulation - using best estimates of hydraulic conductivity, infiltration and boundary conditions;

Simulation 2. Calibrated simulation - calibrated to observed heads by adjusting hydraulic conductivities;

Simulation 3. Quasi 3-D simulation - consisting of a modified base case run in which the porosity of the elements along the section is modified to account for a widening stream tube.

The rationale for performing these simulations was to attempt to resolve the cause of the observed gradient changes along the section in the area of the bedrock high. Two mechanisms - a varying hydraulic conductivity or a change in cross-sectional area could cause such gradient changes. Simulation 2 attributes the entire gradient change to variations in hydraulic conductivity. Simulation 3 (Quasi-3D) attributes the gradient change to a change in cross-sectional area of the streamtube. Unfortunately since FEMWATER is only a two-dimensional model the thickness of the stream tube cannot be varied directly. This behaviour can be mimicked, to some extent, by allowing the porosity to vary along the section. A variable porosity will not improve fits between the simulated and observed gradients. However, the variable porosity will allow velocities and dilution volumes to be modified along the section. Consequently, the use of a variable porosity will enable the effect of a widening streamtube to be incorporated into the transport simulations.

Figure 4.4 presents the results of the first two simulations in the form of piezometric contours along the section. Also presented are observed piezometric heads. The hydraulic conductivity distribution employed for both of these sections is presented in Figure 4.5. No contours have been presented for Simulation Run 3, since these are identical to the base case simulation.

Simulation 1 was performed to evaluate the adequacy of the simple two layer model of the site (i.e. upper and lower homogeneous sands with different hydraulic conductivities based on the interpretation of Morin (1983)) to reproduce the observed head distribution. As can be seen from Figure 4.4 the calculated piezometric contours do a poor job at replicating the measured heads.

The purpose of model Simulation 2 was to examine the magnitude of the hydraulic conductivity contrast necessary to achieve a reasonable match with the observed data. This was not meant to imply that this calibrated distribution represented the actual field values. The required hydraulic conductivity contrast ($2.5 \times 10^{-7}$ m/s to $1 \times 10^{-3}$ m/s), while physically possible for the identified granular deposits at the site, i.e. coarse sand/gravel to silty sand, would appear to be unlikely based on the historical range of hydraulic conductivity reported for the site (Section 3.5.1) as well as the site stratigraphy. Consequently the distribution of hydraulic conductivity for model Simulation 2 is not considered to be realistic portrayal of actual site conditions. More realistic hydraulic conductivity distributions were utilized in the final modeling (Section 6).

#### 4.3.2.2 Transport

The purpose of the preliminary transport simulations was to identify parameters to which the plume migration demonstrated a high sensitivity. They were not intended to accurately portray historical plume movement. As a result many of these simulations used relatively simple input parameters to simplify comparisons between alternate simulations. The simulations were compared to the pH plume because of the greater reliability of the pH data versus that of $Cl^-$ or $^{226}Ra$.

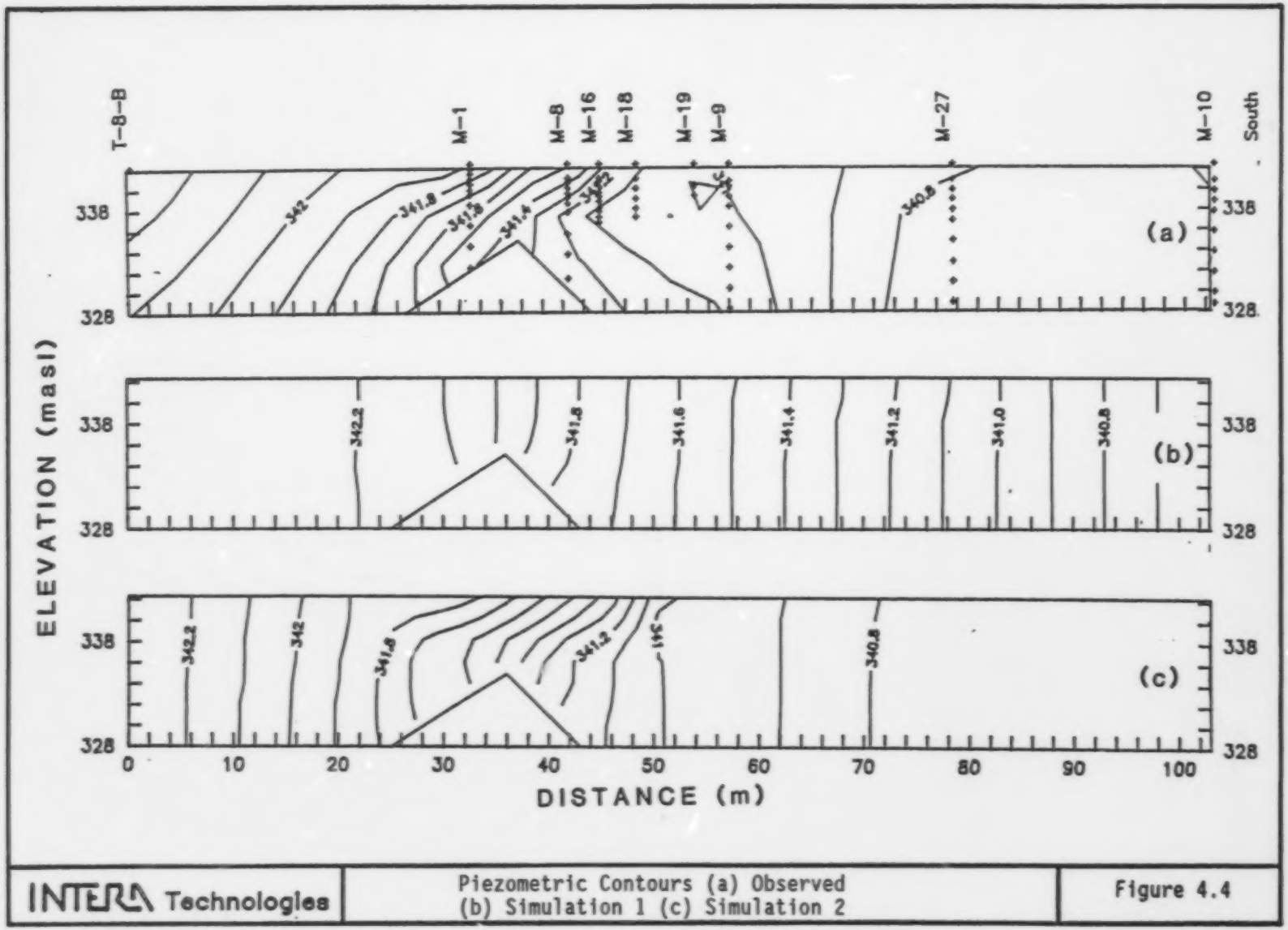


| INTERA Technologies | Piezometric Contours (a) Observed (b) Simulation 1 (c) Simulation 2 | Figure 4.4 |
|---|---|---|

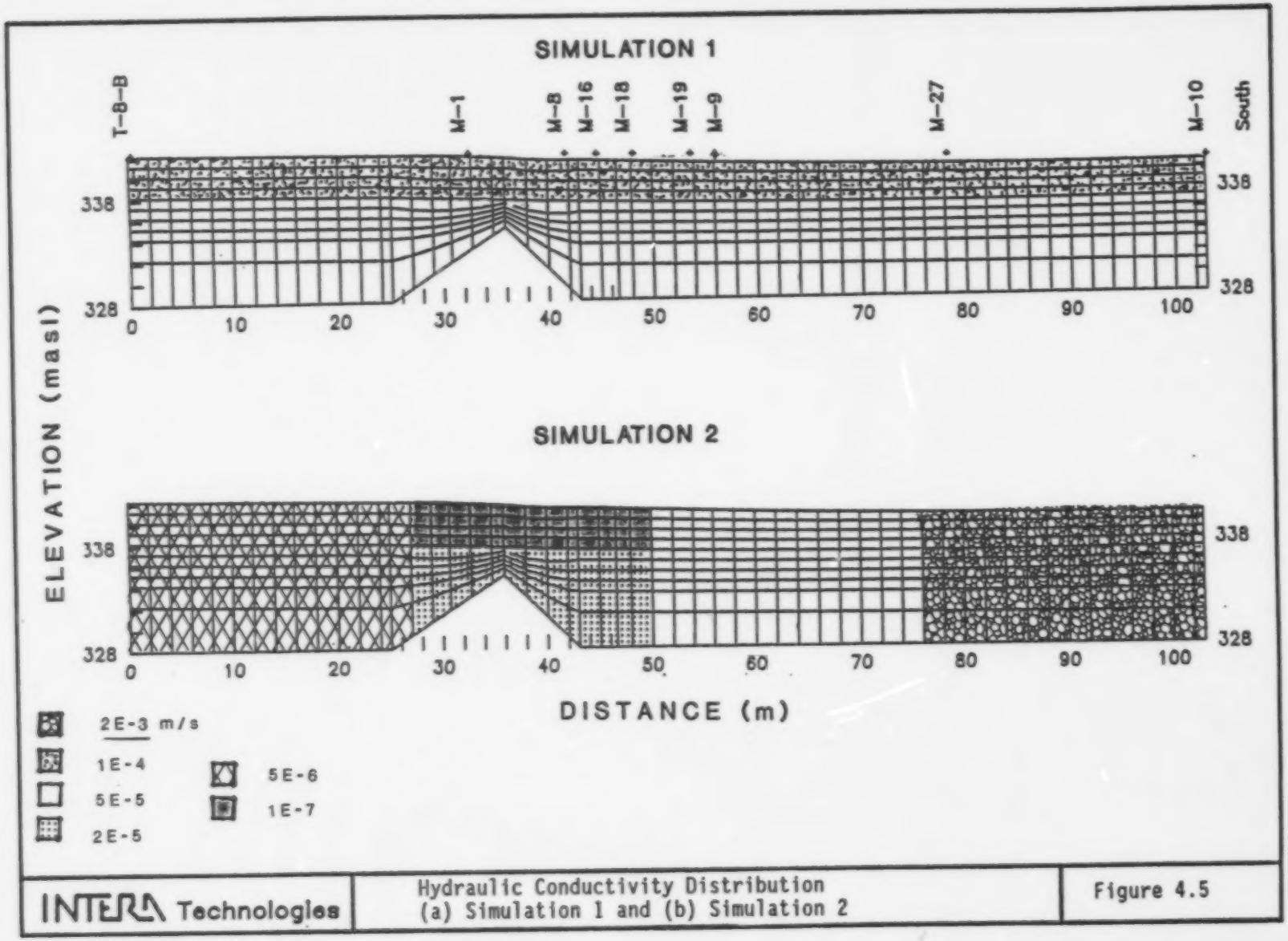


| INTERA Technologies | Hydraulic Conductivity Distribution (a) Simulation 1 and (b) Simulation 2 | Figure 4.5 |
|---|---|---|

Transport simulations performed as part of the preliminary modeling task included:

Simulations 1, 2 and 3: A constant source term (of concentration $C_o = 1$) applied over a length of 2 m (based on Morin, 1983) located adjacent to T-8-B using flow Simulations 1, 2 and 3 and dispersivity, $\alpha$ of 5 m.

Simulation 4: Transport simulation 1 with temporally varying source term (triangular over input period).

Simulation 5: Transport simulation 1 with a smaller dispersivity of 2.5 m.

Simulation 6: Transport simulation 1 with a larger source length or area (20 m).

Transport Simulations 1, 2 and 3 were performed using the steady state flow fields described in Section 4.3.2.1. Concentration contours after 25 years of simulation (1960 to 1984) are presented for each of these runs in Figure 4.6. The major observation made from these Figures was that none of these simulations could accurately reproduce plume concentrations. Several factors were identified which could account for the discrepancy:

1. Location of source may be too distant from piezometer M-1;
2. Area of source may be too small;
3. Uncertainty in source term concentration (i.e. source pH may be greater than 2);
4. Dispersivity may be too small;
5. Retardation may be too high;
6. Poorly calibrated flow field.

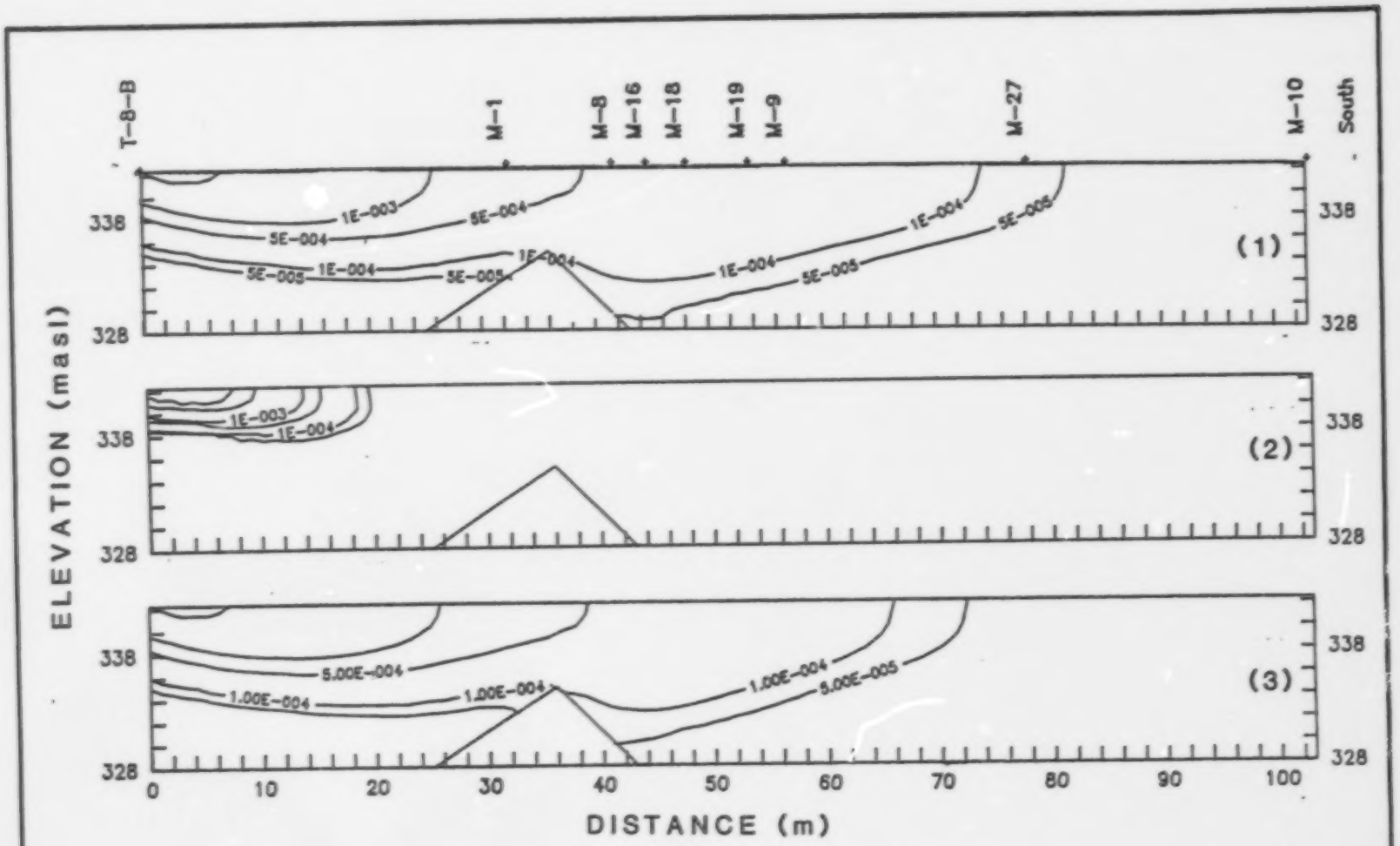


(1) Flow Simulation 1 (2) Flow Simulation 2 (3) Flow Simulation 3

| | | |
|---|---|---|
| INTERA Technologies | Concentration Profiles at 25 Years Using: | Figure 4.6 |

All of these factors could, either by themselves or acting in conjunction, cause the apparent underprediction of the observed concentrations.

Figure 4.7 presents the results for Simulations 4 and 5 in the form of concentration contours at 25 years. Both of these simulations use the same flow system (corresponding to flow Simulation 1). Simulation 4 was identical to Simulation 1 with the exception of a temporal variation incorporated in the source term varying from $C_o = 2$ at $t = 0$ to $C_o = 0$ at $t = 25$ years. This particular shape, although selected somewhat arbitrarily, does represent the general perceived trend of a decreasing source concentration with time. Furthermore, the magnitude of the initial concentration was selected so that the same mass of material, as introduced during Simulation 1, would be added to the flow system over the 25 year simulation period. The results of these simulations would suggest that only a small sensitivity of the concentration profile exists to the shape of the input function.

Simulation 5 was identical to Simulation 1 with the exception of reducing the dispersivity from 5 to 2.5 m. The reduction of the dispersivity caused the leading plume concentrations to recede and peak concentrations to rise.

Figure 4.8 presents the results obtained using a significantly larger source length or area (20 m versus 2 m). These results, in the form of concentration contours at 25 years, correspond to Simulation 6. Concentrations were found to change drastically, by up to two orders of magnitude over a significant portion of the plume.

The transport simulations described to this point have examined a limited number of potentially important model input parameters. Of those examined it is apparent that those of primary importance are definition of the physical flow system parameters and areal extent and location of source term. Parameters of secondary importance are dispersivity and the temporal variation of the source term.

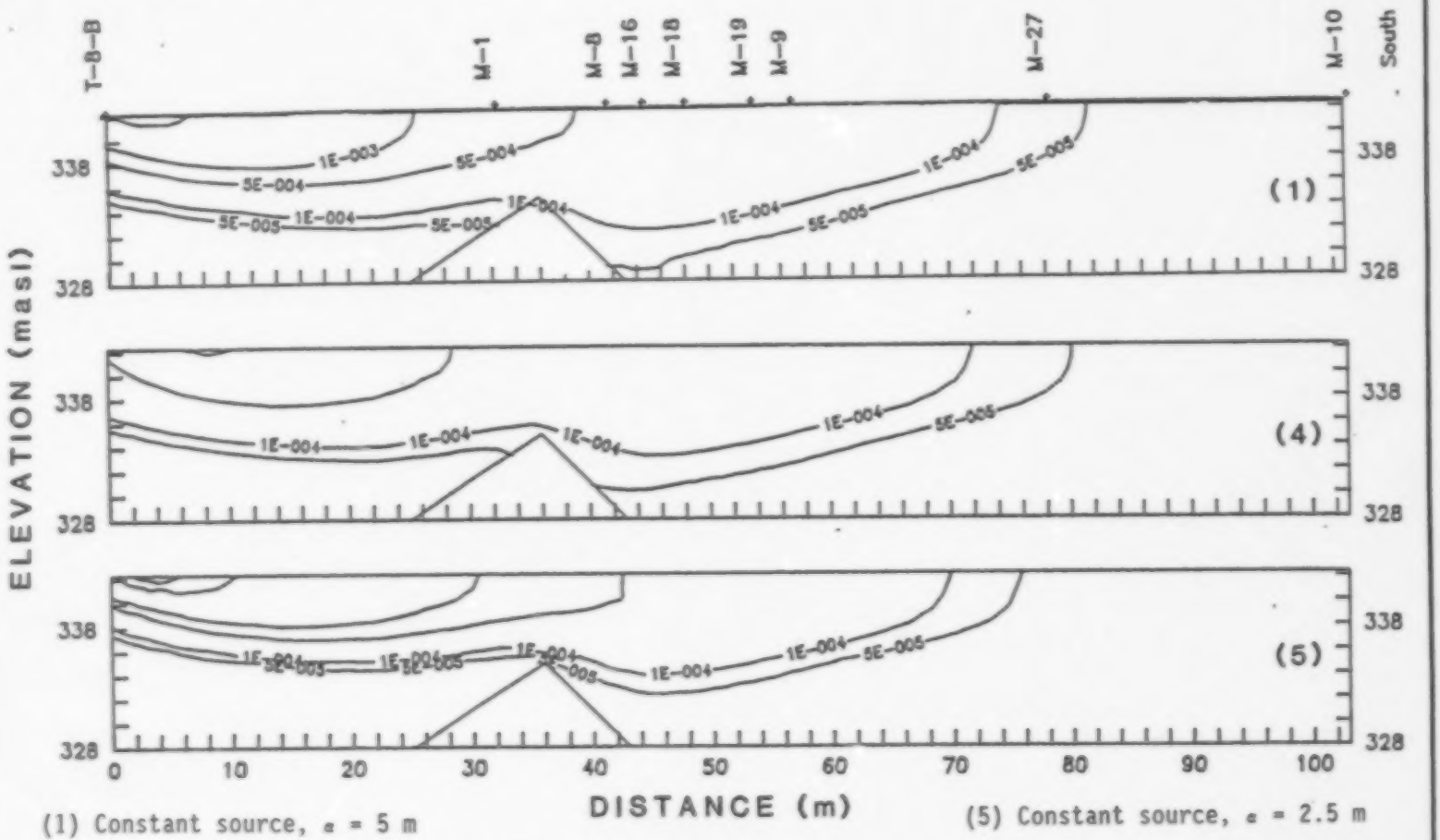


(1) Constant source, $\alpha$ = 5 m

(4) Triangular source distribution, $\alpha$ = 5 m

(5) Constant source, $\alpha$ = 2.5 m

| INTERA Technologies | Concentration Profiles at 25 Years Using Flow System for Simulation 1: | Figure 4.7 |
|---|---|---|

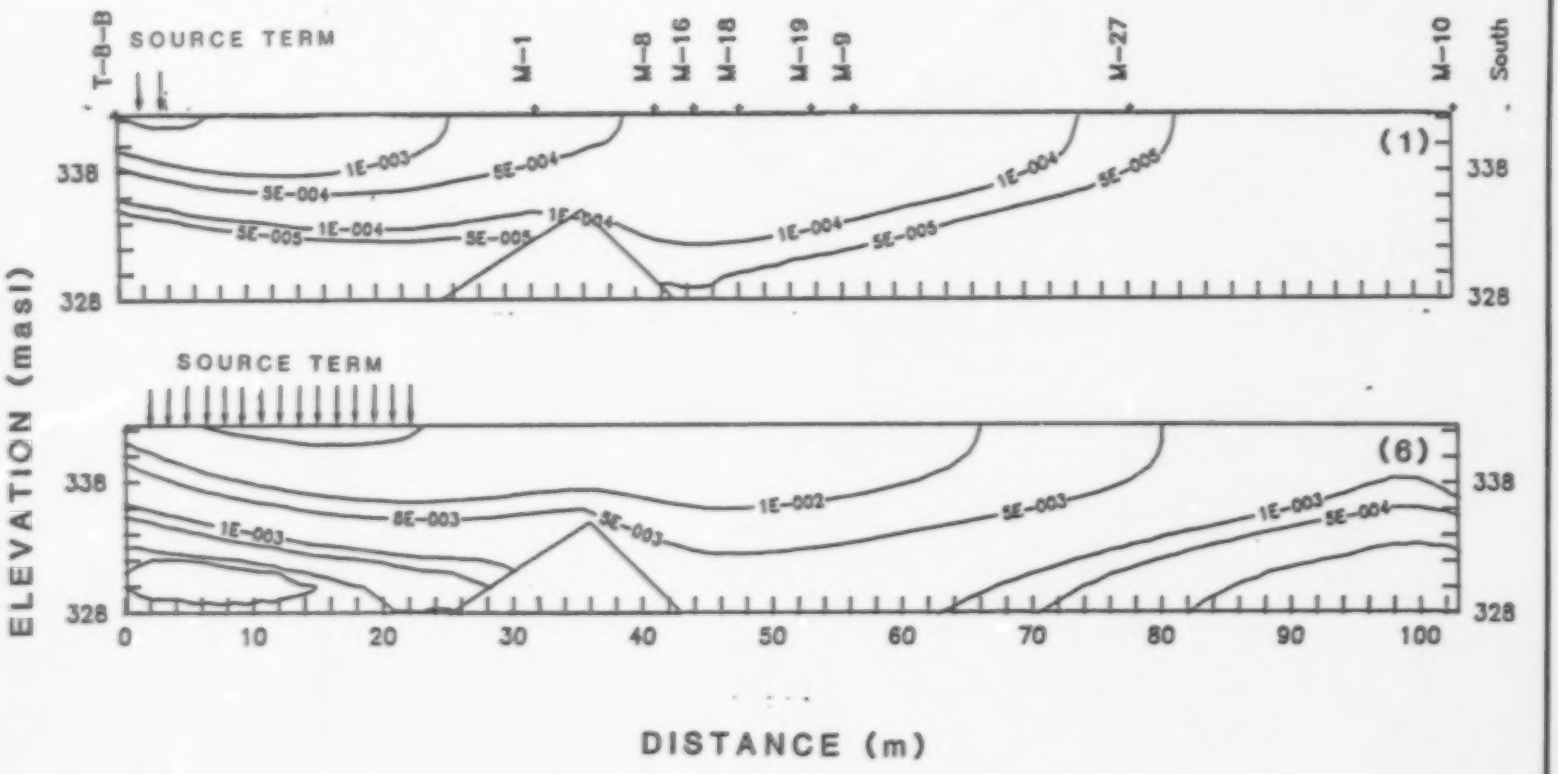


(1) Areal extent of source 2 m

(6) Areal extent of source 20 m

| | | |
|---|---|---|
| INTERA Technologies | Concentration Profiles at 25 Years Using Flow System for Simulation 1: | Figure 4.8 |

## 4.4 CONCLUSIONS AND RECOMMENDATIONS BASED ON PRELIMINARY MODELING

Based on both our review of the available data and the results of the preliminary modeling simulations a number of conclusions were reached:

1) A more thorough testing program should be developed for FEMWATER/FEMWASTE;

2) Physical data describing the hydrogeologic system in the vicinity of plume must be refined;

3) The location and areal extent of the source term should be refined;

4) The analytical data on the pH plume is considered reliable and modeling of this plume is not likely to be problematic;

5) The data on the chloride plume is considered unreliable and modeling of this conservative ion will be problematic. Modeling of conservative species behaviour will require identification of an alternate conservative species or performance of a conservative ion tracer test;

6) The data on the $^{226}Ra$ may be modeled reliably provided sufficient explanation for the erratic plume concentration data and movement is found;

7) The Nordic mine tailings site is acceptable for validation of the FEMWATER/FEMWASTE codes provided the information gaps identified in items 2-6 above were addressed.

Based on these conclusions, INTERA recommended:

1) the implementation of a non-reactive tracer test;

2) the collection of a complete set of water levels;

3) the installation of monitoring points both adjacent to the plume centreline and between T8-B and M-1; and

4) performance of additional in situ hydraulic conductivity measurements.

Based on reviews and comments by several panel members and the data of Morin et al. (1988a) it was concluded that the source of the acidic water to the sand aquifer was likely below the tailings dam and therefore was much closer to M-1 than originally assumed as part of the preliminary modeling. However, because of the difficulty in drilling through the rockfill of the tailings dam and the small likelihood of actually defining by the source location by drilling, no additional work was proposed to define the source location and area.

# 5. RESULTS OF JUNE 1989 SITE INVESTIGATIONS

## 5.1 SCOPE

The detailed review of the existing literature and the results of the preliminary model simulations identified several factors that were both highly uncertain and significant in terms of their impact on model results. These factors included:

1. Definition of physical hydrogeologic system;
2. Location/areal extent of source;
3. Temporal variation of source term.

In addition to the concerns raised by these factors, additional concerns were raised regarding the reliability of some of the data collected previously, including the $Cl^-$ and Ra226 data. Specifically the reliability of the $Cl^-$ data was judged to be so poor (given the source strength concentration and velocity in the aquifer) that it was decided to avoid using this data as part of the modeling effort.

The field investigations performed in June 1989 were undertaken for the purpose of addressing the INTERA recommendations identified in Section 4.4. Activities undertaken as part of this site investigation were mostly directed at improving the definition of the physical hydrogeologic system, since little could be done to reduce uncertainty associated with either the location/areal extent or temporal variation of the source. Specifically activities conducted as part of the site investigations included:

1. Piezometer rejuvenation and drive point installation;
2. Water level measurements;
3. Hydraulic conductivity testing;
4. Tracer testing.

Each of these activities are described in detail in the following sections.

## 5.2 PIEZOMETER REJUVENATION

A visit to the Nordic Main tailings area was made on June 22-27, 1989 by INTERA staff. The first activity undertaken was labelling and restoration of damaged piezometers. It was found that some of the piezometers installed earlier had been protected by a steel surface casing. The polyethylene tubing of these piezometers were generally in reasonable shape requiring only cleaning and relabeling. Tubes were identified by plumbing the vertical depth and matching to the depths reported by Morin (1983). The multi-level piezometers that were installed in the second field series (M-20 to M-35) did not have the benefit of protective surface casings and consequently most of these piezometers had tubes that were broken or had become extremely brittle. These tubes were also cleaned, identified, labelled and, where required, tubing was replaced at surface. Protective surface casings, consisting of a 7.6 cm diameter ABS pipe and cap, were subsequently placed over these multi-level piezometers.

As part of this process it was discovered that a number of tubes had become either blocked or broken below surface. In addition two of the piezometers (M-16, M-17) had been constructed using small diameter (less than 5 mm) tubing. Unfortunately most standard water level tapes are at least 5 mm diameter. This fact precluded the measurement of water levels in these piezometers.

Two additional mini-piezometers (DP-1 and DP-2) were installed adjacent to the centreline. These piezometers consisted of steel drive points, approximately 2.3 m in length and having an inside diameter of 32 mm. These drivepoints were installed solely for the purpose of providing additional water level coverage (i.e., not used for collection of groundwater samples). Figure 5.1 shows the location of all monitoring instrumentation in the vicinity of seepage area A as of June, 1989.

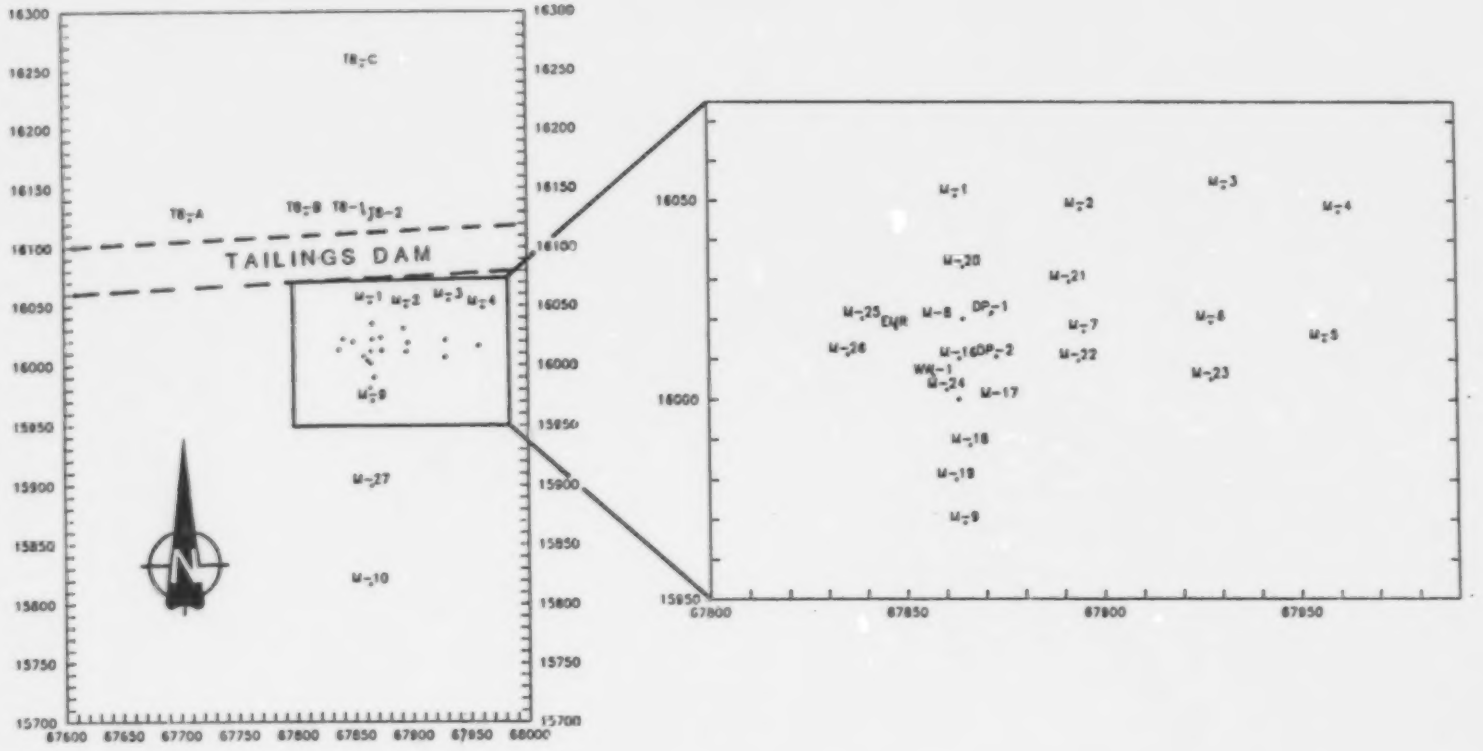


| INTERA Technologies | Location of Monitoring Instrumentation (June, 1989) | Figure 5.1 |
|---|---|---|

## 5.3 WATER LEVEL MEASUREMENTS

As part of the June 1989 site visit a complete set of water level measurements was made in all accessible piezometers at the site and surrounding area. For a variety of reasons, water levels could not be measured in a number of the piezometer tubes. These reasons included broken or blocked tubing below ground and small diameter tubing used in the construction of M-16 and M-17.

A full set of water level elevations using these measured water levels has been calculated and is presented in its entirety in Appendix A. These data have been used to construct a number of piezometric surfaces for various elevations as shown in Figures 5.2 and 5.3. These figures present the water table, and the piezometric surfaces at depths corresponding to 5 m and 10 m. When examining these figures, it should be noted that only those monitoring points used in the construction of the surface have been indicated. Contours depicted in these figures were generated using a commercially available contouring package (SURFER). It can be seen that all three piezometric surfaces exhibit some irregularities. These irregularities may be caused by errors in water level measurement. However, in order to avoid biasing the data we have not attempted to filter the data and have included all water level measurements for these figures. Because the contouring package extrapolates to the edge of the figures, the water level contours are considered most accurate in the immediate vicinity of the piezometers.

In spite of the presence of irregularities several important observations can be made regarding the piezometric surfaces shown in Figures 5.2 and 5.3. As one might expect flow is generally directed southwards under the dam. Streamlines drawn perpendicular to the piezometric contours indicate that groundwater flows around the areas of bedrock outcrop, converging adjacent to the outcrop and diverging once the flow has moved passed this area. It would appear, based on these piezometric surfaces, that the assumption that the centre-line piezometers defined by Morin (1983) correspond to a streamline is, in the

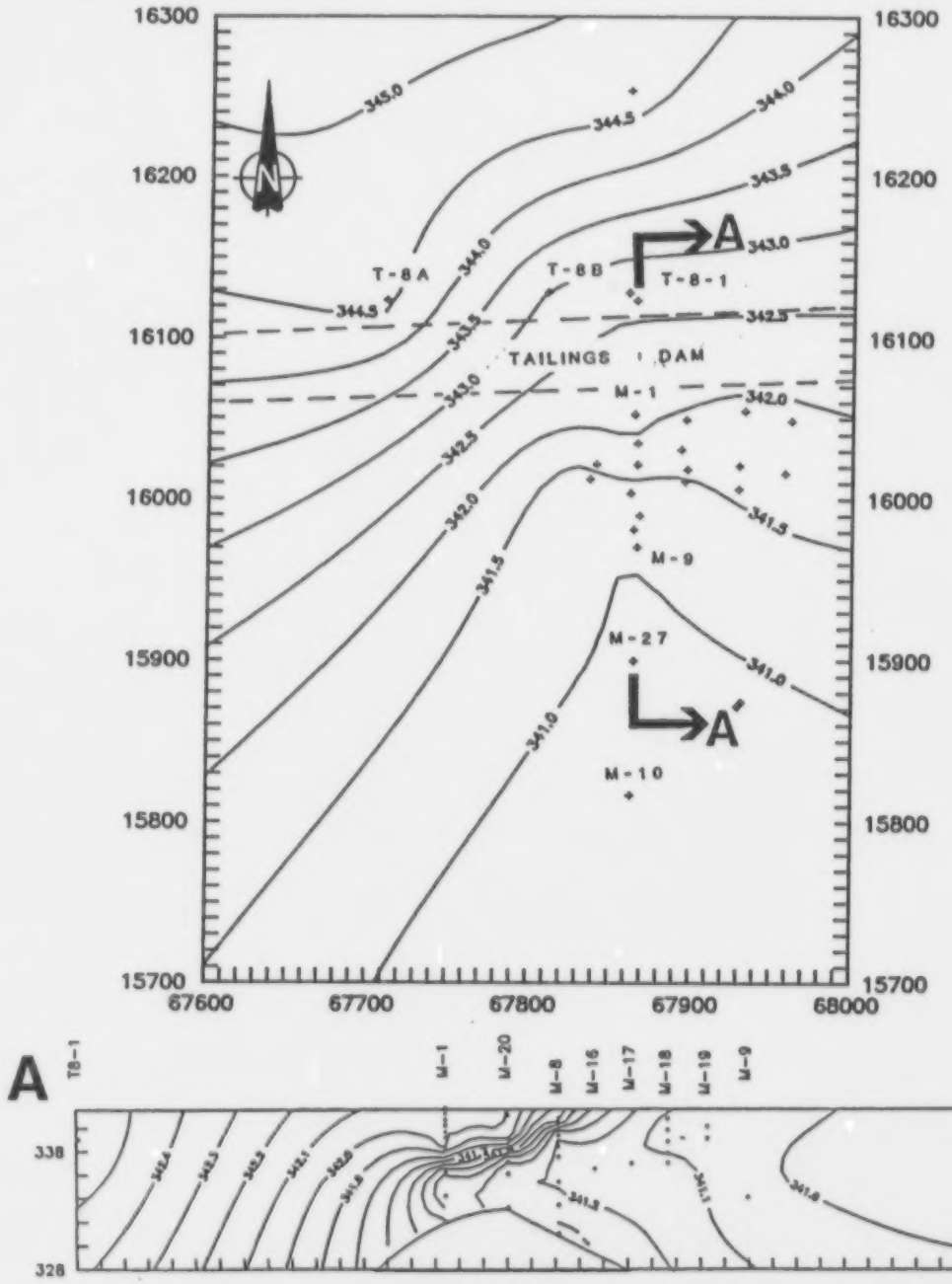


| | |
|---|---|
| Drawn by | Date |
| Checked by | Date |
| Revisions | Date |
| | |

Water Table and Piezometric Cross-Section for June 1989

INTERA Technologies

Figure 5.2

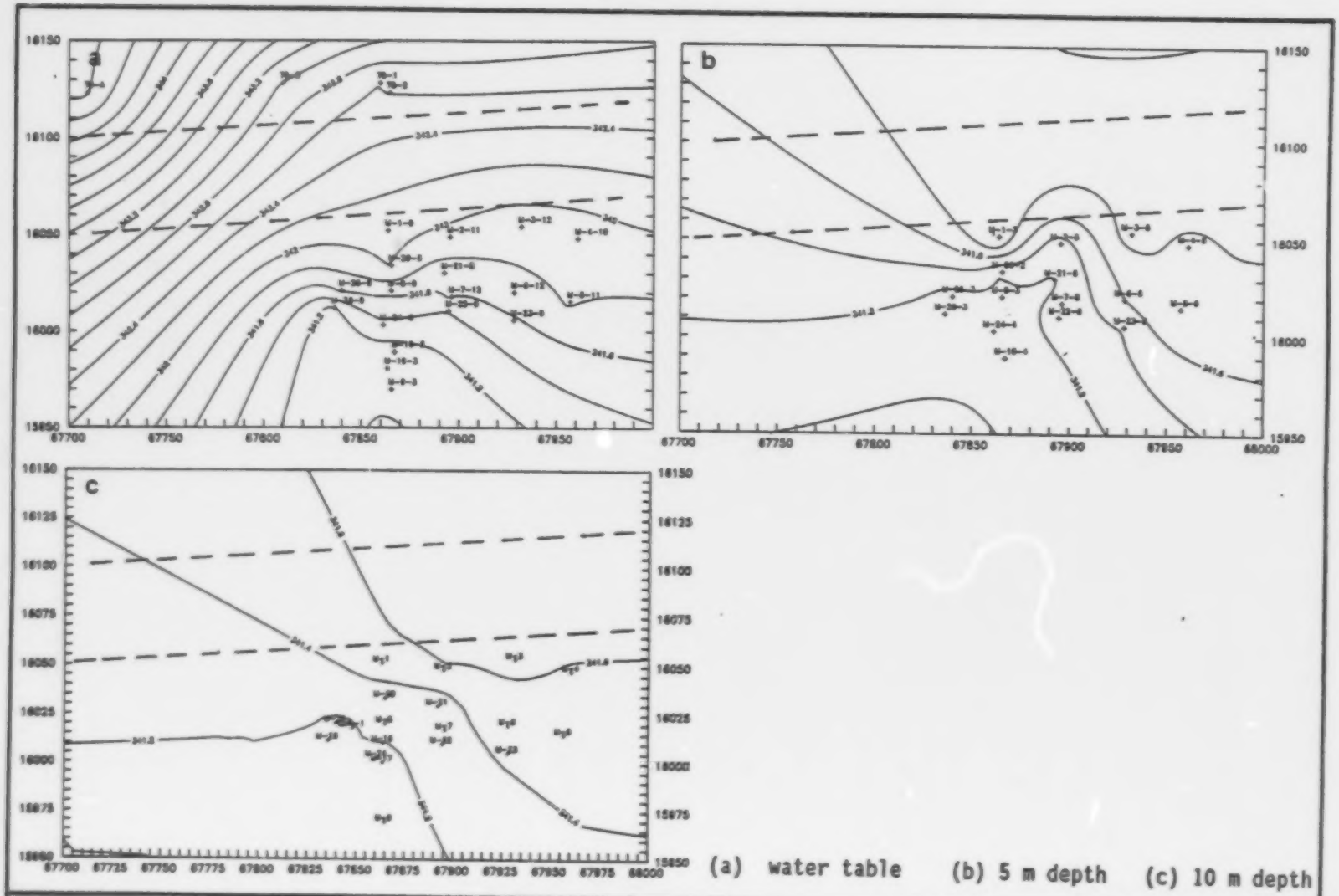


(a) water table (b) 5 m depth (c) 10 m depth

| INTERA Technologies | Piezometric Surfaces (masl) for June, 1989 | Figure 5.3 |
|---|---|---|

vicinity of M-1 and M-10, a reasonable one. The three piezometric surfaces indicate that this general trend is present throughout the overburden thickness. In addition, these three surfaces can be used to identify and quantify areas of vertical flow. For example it can be seen that over most of the region of interest the flow contains a downward vertical component. This velocity component is most significant in the vicinity of M-1 and M-20 (i.e., the northern portion of the centreline section) and becomes almost zero in the vicinity of M-9 and M-19.

A vertical cross-section through Morin's (1983) centreline piezometers (from T-8 and M-10) is also presented in Figure 5.2. This section is quite similar to that presented earlier, as Figure 3.9, which was based on Morin's (1983) data for May, 1980 and June, 1981. Both sections exhibit high head loss between M-1-2 and M-1-3, M-20-2 and M-20-4, and M-8-7 and M-8-8. The magnitude of this head loss is slightly higher for the June 26, 1989 data (up to 0.7 m) compared to that reported earlier (maximum of 0.4 m). In addition the heads corresponding to the June 1989 data are slightly higher (average of 0.2 m) than those of May 1980/June 1981. Generally however the two profiles are quite consistent, a fact which would indicate the absence of any gross measurement errors.

## 5.4 HYDRAULIC CONDUCTIVITY TESTS

One of the main objectives of the June 26, 1989 field trip was to perform in situ hydraulic conductivity tests. Because of the small diameter tubes that were used in the construction of the multi-level piezometers it was not practical to conduct hydraulic conductivity tests in these installations. Consequently, tests were conducted in the mini-piezometers installed as part of this site visit (described previously), in monitoring well WW-1 and in a series of nested piezometers (designated EMR) installed by Morrison Beatty for CANMET in 1980 (Morrison and Beatty, 1980). Both of these piezometers (WW-1 and EMR series) had been installed just west of the plume centreline (see Figure 5.1). Tests consisted of either slug tests or low volume pump tests. These tests were selected so as to minimize the perturbation on the centreline plume.

Slug tests were conducted on DP-2 and WW-1 and involved removing a finite volume of water from the piezometer and measuring the response in water levels. The method proposed by Hvorslev (1951) was used to determine a value of hydraulic conductivity for these tests. Piezometer WW-1 responded very quickly to the removal of the slug, and consequently only a bounding value (i.e., $>1 \times 10^{-4}$ m/s) could be determined from this test. Piezometer DP-2 responded much more slowly than WW-1 and yielded a hydraulic conductivity of approximately $5.0 \times 10^{-6}$ m/s. Piezometer DP-1 was found to respond extremely slowly to removal of a slug of water. It is uncertain whether the relatively slow responses of DP-1 and DP-2 were attributable to the installation of the screen in a low-permeability (i.e., silt or peat) layer or caused by clogging of the screen during installation. The rate of water level recovery in piezometer DP-1 suggests a hydraulic conductivity of about $1 \times 10^{-8}$ m/s for the soil surrounding the screen of DP-1.

A number of the nested EMR series piezometers (EMR-1 and EMR-C) showed a transient response to pumping. The piezometers that exhibited a measurable and steady state response were subjected to a low-volume (<1 L/minute) short duration (typically 10 minutes) pumping tests which were analyzed using the Theim (1906) equation. The results of these tests, together with the slug tests analyzed for DP-1, DP-2 and WW-1, are summarized in Table 5.1. These values demonstrate a much wider variance than the values of hydraulic conductivity reported for the site (i.e., $5 \times 10^{-5}$ - $1 \times 10^{-4}$ m/s) especially for the lower bound, which is significantly lower than that previously reported by Morin (1983) for the hydraulic conductivity of the upper sand aquifer. It is also interesting to note that DP-1 and DP-2 are located approximately 2.6 m east of M-8 and M-16 at depths that would intersect some of the high head loss zone exhibited on the piezometric cross-section shown in Figure 5.1.

Table 5.1 Summary of Hydraulic Conductivity Measurements

| Piezometer | Screened Interval Depth (m) | Test Method | Hydraulic Conductivity (m/s) |
|---|---|---|---|
| DP-1 | 1.3 - 2.0 | Slug | $1.0 \times 10^{-8}$ |
| DP-2 | 1.4 - 1.9 | Slug | $4.6 \times 10^{-6}$ |
| WW-1 | | Slug | $>1.0 \times 10^{-4}$ |
| EMR-A | 4.1 - 4.6 | Pump | $7.3 \times 10^{-5}$ |
| EMR-B | 2.6 - 3.0 | Pump | $6.1 \times 10^{-5}$ |
| EMR-D | 8.7 - 9.1 | Pump | $8.9 \times 10^{-5}$ |
| EMR-E | 7.1 - 7.6 | Pump | $1.4 \times 10^{-4}$ |

## 5.5 TRACER TESTS

Based on our review and assessment of the available physical hydrogeologic data and the limited usefulness of the $Cl^-$ data in helping to define the flow system, INTERA proposed that a tracer test be conducted in the vicinity of the centreline monitoring section (M-1 to M-10). After some discussion with AECB officials, approval to proceed with the tracer test was given.

The tracer selected for the experiment was Lissamine FF, an organic dye frequently used as a groundwater tracer, and reported to be stable down to a pH of 3.0 (Davis et al., 1985; Smart and Laidlaw, 1977). Subsequent laboratory testing with $H_2SO_4$ performed in this study confirmed the fluorescence stability of Lissamine FF to pH 3.0. The tracer test was designed based on a number of factors:

1. Our understanding of the hydrogeologic system (e.g., based largely on review of available literature);
2. Existing monitoring network;
3. Anticipated background concentrations;
4. Sensitivity of fluorometer used for tracer detection.

Based on these factors it was decided to inject 500 mL of 1000 mg/L Lissamine FF solution in monitoring point M-20-4. Based on reported groundwater velocities (500 m/yr reported by Morin, 1983) it was anticipated that breakthrough would be observed relatively quickly (2-3 days) at M-8, and that peak concentrations would be on the order of 500 ug/L. Background Lissamine concentrations (i.e., natural fluorescence) were assumed (and later verified in the field) to be on the order of 10 ug/L.

Tracer was injected on June 23, 1986 into monitoring point M-20-4 and flushed using 1 L of distilled water. Lissamine readings were conducted on samples collected from M-8-5 through M-8-9 starting approximately 5.5 hours after tracer injection. On June 24, the monitoring network was expanded to include

intervals M8-3 and M8-4. Monitoring by INTERA continued on average 3 times per day for approximately 5 days over which time no discernable tracer was detected in any of the monitored intervals in M-8. Additional monitoring was conducted by AECB personnel until August 14, 1989. This monitoring was performed at decreasing time intervals and included a wider circle of monitoring points (including WW-1, EMR-B, and DP-2). However, no tracer was detected in any of these monitored piezometers.

The lack of any discernable tracer in the monitoring points in M-8 may be explained by the following mechanisms:

1. Migration velocity of the tracer is much less than anticipated;
2. Unforeseen chemical interferences caused removal of Lissamine from the aqueous system;
3. Uncertain flow field.

The velocity of the tracer could be slower than anticipated if either the interstitial groundwater velocity is much slower (e.g., if the hydraulic conductivity were much less) or the tracer were retarded due to a reversible chemical process (due to absorption onto aquifer media).

It is also possible that Lissamine is being permanently removed from solution although there is no published information to suggest that such a mechanism does indeed exist.

Finally it is possible that the centreline between monitoring wells M-20 and M-8 is not coincident with a flowline and that the tracer migrated between M-8 and adjacent monitoring wells.

To test these alternate hypothesis it was suggested that a larger slug of high concentration tracer be injected into one of the upstream monitoring points, and that all monitoring points be screened for Lissamine on collection of the final set of samples. Ten litres of 1000 mg/L solution was injected into M-1-8 on August 25, 1989. Interval M-1-8 likely intersects some of the peat

layer. The tracer concentrations measured during the final sampling, 18-20 days after tracer injection, could not be used to reliably define a mean groundwater velocity and dispersivity at the site. The distribution of tracer measured in the final sampling was highest near the injection interval and decreased to levels above background (>1.5 background or >15 ug/L) to a maximum distance of 21.7 m at M-19. Assuming this front of low concentration tracer was unretarded, a linear groundwater velocity of 1.1 m/day can be calculated from this test. However calculated mass recoveries of the tracer test were extremely low (<5%) rendering interpretation of the tracer test difficult and of questional reliability.

# 6. FINAL MODEL

## 6.1 CHANGES TO PRELIMINARY MODEL

The model used in making the final set of flow and transport calculations and predictions was conceptually quite similar to the preliminary model. It differed in the following key areas:

1. Orientation of the section;
2. Source location;
3. Length of the section;
4. Hydraulic conductivity distribution.

It was originally believed based on Morin (1983) that the source of the acidic water was centred near T8-B. An analysis of water level data collected during the June 1989 field visit (see Figure 5.2) indicates that the streamline corresponding to the centre line instrumentation most likely does not pass through T-8B but lies much closer to T-8-1. Consequently the orientation, length and upper Dirichlet boundary condition of the cross-section was changed to be consistent with this flow path (i.e., through T-8-1).

Discussions held after the presentation of the preliminary model and data given by Cherry et al. (1984) and Morin et. al. (1988a) suggested that the actual location of the source was probably few meters north of M-1 and south of T8-1 and T8-2 (i.e. below the dam). As a result the source area was moved much closer to M-1. A number of locations ranging from 1 m to 10 m north of M-1 were examined. Eventually a source distance of 2 m to 6 m north of M-1 was selected for the transport predictions based on anticipated flux rates (See Section 6.2.2.2). It must be noted, however, that there is little physical evidence for such a choice and therefore the exact source location and width remains uncertain.

The revised source location lead to some additional implications. The shorter travel distance implied a slower rate of plume movement suggesting that both a shorter section could be used to model the future plume movement and that a smaller dispersivity may be more appropriate (see for example discussions in Section 4.2.3).

Some additional changes were made to the material properties of the model. Some of these changes resulted from discussions held with AECB after the presentation of the preliminary model. This included the incorporation of a 10:1 horizontal: vertical anisotropy ratio. In addition, it was necessary to include a low permeability silt layer in order to obtain an acceptable match with measured piezometric levels. This aspect is discussed in detail in Section 6.2.2.1.

## 6.2 NUMERICAL MODEL

### 6.2.1 Mesh

The mesh corresponding to the final model is illustrated in Figure 6.1. The underlying philosophy followed in the design of this mesh was to use a fine mesh in those regions where transport would occur. In those regions where transport is not a concern (e.g., near the constant head boundaries), much larger elements were used. The main reason for this approach is due to the more severe constraints to which the numerical solution of a convective dispersion equation must adhere versus a solution to the groundwater flow equation. As a result elements on the order of 1 m were used in the transport region whereas elements up to 8 m were used adjacent to the boundary. A total of 528 elements consisting of 588 nodes were used in constructing this mesh.

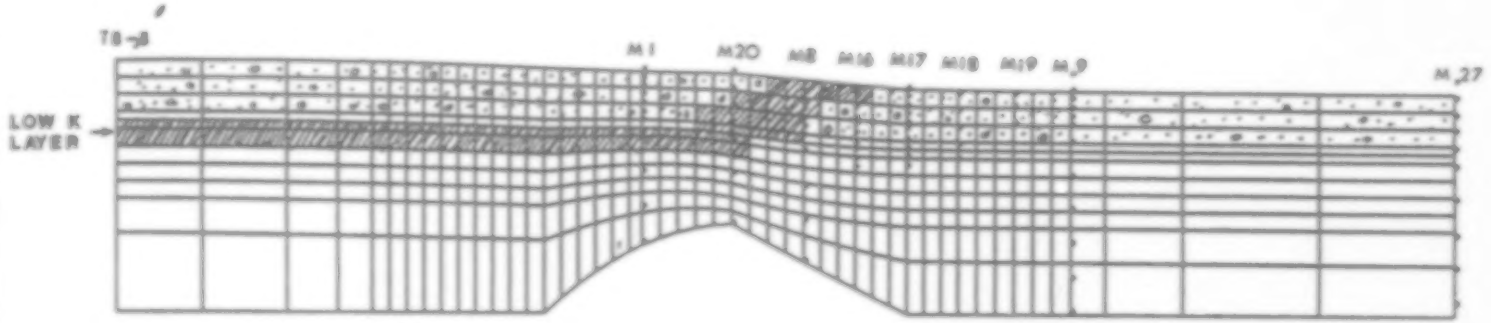


| INTERA Technologies | Numerical Mesh used in Final Model | Figure 6.1 |
|---|---|---|

### 6.2.2 Simulation Runs

#### 6.2.2.1 Flow Calibration

The major differences between the final flow model and the preliminary model include the orientation and length of the section (T8-1 to M-27 versus T8-8 to M-10 previously) and the data set used for comparison. Previously a combined data set based on data for May 1980 and mid June 1981 was used to set Dirichlet boundary conditions and to serve as calibration data. The final model used water levels measured on June 25, 1989. Hydraulic conductivity was varied for a number of simulations as described in the following sections. The remainder of the flow model is virtually identical, conceptually, to that employed previously. For example, a steady state flow system having a spatially uniform recharge of $6 \times 10^{-9}$ m/s (approximately 20 cm/yr) was adopted.

Figure 6.2 shows the piezometric head distribution along the modeled section for both measured and simulated data. The measured piezometric head distribution shown in Figure 6.2a is drawn assuming homogeneous material properties and interpolates between data points. Consequently the reliability of the contours shown in Figure 6.2b is greater in the area of M-1 to M-19 than in areas where the measurement points are sparse (i.e. T8-1 to M-1 and M-9 to M-27).

Model simulations were conducted for a variety of conditions. The first of these simulations (Figure 6.2b) employed a similar hydraulic conductivity distribution to the preliminary base case model (Simulation 1), employing an upper sand of $1 \times 10^{-4}$ m/s and 4 m thick and a lower sand of $5 \times 10^{-5}$ m/s and approximately 10.0 m thick. Boundary conditions were 342.6 masl along the upgradient (left hand) edge and 340.96 masl along the downgradient (right-hand) edge. The distribution of piezometric contours is similar to those exhibited by the preliminary model (Figure 3.9) consisting of near vertical equally-spaced contours. The second simulation was identical to th evious simulation with the exception of the anisotropy ratio which was change from 1:1 to 10:1 (horizontal: vertical) by reducing vertical component of hydraulic

conductivity. This simulation, depicted in Figure 6.2c, shows the resulting impact of such an anisotropy change. When compared to 6.2b it can be seen that the existence of anisotropy serves to magnify the head loss associated with any vertical component of flow resulting in a higher density of head contours in these areas. Areas where the flow direction is predominately horizontal are largely unaffected by the anisotropy change. It is also of interest to note that even with an anisotropy change of 10:1 the flow lines in the near surface do not change appreciably indicating that surface recharge is a minor component of total aquifer flux. Finally and most importantly, inclusion of anisotropy to the base model does not reproduce the pattern of piezometer contours measured at the site.

In examining Figures 6.2b and 6.2c it can be seen that a major area of discrepancy exists in the vicinity of M-1-3, M-20-4 and M-8-7. Such deviations were also apparent in the preliminary modeling results presented earlier. It was previously suggested that one possible mechanism that could account for the observed piezometric pattern would be enhanced infiltration under (and caused by) the tailings dam itself. To explore the possibility that such a mechanism could account for the observed head distribution a simulation using enhanced ($6 \times 10^{-7}$ m/s or 20 m/yr) infiltration over a 13 m long portion of the section was conducted. The piezometric distribution resulting from this simulation (presented in Figure 6.2d) demonstrates no significant change from the contours of Figure 6.2c. Although further increases in the enhanced infiltration magnitude may give the desired response it is unlikely that the necessary increase could be physically justified.

It is much more likely that heterogeneity, such as the peat and silt layers proposed by Blair et al. (1980) (see Figure 3.7), are the cause of the high head loss zone in the vicinity of M-1, M-20 and M-8. To determine if the existence of such a layer (possibly silt) could cause such a head loss zone an additional simulation was performed. This simulation used the conditions comparable to Figure 6.2c (with anisotropy and uniform recharge) and incorporated

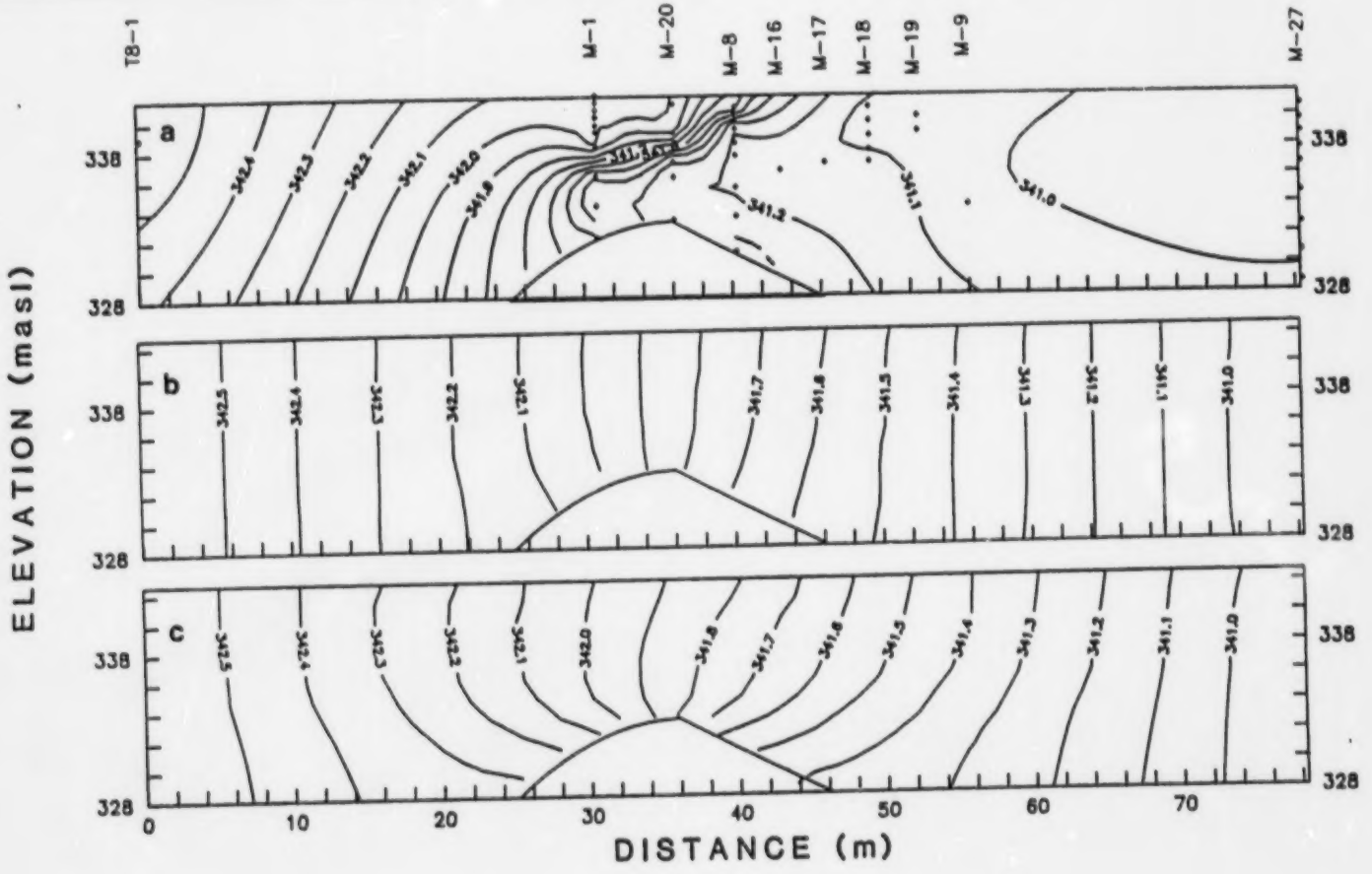


(a) Observed (b) Upper ($10^{-4}$) and Lower ($5 \times 10^{-5}$) Sand (c) Anisotropy 10:1

| INTERA Technologies | Piezometric Contours along Plume Centreline | Figure 6.2 |
|---|---|---|

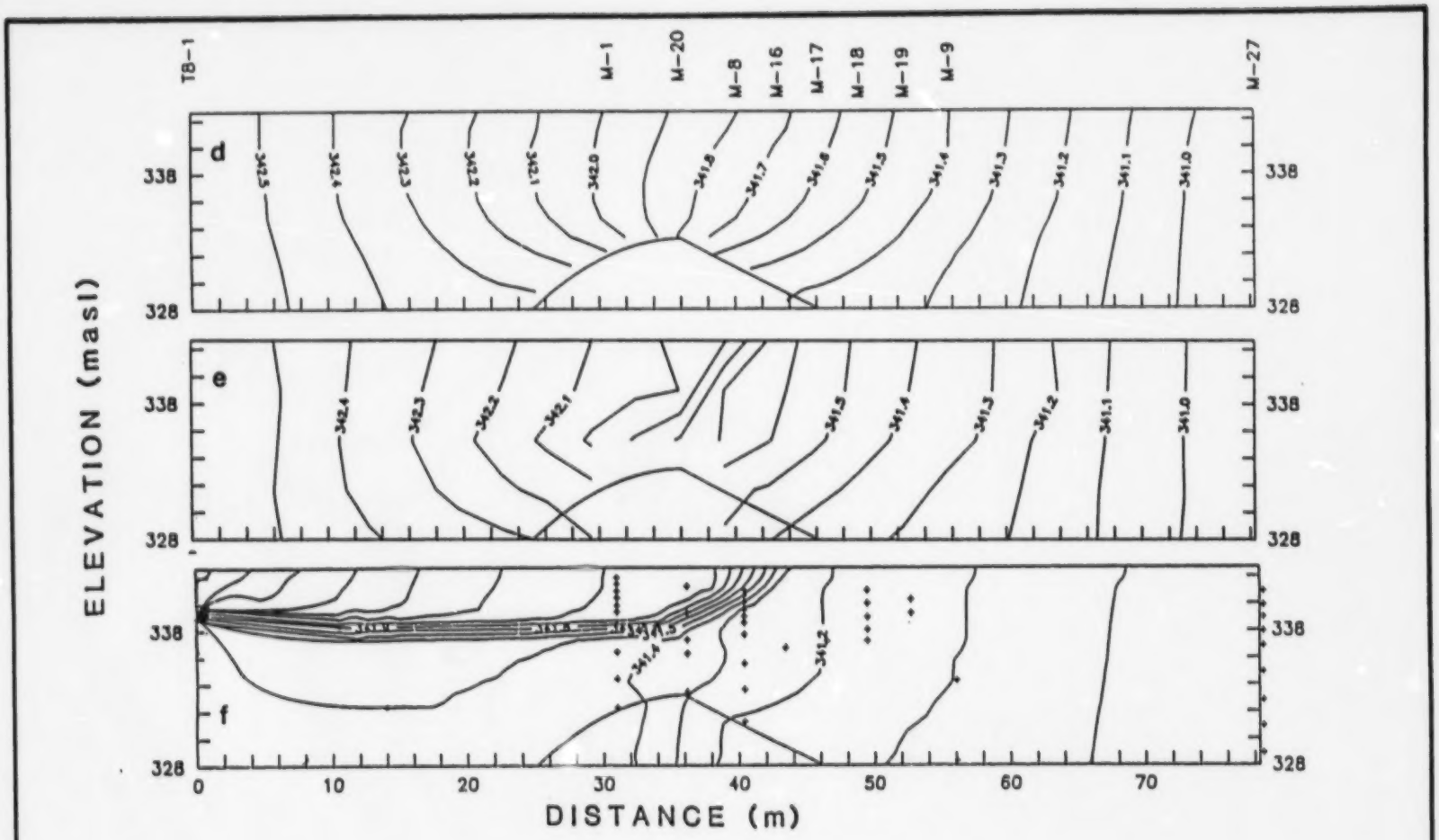


(d) focused recharge (e) silt layer (f) silt layer and revised boundary conditions

| INTERA Technologies | Piezometric Contours along Plume Centreline (cont'd) | Figure 6.2 |
|---|---|---|

a heterogeneous zone having a hydraulic conductivity of 1 x $10^{-9}$ m/s and a distribution similar to that identified in Figure 6.1. The results of this simulation (Figure 6.2e) show that such a low permeability layer does indeed improve the fit in the vicinity of M-1, M-20 and M-8. However, the magnitude of the simulated head loss is lower than that observed in the field. In addition the distribution of head contours around this head loss zone (i.e., the areas upstream and downstream of bedrock high) remains approximately evenly distributed. The measured head contours, on the other hand, indicate that much more head loss occurs upstream of M-8 than downstream of it.

Additional simulations showed that the distribution of piezometric contours was largely unaffected by the actual hydraulic conductivity of the low permeability layer. The explanation for this phenomena is that the layer merely serves to isolate (and hence control) a small portion of the grid (i.e., upper left hand quadrant). Changes to the silt layer will leave the major flow path, from the lower left hand quadrant to the discharge point at the right-hand side, unaffected. A series of additional simulations indicated that only two possible mechanisms could result in a redistribution of the piezometric head contours. One mechanism involved placing a thick zone of reduced permeability below the inferred silt layer. This resulted in a shift of piezometric contours from the right-hand side of the section to the left-hand side. The second mechanism is to reduce the head along a portion of the left-hand boundary. We have elected to adopt the latter of the two mechanisms identified above. There are two reasons for this choice:

1. The first mechanism would require the use of an extensive quantity low permeability material. However, there is little evidence to suggest that such large scale heterogeneities of this magnitude exist at the site.

2. Secondly, although no head measurements at depth are available at T-8-1, it would seem logical that if the low permeability layer were extended horizontally to the left hand boundary that a head drop of approximately 1.0 m would exist on this boundary. This head loss is comparable to that observed in piezometer M-1.

We have therefore adopted the second mechanism since it is, at least conceptually, more correct. In addition, an extensive low permeability layer is likely more consistent with our understanding of the physiography of former tailings area (i.e., an extensive bog that ended about where the low permeability unit is thought to emerge at M-8 and M-16) and is locally consistent with hydrogeologic interpretations provided by Blair et al. (1980) and Morin (1983).

The low permeability layer is conceptually equivalent to the location north of M-1 of peat and silt layers identified by Blair et al. (1980). The low permeability unit that emerges to surface near M-8 and M-16 is likely equivalent to the low permeability peat layer suggested by Blair et al. (1980) and is supported by hydraulic testing of piezometers DP-1 and DP-2 described in Section 5.4 of this report. Consequently there is hydrogeologic evidence from this and earlier studies that supports the existence of a low permeability (silt) layer as shown in Figure 6.1.

Figure 6.2f shows the piezometric head distribution that results from assuming a constant head of 342.6 masl above and 341.5 masl below the silt layer (having a hydraulic conductivity of $5 \times 10^{-6}$ m/s along the left-hand boundary. Comparing Figure 6.2f with the observed data of 6.2a shows a reasonable match in those areas where data points exist. Regions having low concentrations of data points (e.g., between T-8-1 and M-1) show poor similarity. This apparent "poor fit" is attributable to the uniform interpolation/extrapolation that is performed by the contouring program on the observed points. If, for example, it were known that an equivalent low permeability silt layer was continuous to the left-hand boundary, it is unlikely that the contours presented in Figure 6.2a would be representative. This aspect points to the danger of interpolation between data points that are too widely spaced.

For the purpose of performing transport calculations therefore, we have assumed that the steady state flow field presented by Figure 6.2f is a reasonable representation. This representation includes anisotropy, uniform recharge and a heterogenous low permeability unit that extend north below the tailings dam to T-8-1. Definitely within the primary area of concern (i.e., in the vicinity

of the source and plume) the adequacy of the model fit can be verified by comparison to known data.

6.2.2.2 Transport Calibration

In calibrating FEMWASTE there are several factors that are key in controlling the shape and magnitude of the concentration profiles at the Nordic Tailings Area. These factors include:

1. Location of source;
2. Size of source;
3. Source strength over time;
4. Dispersivity of the natural system;
5. Retarded interstitial solute velocity.

Many of the above factors are not independent of each other from the standpoint that changes in one parameter could potentially be off-set by changes in another. Source location and retarded interstitial solute velocity are examples of this type of interdependence. By placing the source twice as close to the observation point and reducing the interstitial solute velocity by a half one would see a similar breakthrough curve at the observation point. "Similar" and not identical since dispersion would be greater (assuming the same dispersivity) in the higher velocity case. It is important, therefore, to realize that the solution provided by groundwater transport models may not be (and typically will not be) unique and that several combinations of parameters may yield similar solutions. In some cases specific "solutions" may be eliminated if the resulting fitted parameters are outside of a feasible or credible range. The approach followed in calibrating the transport model is based on this philosophy, that all parameters must correspond to a credible range. Specifically the following ranges were used as our best estimates of likely parameter ranges:

Location of source: 1 to 10 m north of M-1
Size of Source: 1 to 10 m
Longitudinal Dispersivity: 0.5 to 2 m
Retarded Interstitial Velocity: 1 to 2 m/yr.

Of the estimates above, the parameter having the lowest uncertainty (and smallest range) is the retarded interstitial velocity. This estimate was made by Morin (1983) and can be substantiated by examining subsequent concentration profiles. Given that in 1983/84 the source had been in existence only about 17.5 years, then for an undispersed system the source would be located 17.5 to 35 m from the plume edge. If one assumes that the edge of the plume is located in the vicinity of M-17 or M-16 (i.e., near 4.5 and 5.0 pH contours in 1984 or 25 pCi/L contours) then the source could be located from 1 to 17.5 m north of M-1. In reality it is unlikely (due to dispersion and dilution) that the plume would be located close to this upper limit, and therefore a limit of 10 m was selected. In order to refine this estimate of source location a number of simulations were conducted:

1. Source located between 2 and 4 m north of M-1 (i.e. source width = 2 m);
2. Source located between 2 and 6 m north of M-1 (i.e. source width = 4 m);
3. Source located between 2 and 9 m north of M-1 (i.e. source width = 7 m).

These simulations used the following assumptions and properties:

1. Constant concentration (over time) of unit magnitude;
2. Uniform spatial distribution of source;
3. Solute velocity of approximately 1 m/yr;
4. Dispersivity of 1 m.

The results of these simulations are presented in Figure 6.3 in the form of concentration profiles at 17.5 yrs (corresponding to start of plume until 1983/84). In order to correctly interpret the results of these (and all subsequent) simulations it is important to remember several key points. First, the mesh used in performing the simulations is refined in middle of the section (between 15 and 58 m from left hand edge). Outside of this range the numerical results will be much less reliable since they will be subject to numerical dispersion (for upwind weighting) and numerical overshoot-undershoot (Reeves et al., 1985). Secondly, based on the results of the verification problems, it would appear that the model's solution is accurate within two to three orders of magnitude of the source concentration. Consequently values less than $10^{-3}$ should be viewed with caution. Bearing this in mind we can now turn our attention to Figure 6.3. If one assumes that the average historical input concentration for pH is approximately pH = 3 then the $10^{-2}$ contour would represent the pH = 5 contour. From Figure 3.10, one can see that the pH=5 contour should lie between M-1-3 and M-1-4, M-8-4 and M-8-5 and intersect the surface between M-17 and M-18. Comparing with Figure 6.3, it can be concluded that the two meter wide source does not provide sufficient hydrogen ion flux to yield an acceptable concentration match. In this case the $10^{-2}$ contour is too shallow and has not migrated deep enough. Conversely the $10^{-2}$ contour for the 7 m wide source has migrated too far horizontally, although the extent of vertical migration is approximately correct. The extent of vertical migration for the 4 m wide source is comparable to the 2 m wide source, a fact which would imply that the low permeability silt layer is limiting the plumes movement in this direction. The 4 m wide source does a better job, however, of matching the horizontal position of the $10^{-2}$ contour.

Based on these observations it would appear that it is unlikely that a 2 m wide source could add sufficient contaminant volumes to generate the observed concentration plume for reasonable flux rates. However it is conceivable that the 7 m wide source could reproduce the concentration contours acceptably if either the contaminant flux rate was decreased or the contaminant

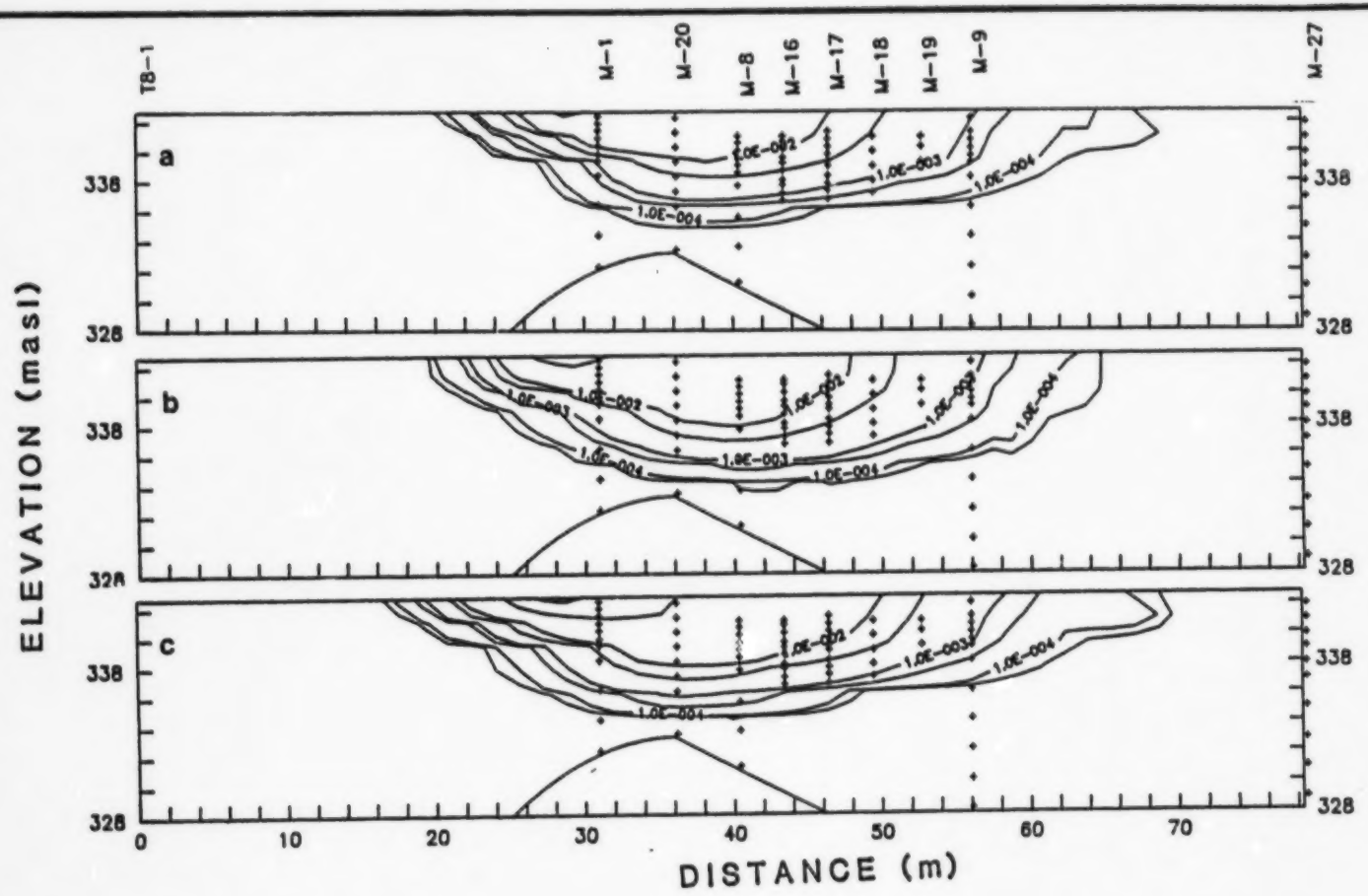


(a) 2 m (b) 4 m (c) 7 m

| INTERA Technologies | Concentration Profiles for Various Source Widths | Figure 6.3 |
|---|---|---|

was more highly sorbed. To examine this latter possibility and also to demonstrate the sensitivity of the contaminant plumes to the effective interstitial velocity two separate simulations were performed in which the kd was varied to yield interstitial velocities that were 50% higher and half those of the base case simulation. The results of these simulations are presented in Figure 6.4 in the form of concentration profiles after 17.5 years. The simulation corresponding to the higher kd (yielding a solute interstitial velocity on the order of 0.5 m/yr) shows, as one might anticipate, much slower movement of the plume compared to the 1 m/yr simulations. Based on this comparison it can also be seen that the quantity of contaminant mass present as solute has decreased due to the sorption of a higher percentage onto the aquifer medium. The converse (i.e., more dissolved solute and faster movement) is generally true for the less retarded interstitial velocity (1.5 m/yr). An exception to this is the forward horizontal movement of the $10^{-2}$ contour which is largely unchanged between the concentration profiles corresponding to the two "fastest" profiles. This is largely attributable to the existence of the low permeability silt layer which is approximately coincident with this contour.

Another general observation which can be made regarding these profiles is the degree of dispersion that exists. The lower kd plumes contain a much higher degree of smearing resulting from their higher velocities. This could be offset by using a lower dispersivity, however, it should be pointed out that there are numerical and practical constraints which prohibit the use of extremely small dispersivities over significant scales for numerical grid-based solution codes such as FEMWASTE.

To examine the sensitivity of the simulations to dispersion three additional simulations were made. These simulations used similar assumptions to those employed in the earlier simulations although in this case a source of 4 m width was used. While the use of a 7 m wide source can feasibly reproduce the observed concentration profiles, this would necessitate using a slower moving plume than that observed in the field. The results of three simulations using a longitudinal dispersivity of 2 m, 1 m and 0.5 m is shown in Figure 6.5.

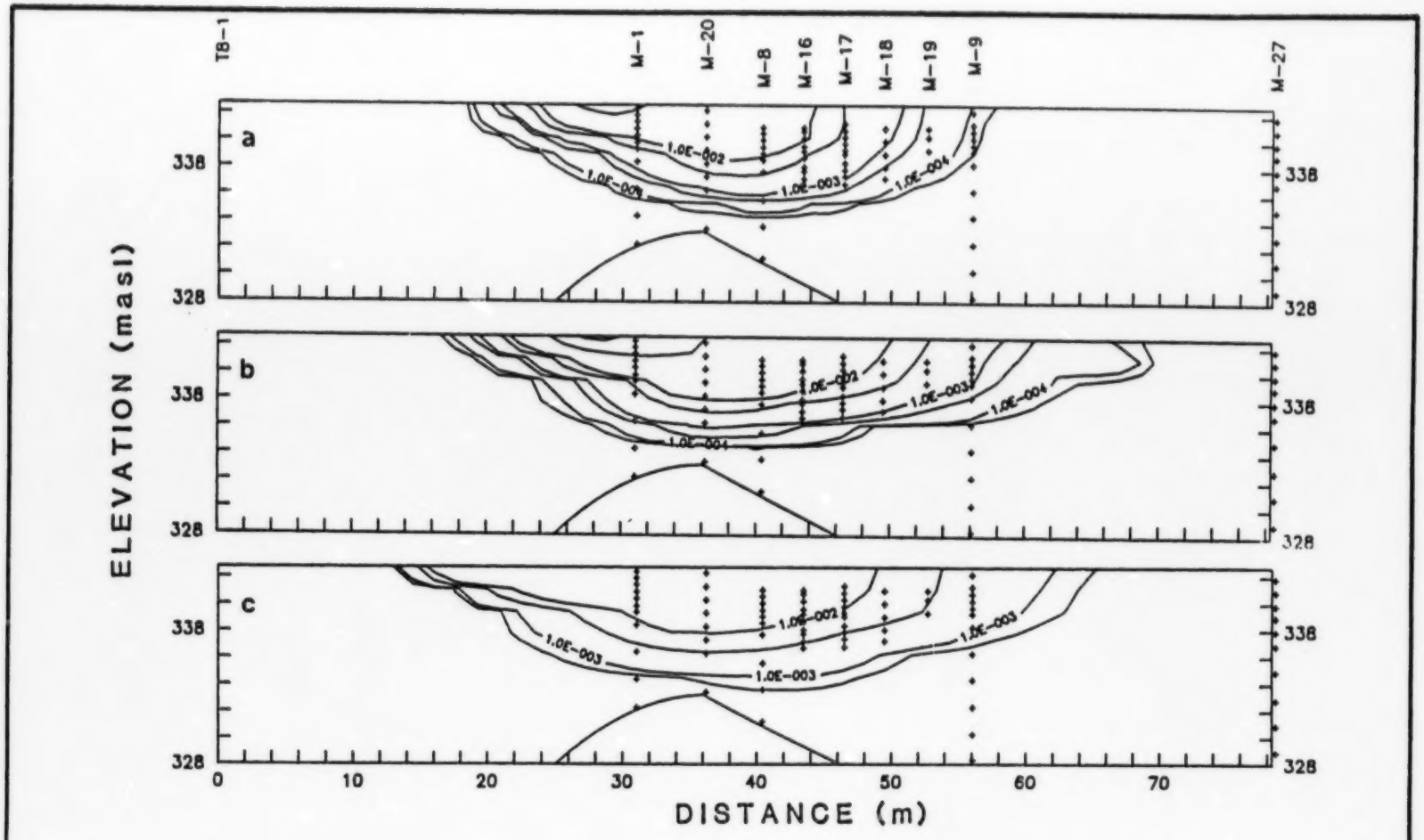


(a) kd = .03 (b) kd = .015 (c) kd = .01

| INTERA Technologies | Concentration Contours for Various kd | Figure 6.4 |
|---|---|---|

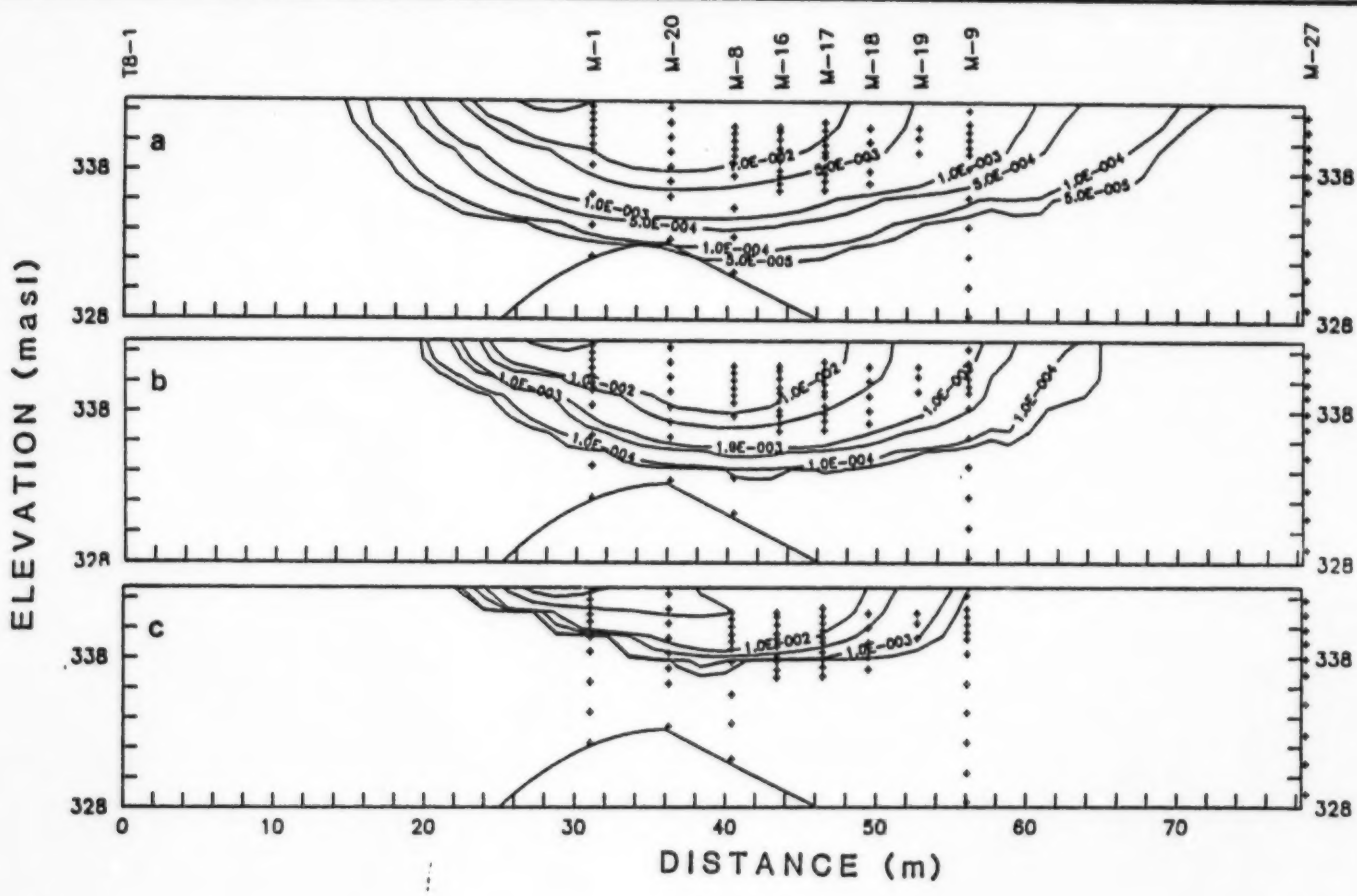


(a) $\alpha_L$ = 2 m (b) $\alpha_L$ = 1 m (c) $\alpha_L$ = 0.5 m

| INTERA Technologies | Concentration Contours for Various $\alpha_L$ | Figure 6.5 |
|---|---|---|

Several interesting observations can be made regarding these figures. For example, the concentrations in the vicinity of the silt layer are again largely unchanged (e.g., note the forward position of the $10^{-2}$ concentration contour). The remainder of the plumes behave much as one would expect demonstrating higher peak concentrations and less smearing with reduced dispersivities. For the conditions modeled it can be seen that a dispersivity of 0.5 m will give a maximum concentration of greater than 0.1 of the input concentration. If one assumes the average input pH is on the order of 3 this would result in concentrations of less than pH = 4 at M-1, an observation which cannot be substantiated based on available field data. It is difficult to make conclusive statements regarding the most appropriate upper bound for the field dispersivity. The concentration profiles in the region upstream of the silt layer are virtually identical for a dispersivity of either 1 or 2 m, and the area downstream contain concentrations that are unreliable, both from a numerical simulation standpoint and from a data reliability standpoint (e.g., the contribution above background).

To summarize therefore, although this calibration has not definitely identified the specific (or only) set of input parameter values that could reproduce observed concentration levels it has yielded bounds on what may be considered feasible parameters based on our current conceptual model. For example:

1. Source size - the source is probably at least 4 m in width and possibly up to 7 m but is unlikely to be 2 m;

2. Source location - given the reported rate of plume movement it is unlikely that the edge of the source is located more than a couple of meters from M-1;

3. It is unlikely that a dispersivity of less than 1 m is appropriate in the high velocity region upstream of the silt layer.

The results of the final calibration run for pH are presented, along with measured field data for 1983 and 1984 in Figure 6.6. This model uses a 4 m wide source, a dispersivity of one meter, a constant input pH = 3, a retardation factor of 86, and a simulation time of 17.5 years. In view of the significant differences that exist between the 1983 and 1984 measured data the calibrated concentration profile gives an acceptable fit. The vertical extent of the 4.5, 5.0 and 5.5 contours is reasonable with some minor deviation in the lower points of M-1. The adequacy of the model to predict the horizontal movement of the plume is more difficult to assess owing to the anomalous source in the vicinity of M-17. Based on the horizontal progression of the 5.0 and 5.5 contours (excluding 1983 5.5 contour) it would appear that the simulated horizontal plume velocity is reasonable.

Figure 6.7 provides a correlation plot of the pH data for the 1983/84 calibration of the centreline piezometers with the actual measured pH data in 1983 and 1984. The straight line shown on these plots shows a perfect correlation (i.e. correlation coefficient, = 1). The plots also show the calculated correlation coefficient which potentially ranges from 0 to 1 and provides a normalized and scale free measure of the association between two variables assumed to be normally distributed. As such the correlation coefficient provides a quantification of the correlation between the measured and calculated (calibrated) pH values. The correlation coefficient between the calibration model and the 1983 pH data are 0.77 and the 1984 pH data are 0.69 suggesting a slightly better correlation between the calibrated model and the 1983 pH data.

The final model calibration for the Ra226 data is shown in Figure 6.8. This model was virtually identical to the pH model, although it assumes uniform input concentration of 3,000 pCi/L over the simulation period. This value was based largely on two factors, the range reported by Blair et al. (1980) of 1,000 to 5,000 pCi/L and the "required" concentration to give an acceptable match using the pH calibrated model. Figure 6.8 also shows measured Ra226 concentrations for 1983 and 1984. These data, like the pH data demonstrate some significant differences most notably with respect to the existence of peak concentrations.

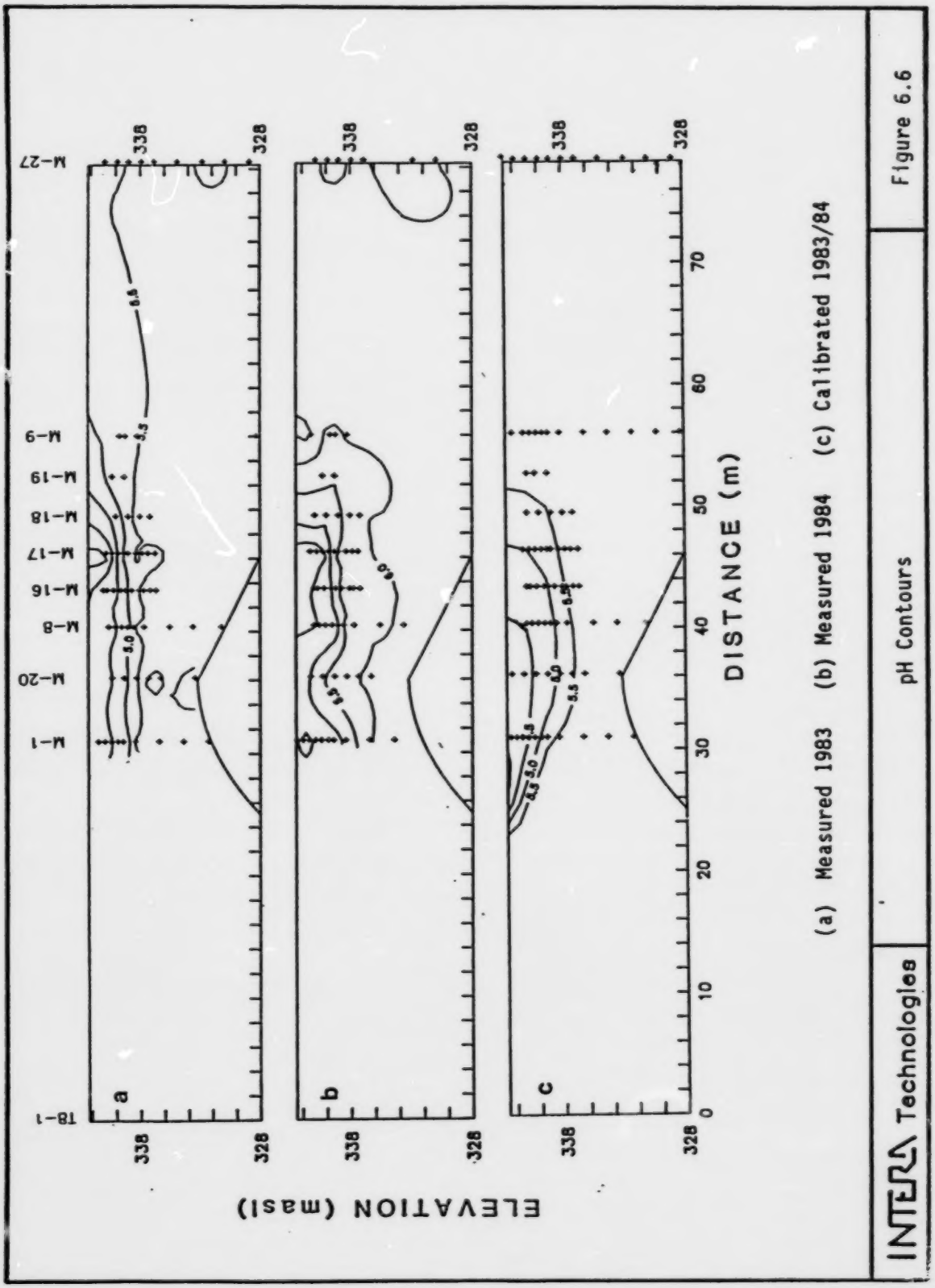
ELEVATION (masl)
DISTANCE (m)
M-27
M-9
M-19
M-18
M-17
M-16
M-8
M-20
M-1
TB-1
338
328
0
10
20
30
40
50
60
70
a
b
c
5.5
5.0
4.5
4.0
3.5
3.0
(a) Measured 1983 (b) Measured 1984 (c) Calibrated 1983/84
INTERA Technologies
pH Contours
Figure 6.6

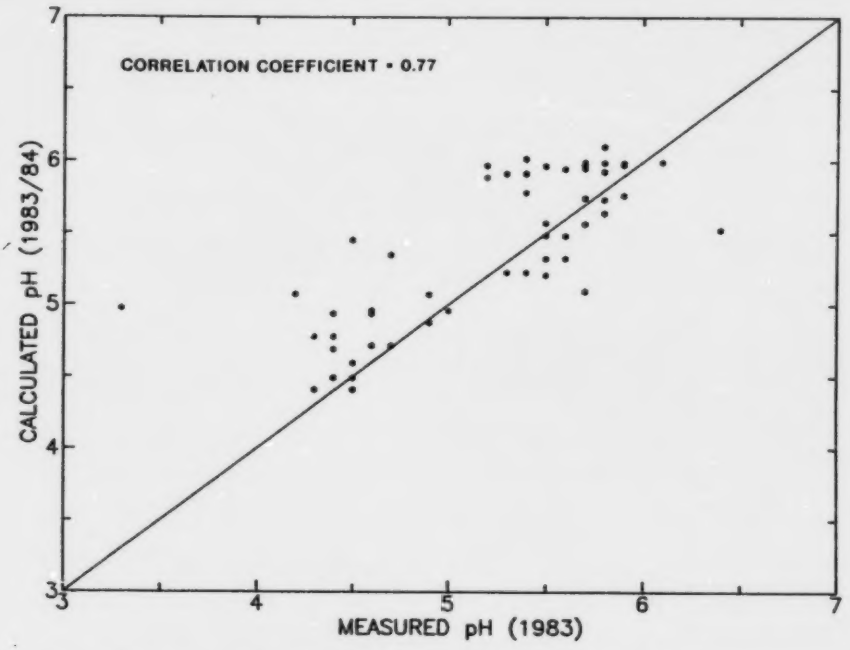


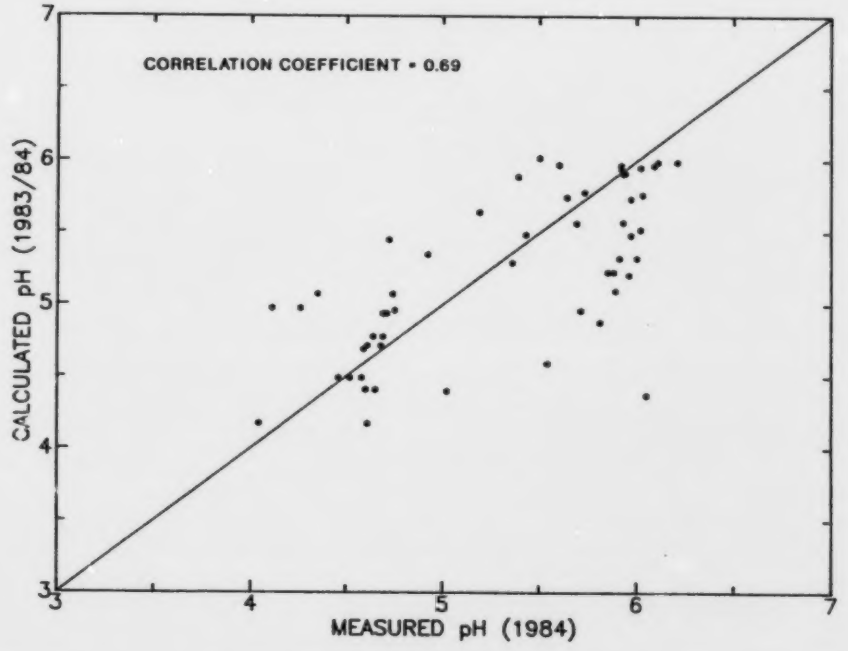


| | |
|---|---|
| Drawn by | Date |
| Checked by | Date |
| Revisions | Date |
| | |

Correlation plots for model calibrated and measured pH for 1983 and 1984

INTERA Technologies

Figure 6.7

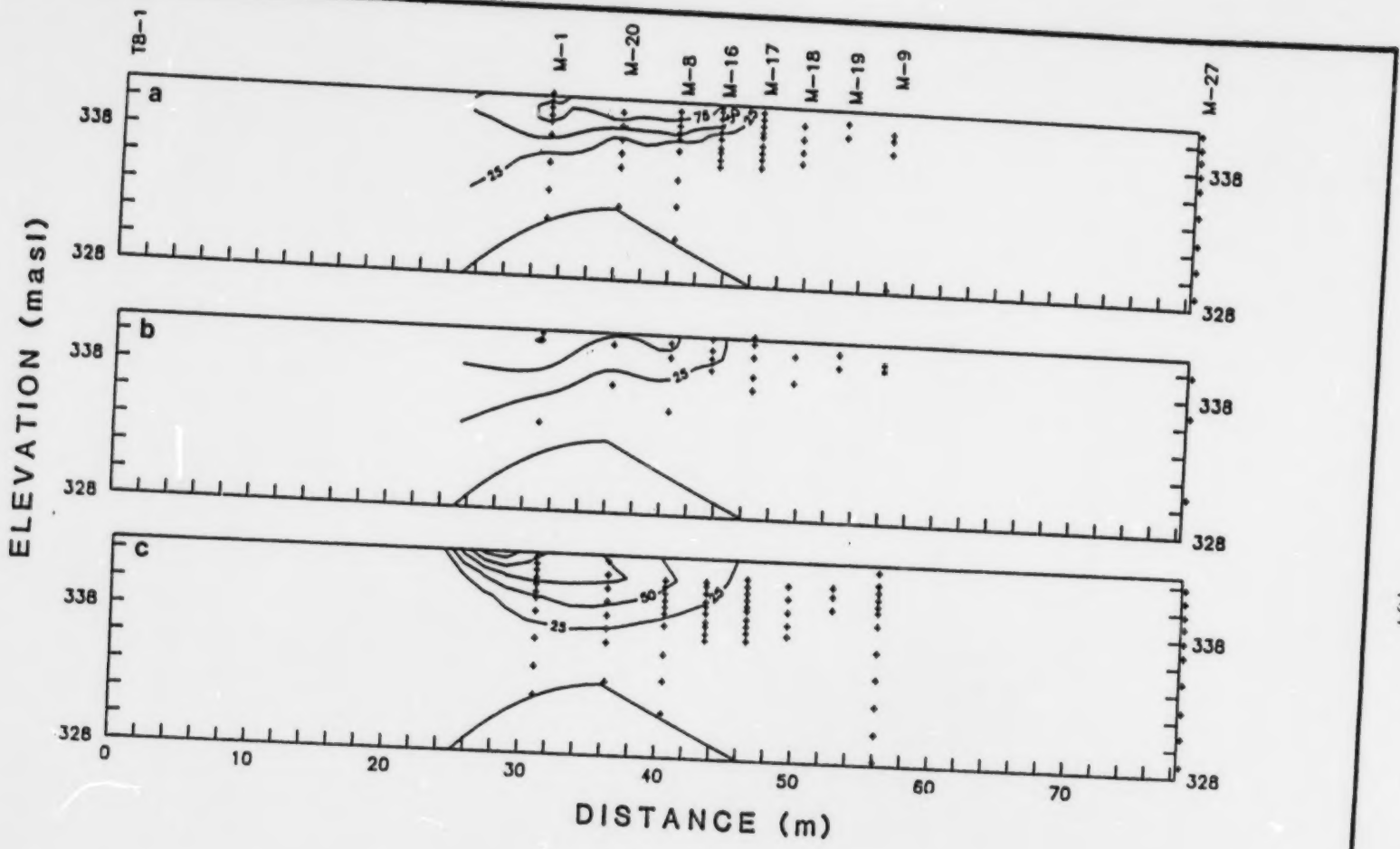


(a) Measured 1983 (b) Measured 1984 (c) Calibrated 1983/84

| INTERA Technologies | Simulated Ra226 Contours (pCi/L) | Figure 6.8 |
|---|---|---|

The simulated contours do a reasonable job of matching the 25 pCi/L contour (since little difference exists between the two measured data sets) and of "falling between" the 1983 and 1984 measured contours for 50 and 75 pCi/L.

Figure 6.9 provides the correlation plots and correlation coefficients for the Ra226 data calculated in the calibration exercise. Figure 6.9 shows slightly better correlation of calibrated model to the 1984 Ra226 data (correlation coefficient = 0.93) than the 1983 Ra226 data (correlation coefficient = 0.87). The apparently better correlation of the Ra226 data over the pH data as expressed in the correlation coefficient may be due to the confounding influence of acid precipitation on the pH plume as the site, the limitation of the model to simulate over three orders of magnitude and the range of the observed data.

### 6.2.2.3 Transport Predictions

The calibrated transport models do a reasonable job of matching historical data for both Ra226 and pH given the uncertainty that exists in the measured data and the characterization of the physical flow system at the site. The next step in this analyses is to perform predictions for the 1989 field data based on the calibrated pH and Ra226 models.

In general, it is probably reasonable to assume that the assumptions and parameter estimates used in constructing the calibrated model do not change over the prediction period. One notable exception to this assumption may be the source strength which could, and is likely, changing over time. For example the pH of the pore water will likely continue to decrease until some form of control (e.g., amount of available pyrite or oxygen, bacteriological factors, etc.) is invoked. Based on measurements conducted on other similar tailings it would appear that a lower pH limit would be about 1.5 (Blowes and Gillham, 1988).

It is likely that the Ra226 concentration of the source term is decreasing with time since there is a finite quantity of Ra226 available and its release will be governed by acid leaching. However it must be recognized that considerable uncertainty exists surrounding the source term's variance over time. For this reason, two sets of predictive simulations were performed for 1989:

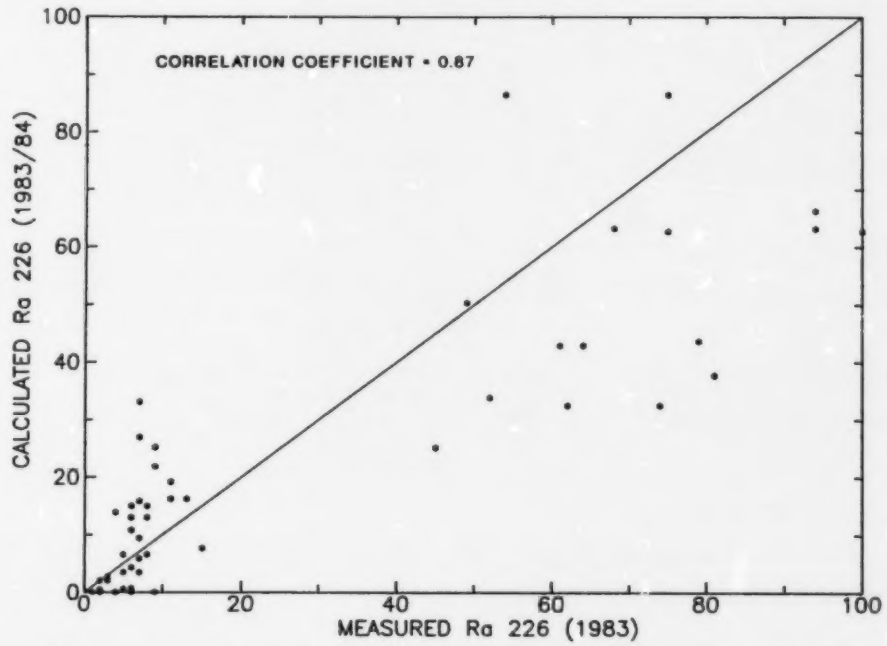


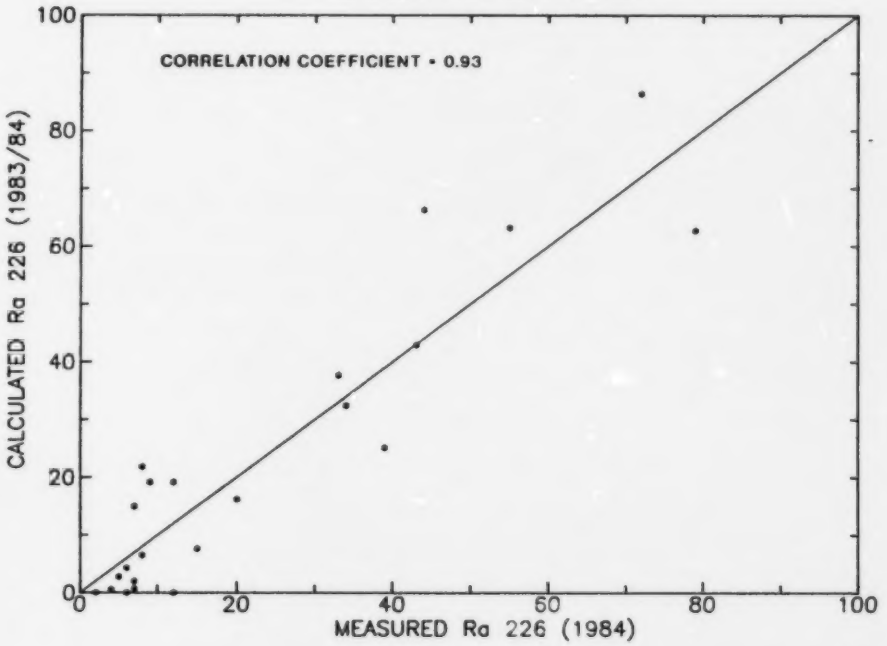


| | |
|---|---|
| Drawn by | Date |
| Checked by | Date |
| Revisions | Date |
| | |

Correlation plots for model calibrated and measured Ra 226 for 1983 and 1984 (pCi/L)

INTERA Technologies

Figure 6.9

1. Predictive runs using the same source concentration employed for calibration purposes;

2. Sensitivity simulations in which the source term was adjusted over the prediction period. In the case of pH, the source term was assumed to decrease linearly from a value of 3 at the end of the calibration period to a value of 1.5 at the end of the prediction period (approximately 5.5 years later). For Ra226, the input concentration was assumed to vary linearly from 3000 pCi/L to 500 pCi/L from the end of the calibration period to 1989.

The results of these simulations have been presented in Figure 6.10 for pH and Figure 6.11 for Ra226. Also presented in these figures are concentration profiles corresponding to 1995 for the constant source (i.e., predictive) simulation. The assessment and interpretation of these profiles is undertaken in Chapter 7 where they are compared to the measured 1989 field data. At this point, it is sufficient to say that both predictive and sensitivity analyses simulations demonstrate anticipated behaviour. It is worthwhile to note the extent and magnitude of the deviation between sensitivity and predictive runs since this represents the maximum difference that could be attributed to source term deviations. For both pH and Ra226 the changes are most significant in closer proximity to the source location. At the leading edge of the plume the two profiles (sensitivity and predicted) are indistinguishable.

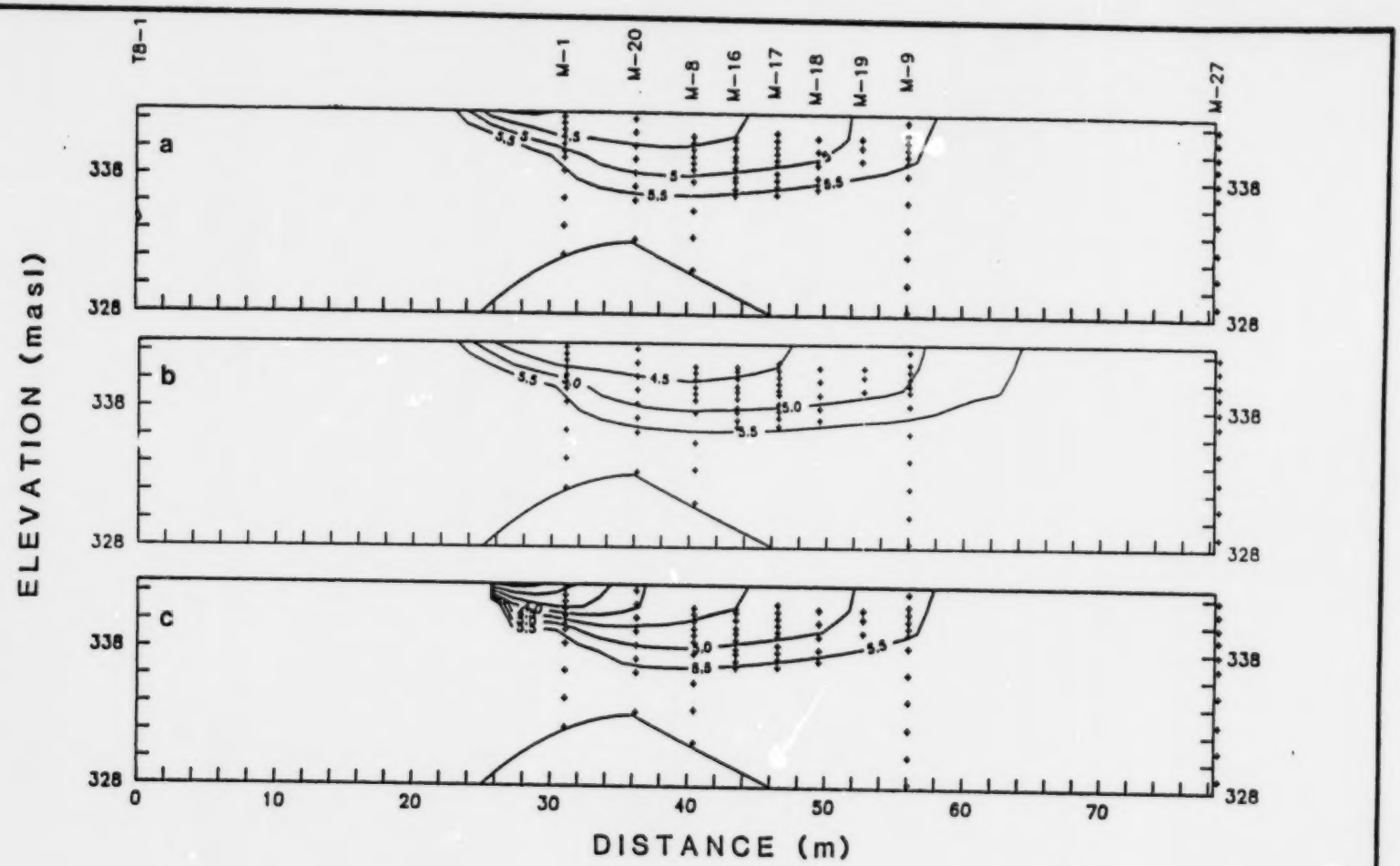


(a) Prediction 1989 (b) Prediction 1995 (c) Sensitivity Run 1989

| INTERA Technologies | pH Contours | Figure 6.10 |
|---|---|---|

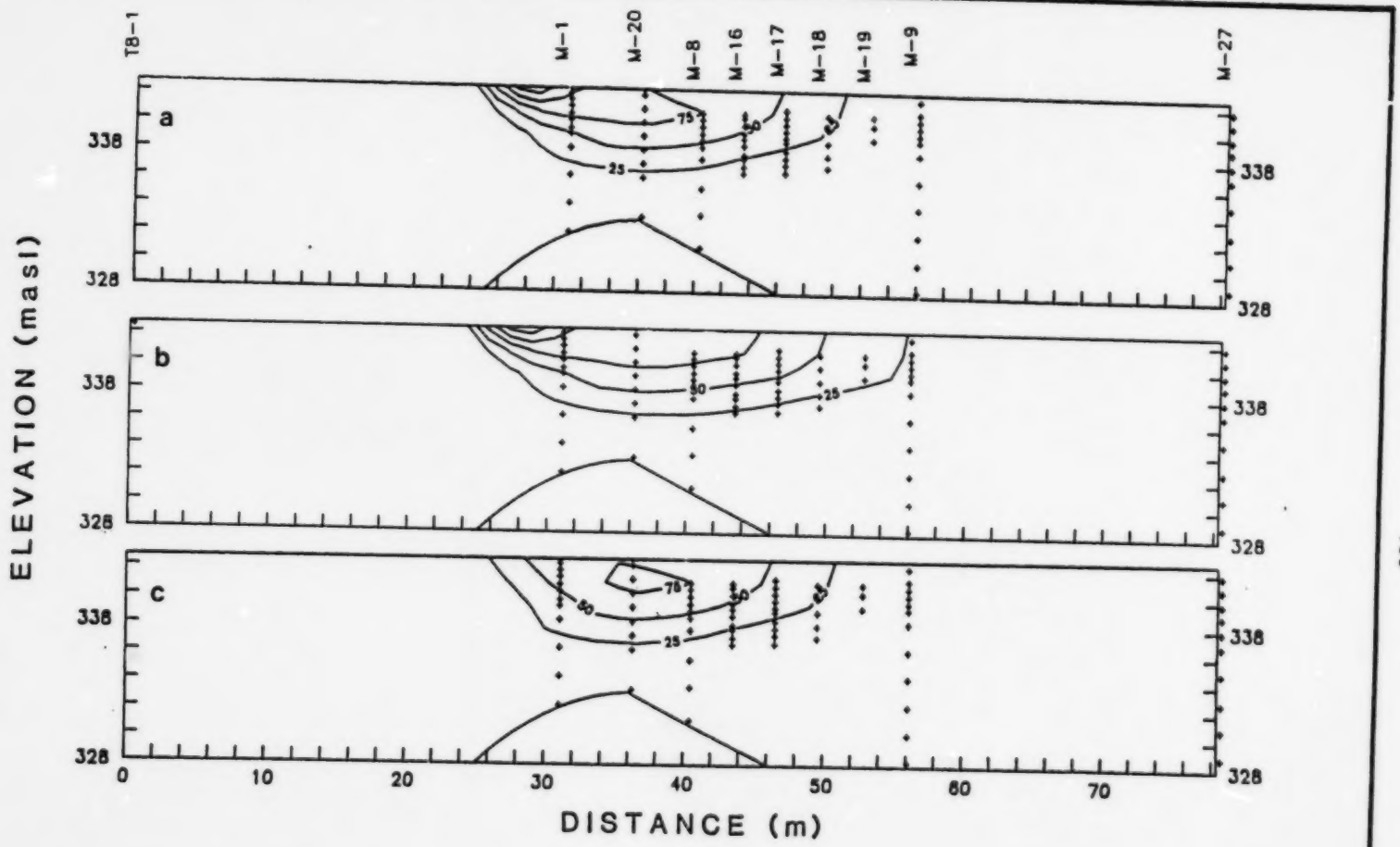


(a) Prediction 1989 (b) Prediction 1995 (c) Sensitivity Run 1989

| INTERA Technologies | Comparison of Measured Simulated Ra226 (pCi/L) | Figure 6.11 |
|---|---|---|

# 7. ACCURACY OF MODEL

## 7.1 DESCRIPTION OF SEPTEMBER 1989 GROUNDWATER SAMPLING

A field visit was made from September 12 - 15, 1989 for the purpose of collecting groundwater samples for chemical analyses. Prior to collection of samples, water levels were measured and recorded for all seepage area A centreline piezometers. Water levels were within 0.3 m of those measured during the June, 1989 field trip and have been presented in Appendix A. The change in hydraulic gradient between these two measurements periods was found to be small generally being less than 10%.

Groundwater samples were collected using the protocols outlined in Morin (1985) which involved pumping the piezometer at rate of approximately 0.5 L/min into a 200 mL (water bathed) flow cell. The pumping was continued until either the pH stabilized (less than 0.02 pH units/min) or until a maximum of five litres had been removed. The pH probe and meter were calibrated using pH 4 and pH 7 standards before the sampling and checked on an hourly basis. Results of duplicate measurements showed excellent ($\pm$.02 units) agreement. Figure 7.1 shows the results of the pH measurements conducted during the September sampling program. Also presented in Figure 7.1 are pH concentration profiles based on the results of Morin data (1983 and 1984). Several observations can be made from this data:

1. The 1984 data appears to contain several anomalous regions (e.g., 5.5 contour location and existence of 6.0 contour);

2. Based on a comparison of 1983 and 1989 data, the 5.0 and 5.5 contours have exhibited significant downward movement (up to 6 m) although the magnitude of this movement varies spatially.

3. The 4.5 pH contour appears to have changed little (either horizontally or vertically) from the 1983 data.

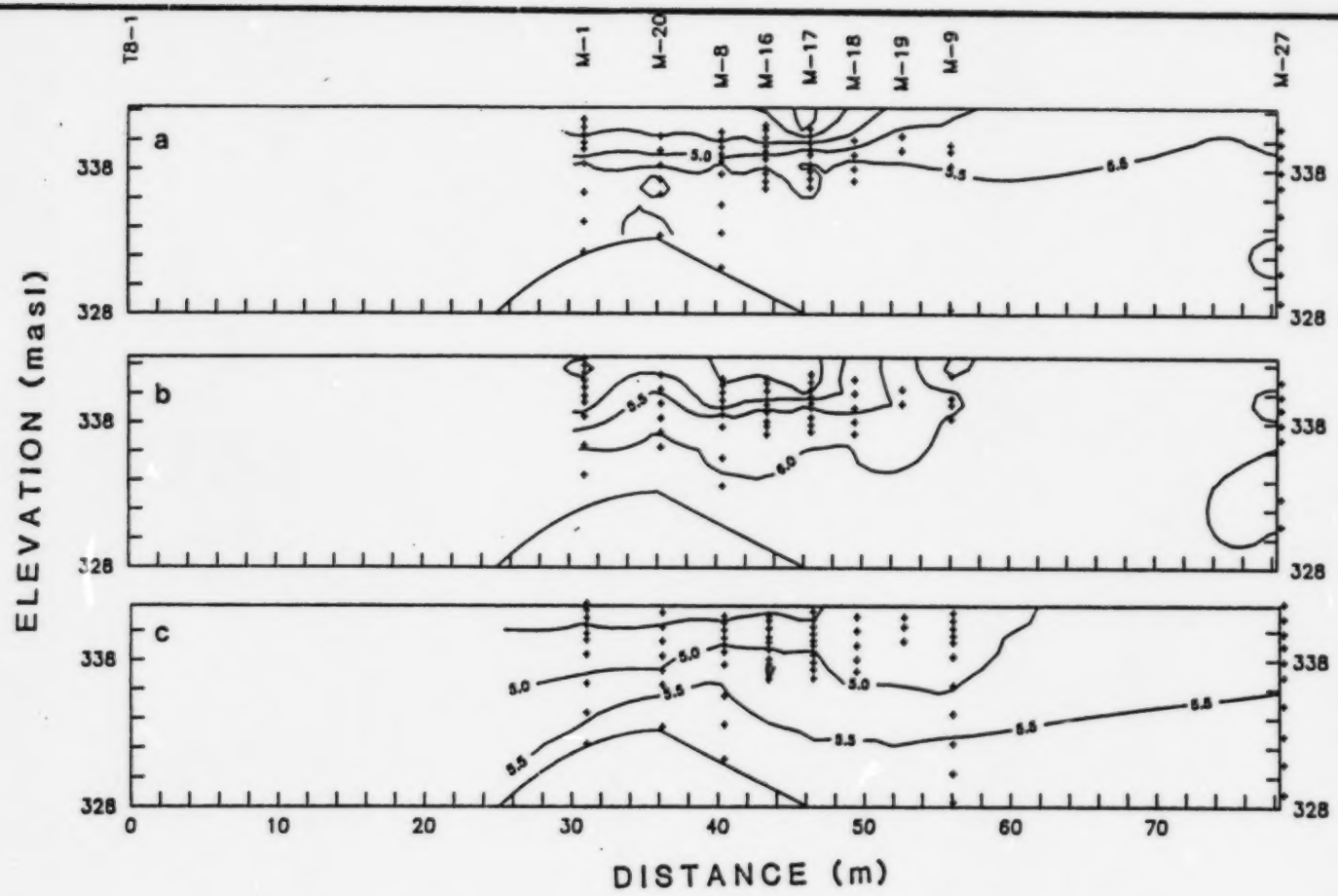


(a) 1983 (b) 1984 (c) 1989

| INTERA Technologies | Measured pH Concentrations | Figure 7.1 |
|---|---|---|

4. The leading edge of the 5.0 contour has exhibited both significant vertical and horizontal movement.

The implications of these findings are discussed in Section 7.2 in terms of their impact on the model predictions.

After pH measurements had been collected, 4 L samples were collected for Ra226 analyses. The sampling procedure again followed the protocols outlined in Morin (1985), in order to reduce variability between subsequent sampling events. Ra226 samples were filtered using a 0.45 um filter and subsequently acidified to a pH of approximately 1.5. Ra226 analyses were performed by Rio Algoma Process Development Laboratory, again to minimize variation between sampling events. The criterion followed in selecting the sample points for Ra226 analyses were to provide adequate coverage of the area of interest (M-1 to M-9). As part of this sampling effort a total of 32 samples (including 3 sets of duplicate samples) were submitted for analyses. The duplicate samples were collected for quality assurance reasons (to test the ability of the laboratory to duplicate its results over a range of concentrations). Duplicate sample results were:

| | | |
|---|---|---|
| M-1-6 (pCi/L) | 44 | 64 |
| M-8-6 (pCi/L) | 21 | 21 |
| M-9-3 (pCi/L) | 7.1 | 8.2 |

These values would indicate very good reproducibility at low and mid concentration levels with much less accuracy for high concentrations.

The results of the Ra226 analyses are presented in the form of concentration profiles in pCi/L in Figure 7.2 and in Appendix B. Also presented are the Ra226 concentrations based on Morin's data (1983, 1985). The main observations that can be made from this data are:

1. Little discernable movement for the 25 pCi/L concentration contour;
2. Ra226 concentrations are generally decreasing over time.

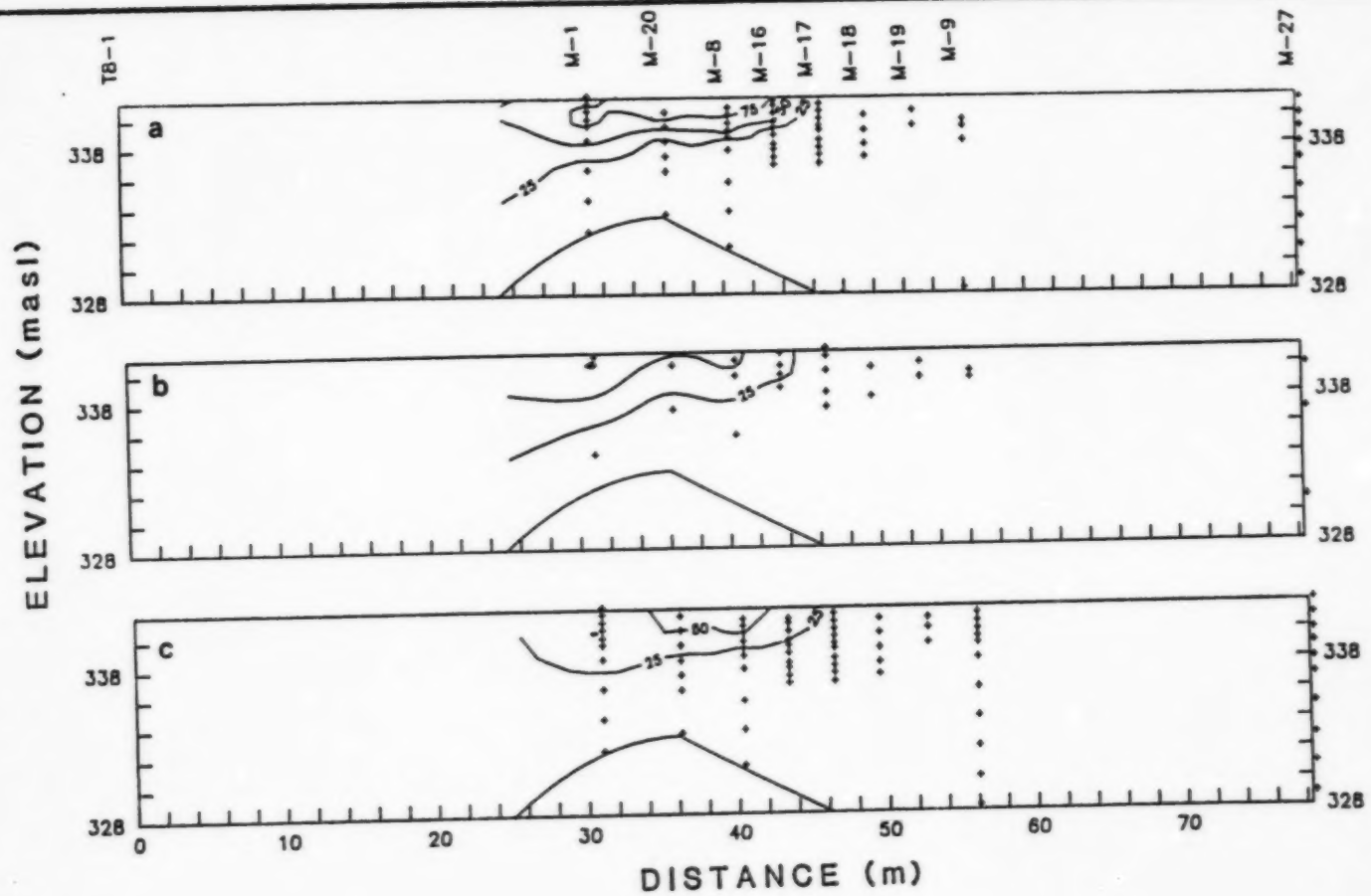


(a) 1983 (b) 1984 (c) 1989

| INTERA Technologies | Measured Ra226 Concentrations (pCi/L) | Figure 7.2 |
|---|---|---|

The implications of these observations in terms of their impact on predictions are discussed in the following section (Section 7.2).

## 7.2 COMPARISON OF PREDICTED AND MEASURED DATA

### 7.2.1 pH

Figure 7.3 presents measured and simulated concentration profiles for pH for 1989. At first glance it would appear that the shape of the pH profile is remarkably different from the predicted and sensitivity analysis simulations. However several aspects should be kept in mind when evaluating this comparison:

1. The consistency of the measured data over time;
2. The fit of the calibrated model.

For example, it would appear based on a comparison of 1983, 1984 and 1989 data that the pH data reported in 1984 is generally anomalous. It is possible that infiltration may have contributed to these apparent anomalous readings, however based on dilution calculations it is unlikely to be the sole cause. It is possible that temperature may have played a role in elevating the pH readings taken in November, 1984. Whatever the cause, this data could not be discounted prior to making the predictions. Consequently, the calibration of the model was based on an average of the 1983 and 1984 data. Secondly, it is unlikely that even if the pH data for 1984 had been discounted that the model could have accurately predicted the significant (vertical) movement of the pH = 5.0 and 5.5 contours. It is likely that a significant portion of this movement is attributable to infiltration of acid rain. Again the magnitude of this effect could not be discerned based on 1984 data.

In spite of these difficulties and the apparent differences in plume shape the model predictions for pH are not all poor. An examination of specific values for monitoring points (presented in Appendix B) indicated that for the vast majority of these points the difference between measured and predicted values was less than 0.5 pH units. Further it can be seen that the model does

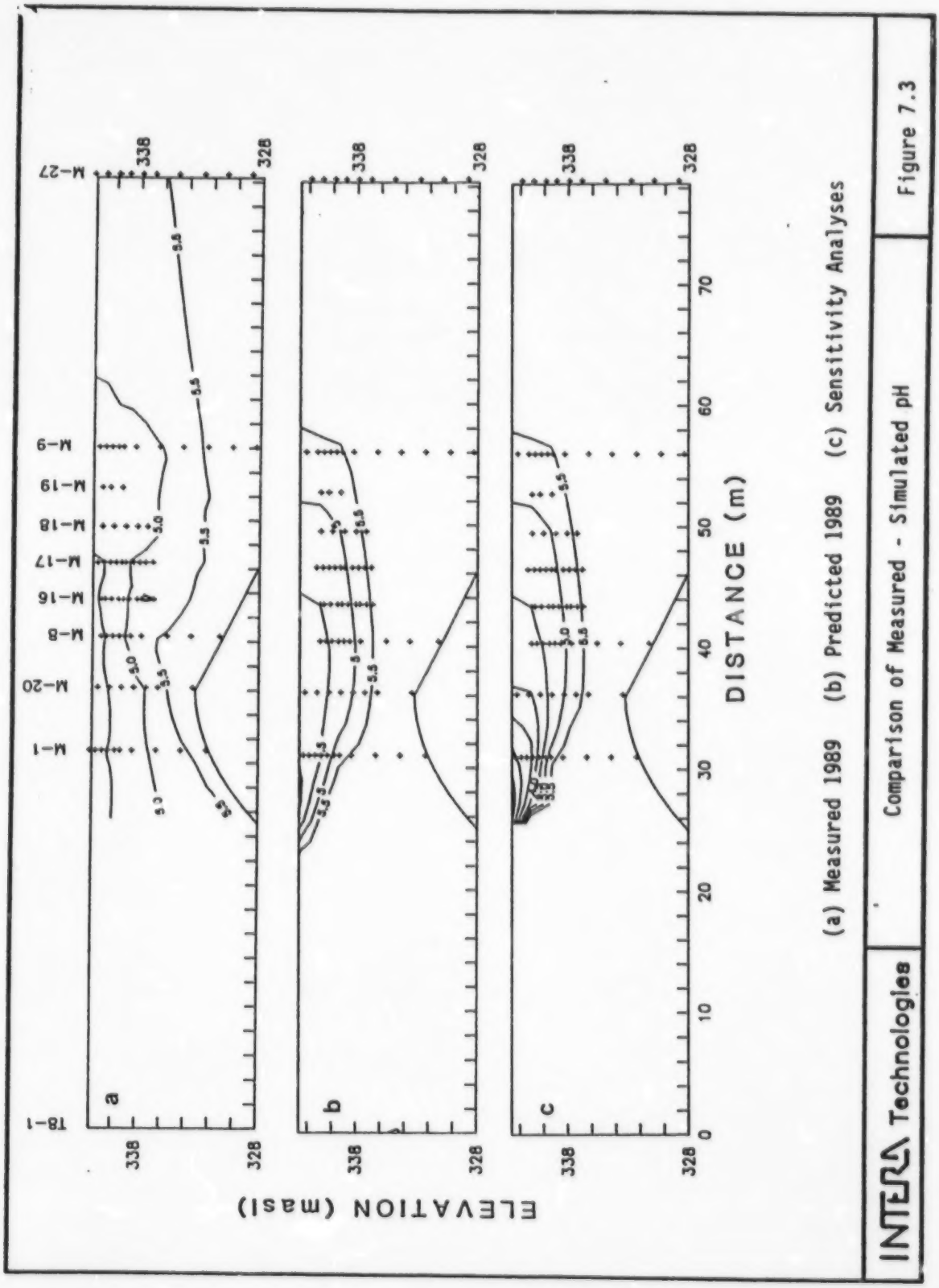


(a) Measured 1989 (b) Predicted 1989 (c) Sensitivity Analyses

INTERA Technologies | Comparison of Measured - Simulated pH | Figure 7.3

a better job of predicting both high concentrations (i.e., low pH values) and values near the centre of the monitoring section. For example values predicted for M-20, M-8, M-16, M-17 and (to a lesser extent) M-18 are quite close. The model does overpredict pH in the lower monitoring points of M-1, however this deficiency was also noted in the calibrated model based on the 1983/84 data.

Visual and quantitative measures of the relationship between model predicted pH and actual measured values for September 1989 are given in Figure 7.4. The scatter plot of predicted (calculated) and measured values shows better fit for the low pH values (<5.5) and model over prediction of pH for pH values greater than 5.5. The model overprediction of high pH values is likely attributable to vertical movement of pH 5.0 - 5.5 contours to depth which may be due to the effects of acid rain infiltration. The calculated correlation coefficient for the 1989 predicted vs. measured pH data is 0.73 similar to calibrated correlation coefficients of 0.69 to 0.77.

The model's ability to simulate and predict pH is considered acceptable only in areas where plume movement has been observed or for higher concentrations (i.e. low pH). There are a number of reasons for this, including the magnitude of interference effects, non-linear retardation behaviour, and the influence of heterogeneities on plume velocity. In addition, given the numerical limitations of the code one cannot rely on model results that are on the order of $10^{-3}$ (or less) than the source term (i.e. pH $\geq$ 6).

### 7.2.2. Ra226

The measured and simulated 1989 concentration profiles for Ra226 are presented in Figure 7.5. The same factors used in assessing the pH profiles should be remembered when assessing these profiles, namely the adequacy of the calibrated model and the consistency and reliability of the data. Based on the measured data profiles presented earlier (Figure 7.2) it can be seen that the data does show a fairly consistent trend, that of reducing Ra226 concentrations over time. However it is also apparent that the estimated plume velocity is much

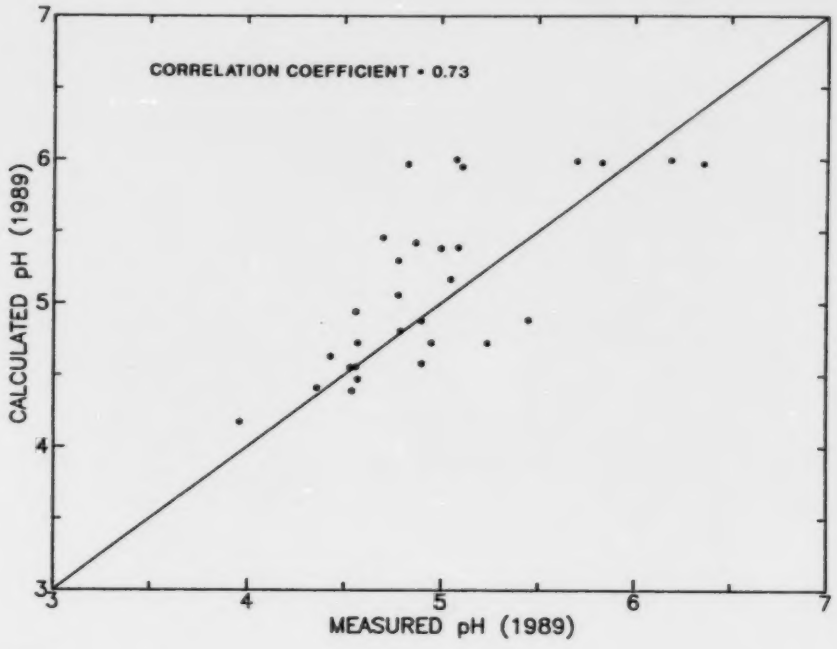


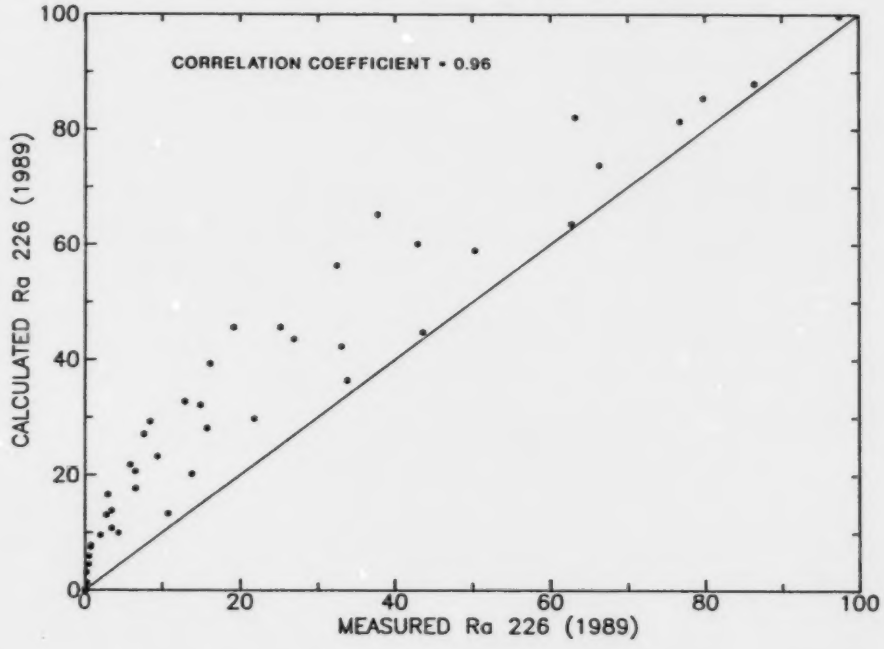


| | |
|---|---|
| Drawn by | Date |
| Checked by | Date |
| Revisions | Date |
| | |

Correlation plots for predicted and measured pH and Ra226 for 1989

INTERA Technologies

Figure 7.4

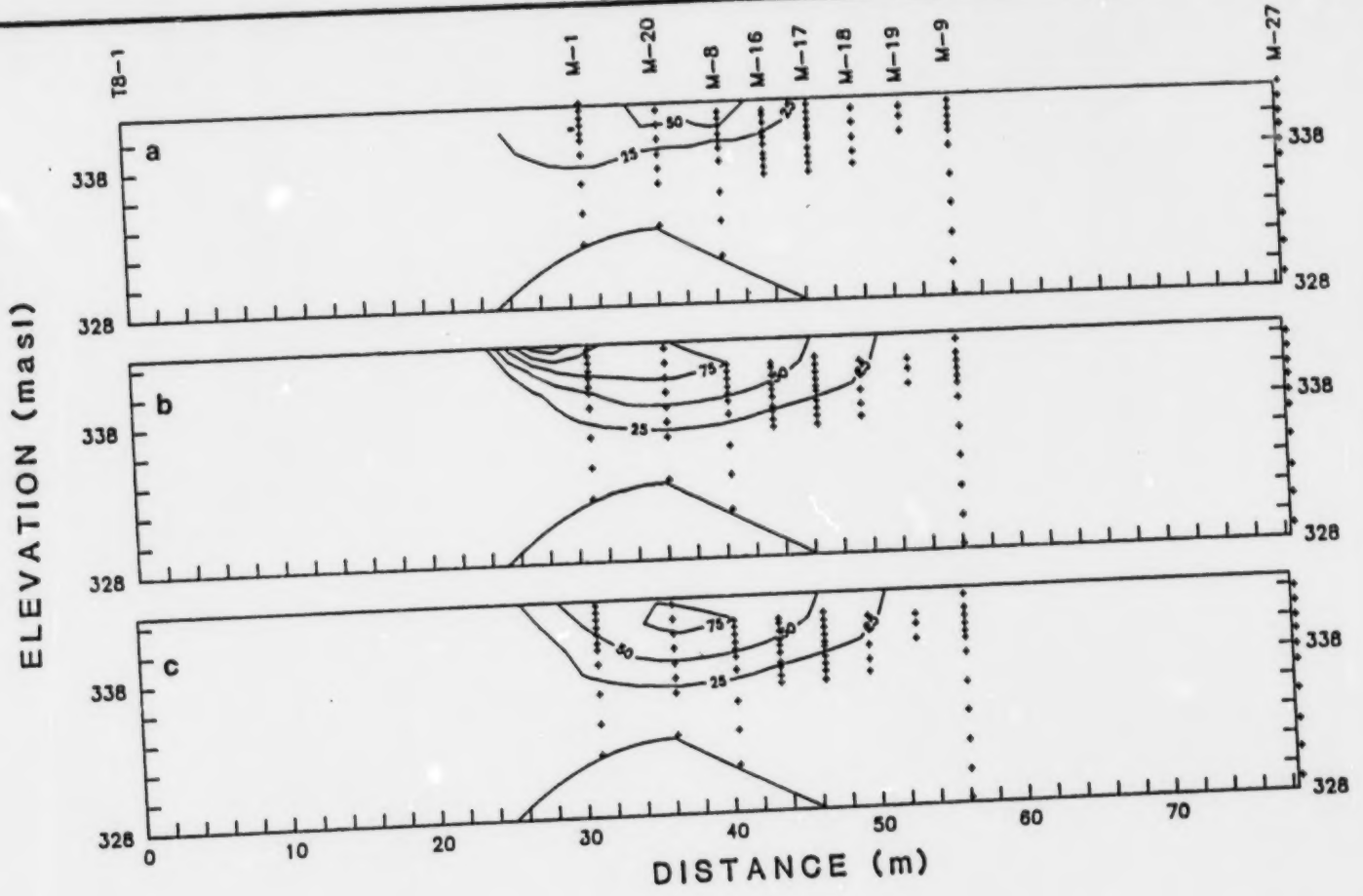


(a) Measured (b) Predicted (c) Sensitivity Analyses

| INTERA Technologies | Simulated Ra226 Contours (pCi/L) | Figure 7.5 |
|---|---|---|

less than the reported 1 or 2 m/yr. In fact based on the position of the 25 pCi/L contour (figure 7.2) it would appear no significant migration of the plume has occurred between 1984 and 1989. For this reason, the plume movement predicted by the model is much in excess of that measured in the field. In addition the peak concentrations of both the predicted (using constant source concentration) and sensitivity analysis (using a decreasing source) simulations are in excess of those predicted in the field. It is conceivable that the source term is dropping at an even faster rate than the linear model assumed in the sensitivity analyses simulation. However it is doubtful that even if the concentration were set to zero over the prediction period, that this could fully account for the apparent reduction in mass between 1983 and 1989.

The scatter plot of model predicted and actual field measured values of Ra226 are also shown in Figure 7.4. This figure shows a strong correlation between the predicted and measured Ra226 values with a correlation coefficient of 0.96. However this strong correlation is an artifact of the Ra226 data due to the significant lack of movement of the Ra226 plume and therefore similarity of the 1983/84 and 1989 data. Figure 7.4 does show that there was significant overprediction of Ra226 concentrations by the model.

# 8. CONCLUSIONS AND RECOMMENDATIONS

Based on the comparison of predicted and actual 1989 pH and Ra226 plume concentrations described in this study, the FEMWATER/FEMWASTE models have limited potential application for the accurate prediction of the migration of aqueous contaminants from uranium mine tailings areas. Although only pH and Ra226 migration were evaluated in this study, the FEMWATER/FEMWASTE codes provided adequate predictions only for the low pH (pH < 5.5) or "inner core" and Al $(OH)_3$ region (Cherry et. al., 1984) of the pH plume and only for a five (5) year period from 1984 to 1989. Extrapolation of the prediction period to larger temporal and spatial scales would likely be problematic due to uncertainty in source term concentration, the complex geochemical reactions that characterize acid tailings drainage and metal leaching and additional uncertainties in the physical flow system.

The following sections summarize our conclusions and recommendations regarding capabilities and limitations of the FEMWATER/FEMWASTE codes as determined from the verification tests and validation of a model of Seepage Area "A" of the Nordic Main tailings impoundment near Elliot Lake. Because Seepage Area "A" is the best instrumented and studied uranium tailings site in Canada, it is the best site for assessment of the FEMWATER/FEMWASTE models.

Only limited verification of the FEMWATER code was performed in this study. The verification consisted of comparison to earlier verification tests of a simple unsaturated flow problem by (WESAL, 1987). Although this verification of the partially saturated aspects of FEMWATER was deemed successful, the lack of specific data describing flow in the unsaturated zone at Seepage Area "A" precluded calibration and validation of this aspect of FEMWATER. Consequently the unsaturated flow components of the model have not been calibrated or validated in this study.

Calibration of the saturated flow components of the FEMWATER model was difficult at Seepage Area "A" despite the numerous hydrogeologic investigations and monitoring piezometers completed at the site. To obtain an acceptable fit

between measured and calculated hydraulic heads at this site it was necessary to invoke the presence of an equivalent low permeability layer below the tailings dam that subcrops in the middle of the "centreline" section. Although there is geologic and hydrogeologic evidence to support the existence of this layer, other explanations including streamline intersection with the "centreline" cross-section were also possible. Because FEMWATER is only a two-dimensional model it was not possible in this study to fully evaluate such alternate explanations. Consequently the two-dimensional nature of the FEMWATER model is considered a major limitation in its application of tailings sites. This is particularly a concern as most uranium tailings areas in Canada will likely be located in more complex hydrogeologic environments comprising glacial fluvial deposits and fractured bedrock.

Validation of the FEMWATER codes was not successful in this study due to a lack of data with which to compare the calibrated model. The original $Cl^-$ data was inappropriate for this purpose and the tracer migration experiment did not yield reliable estimates of interstitial groundwater velocities at the site.

The validation of FEMWATER at the Seepage Area "A" of the Nordic Main tailings impoundment has been unsuccessful and further work may be required. Such work should include additional data collection to enable calibration and validation of both the saturated and unsaturated flow aspects of the code. It is anticipated, based on the work completed in this study, that the FEMWATER model would be suitable for simulation of saturated groundwater flow at hydrogeologically simple mine tailings sites where streamlines are easily identified and therefore the two-dimensional aspect of the model in not a significant limitation.

The FEMWASTE model, which predicts dissolved species migration assuming advection-dispersion with Kd-based retardation, likely has less application than the FEMWATER models at uranium mine tailings sites.

The FEMWASTE model was partially verified in this study using both a pulse and continuous source term in one-dimensional uniform flow fields. Such

verification tests showed that the FEMWASTE model, similar to other numerical models, has poor numerical accuracy at relative solute concentrations of $10^{-3}$ and less particularly for pulse source problems. Consequently in some applications, for example with acid sources of 2 to 3 pH, calculated pH values of 5 to 6 and greater may be subject to significant numerical inaccuracies.

The attempt at validation of FEMWASTE at Seepage Area "A" for pH and Ra226 shows that FEMWASTE has only limited application at mine tailings sites. The calibration to 1983/84 data and subsequent validation to 1989 data suggests that only the "inner core" or low pH part of the acid plume can be predicted by FEMWASTE. However we caution the extrapolation of this finding to larger temporal and spatial scales at the Nordic site and to other sites for the following reasons:

- the simple Kd approach used in FEMWASTE is incapable of replicating the complex geochemical reactions that retard pH, metals and radionuclides migration at mine tailings sites;

- the source term will vary significantly over time.

Because FEMWASTE uses a simple Kd or partitioning approach to evaluate retardation, the FEMWASTE model cannot at one time accurately simulate the migration of different pH plumes, metals and radionuclides at mine tailings sites. For acid waters below about pH 5 there is likely no solid phase control of pH (Morin, 1985) and this "inner core" is geochemically less complex than the "neutralization zone" and "outer zone" described by Morin et al. (1988a). The lack of geochemical complexity in the "inner core" may explain the limited success of FEMWASTE at predicting the migration of the low pH plume at the Nordic site.

Migration of higher pH water (i.e. pH >5), radionuclides and metals at the Nordic site and at other uranium tailings sites is likely controlled by precipitation dissolution of the calcite-siderite solid solution, gypsum, Al-OH minerals and Fe-OH minerals (Morin et al., 1988a). Consequently the migration

of these species will be controlled by the solid phase chemistry of the aquifer materials and the groundwater chemistry. Because FEMWASTE in no way accounts for these variables, there is little hope that the model could effectively predict the migration of higher pH waters as well as radionuclides and metals. The significant difference between measured and calculated Ra226 and higher pH concentrations as part of the validation effort supports this conclusion. In the specific case of the Ra226, co-precipitation of Ra226 with siderite, calcite and gypsum (Morin et al., 1988b) may explain the removal of solute from the plume, the apparent stagnation of the plumes leading edge and the diminishing of peak concentrations in the plume. In the case of pH, the site conditions are further complicated by infiltration of acid rain.

A second major limitation in the use of FEMWASTE at tailings areas relates to the specification of the source term. Although FEMWASTE allows temporal variation of the source term to be specified, the FEMWASTE code does not itself consider the geochemical, biological and physical processes responsible for the generation of acidity and leaching of metals in uranium mine tailings. Such chemical processes include the oxidation of pyrite in the unsaturated zone and the subsequent buffering and leaching of metals in the saturated zone of the tailings. The significance of these processes will vary depending upon hydrogeologic conditions and the chemistry of the tailings solids. Because FEMWASTE does not consider these processes there is little hope that FEMWASTE alone could accurately simulate the temporal and spatial variation of source terms at uranium mine tailings sites.

In summary because of the two-dimensional limitations of FEMWATER and the inability of FEMWASTE to accurately predict the migration of pH or metals and radionuclides, it is recommended that the FEMWATER/FEMWASTE models not be used by AECB for accurate parameter evaluation. Further, this study has demonstrated that the data requirements for the application of a model such as FEMWATER/FEMWASTE are very significant. It is unlikely that most sites will ever have sufficient existing data to allow the construction of a model of this type to be used in an accurate predictive capacity.

It may be possible to explain some of the deviation between model calculated and observed values by collecting additional data to verify some of the assumptions made in this study. An example is the permeability and integrity of the lower till layer and the hydraulic gradients across it. This data would confirm (or refute) the assumption of a lower impermeable boundary. Another example is the collection of better stratigraphic information in the vicinity of the hypothesized low permeability material. Similarly cross-hole hydraulic tests could be used to verify the assumption of anisotropy.

Finally, while it is recognized that current modelling technology may not fully satisfy all of AECB's requirements for accurately predicting contaminant migration from tailings areas, the models examined and used as part of this study have some limitations that can be overcome by using alternate models. We would recommend that the AECB consider using a three dimensional (phreatic) groundwater flow model for the purpose of identifying streamtubes that could be coupled to multi-component geochemical model. Such approaches are currently being explored by other research organisations and are generally considered to be the most promising of available modelling technologies for coupled hydraulic geochemical groundwater processes.

## REFERENCES

Ball, J.W., E.A. Jenne, and D.K. Nordstrom, 1979. WATEQ2 - A computerized chemical model for trace and major element speciation and mineral equilibria of natural waters. In: E.A. Jenne (Editor), Chemical Modelling of Natural Waters. Am. Chem. Soc., Symp. Ser., 93:815-835.

Blair, R.D., J.A. Cherry, T.P. Lim and A.J. Vivyurka, 1980. Groundwater Monitoring and Contaminant Occurrence at an Abandoned Tailings Area, Elliot Lake, Ontario. Proceedings of the 1st International Conference on Uranium Mine Waste Disposal, Vancouver. Society of Mining Engineers of the American Institute of Mining Engineers, New York, p. 411-444.

Blowes, D.W. and R.W. Gillham, 1988. The Generation and quality of streamflow on inactive uranium tailings near Elliot Lake. J. of Cont. Hydrology 1(22).

Cherry, J.A., R.A. Blackport, N.M. Dubrovsky, R.W. Gillham, T.P. Lim, D. Murray, E.J. Reardon and D.J.A. Smyth, 1980. Subsurface hydrology and geochemical evolution of inactive pyritic tailings in the Elliot Lake uranium district, Canada. Proc. 3rd Symposium on Uranium Tailings Management, Colorado State University, Fort Collins, CO.

Cherry, John A., Kevin A. Morin, and Neil M. Dubrovsky, 1984. Modelling of Contaminant Migration in Acidic Groundwater Plumes at Uranium Tailings Impoundments: ADNEUT3. Final Report for Energy, Mines and Resources Contract OST83-00284, File number 20ST.23241-3-1663, 105 p.

Christie, L., D.F. Griffiths, A.R. Mitchell, and O.C. Zienkiewicz, 1976. Finite element methods for second order differential equations with significant first derivatives. Int. J. Num. Meth. Engrg. 10:1389-1396.

Cleary, R.W., 1978. Final report 208 project, Fin. Pe. 208 Proj., Nassau, Suffolk Reg. Plan, Bd., Hanppauge, New York.

Davis, S.N., D.J. Campbell, H.W. Bentley and T.J. Flynn, 1985 Ground Water Tracers. National Water Well Association, Worthington, Ohio, 200 pp.

Dubrovsky, N.M., 1986. Geochemical evolution of inactive pyritic tailings in the Elliot Lake Uranium District. Ph.D. thesis, Department of Earth Sciences, University of Waterloo, Waterloo, Ont.

Dubrovsky, N.M., J.A. Cherry, E.J. Reardon, A.J. Vivyurka, 1985. Geochemical evolution of inactive pyritic tailings in the Elliot Lake Uranium District. Can. Geotech. J., 22:110-127.

Duguid, J.O. and M. Reeves, 1976. Material transport in porous media: A finite-element Galerkin model. ORNL-4928. Oak Ridge National Laboratory, Oak Ridge, Tennessee, 198 pp.

Dupuit, J., Etudes Theoriques et Pratiques sur le Mouvement des Eaux dans les Canaux de Couverts et a Travers les Terrains Permeables, 2nd edn, Dunod, Paris, 304 pp., 1863.

Freeze, R.A. and J.A. Cherry, 1979. Groundwater. Prentice-Hall Inc.

Golder Associates and SENES Consultants Ltd., 1987. Assessment of Seepage Control Alternatives at Westner Lake Nordic Mine, Elliot Lake, Ontario. Report prepared for Rio Algom Ltd.

Haverkamp, M., M. Vuclin, J. Touma, P.J. Wierenga and G. Vachaud, 1977. A Comparison of Numerical Simulation Models for One-Dimensional Infiltration, Soil Sci. Soc. Am. J., vol. 41, pp. 285-294.

Intera Technologies Ltd., 1989. Progress Report: Calibration of FEMWATER/FEMWASTE. Prepared for Atomic Energy Control Board.

Moffet, D. and M. Tellier. 1978. Radiological Investigations of an Abandoned Tailings Area, J. Environ. Qual., Vol. 7, no. 3, 1978.

Morin, K.A., 1985. 1984 Geochemical Study of the Acidic Contaminant Plume Near the Nordic Main Tailings Impoundment, Elliot Lake, Ontario. Report for EMR Contract OSQ84-00229, DSS File No.: 26SQ23241-1689.

Morin, K.A., 1983. Prediction of Subsurface Contaminant Transport in Acidic Seepage from Uranium Tailings Impoundments, Volume I and II. Ph.D. thesis, Department of Earth Sciences, University of Waterloo, 713 p.

Morin, K.A. J.A. Cherry, T.P. Lim and A.J. Vivyurka, 1982. Contaminant Migration in a Sand Aquifer Near an Inactive Uranium Tailings Impoundment, Elliot Lake, Ontario. Canadian Geotechnical Journal, 19, p. 49-62.

Morin K.A. and J.A. Cherry, 1986. Trace amounts of siderite near a uranium-tailings impoundment, Elliot Lake, Ontario, and its implication in controlling contaminant migration in a sand aquifer. Chem. Geol. 56:117-134.

Morin, K.A. and J.A. Cherry, 1988. Migration of acidic groundwater seepage from uranium-tailings impoundments. 3. Simulation of the conceptual model with application to Seepage Area A. J. Contam Hydrol., 2:323-342.

Morin, K.A., J.A. Cherry, N.K. Dave, T.P. Lim and A.J. Vivyurka, 1988a. Migration of acidic groundwater seepage from uranium-tailings impoundments. 1. Field study and conceptual hydrogeochemical model. J. Contam. Hydrol., 2:271-303.

Morin, K.A., J.A. Cherry, N.K. Dave, T.P. Lim and A.J. Vivyurka, 1988b. Migration of acidic groundwater seepage from uranium-tailings impoundments. 2. Geochemical behavior of radionuclides in groundwater. J. Contam. Hydrol., 2:305-322.

Morrison Beatty Ltd., 1980. Hydrogeologic Investigation of the Nordic Tailings Ponds, Elliot Lake Ontario. Prepared for CANMET.

Ogata, A. and R.B. Banks, 1961. A solution of the differential equation of longitudinal dispersion in porous media. U.S. Geol. Survey, Prof. Paper No. 411-A.

Pickens, J.F. and G.E. Grisak, 1981. Scale-Dependent Dispersion in a Stratified Granular Aquifer. Water Resources Research, Vol.17, No.4, pp.1191-1211.

Reeves, M. and J.O. Duguid, 1975. Water movement through saturated-unsaturated porous media: A finite-element Galerkin model, ORNL-4927. Oak Ridge National Laboratory, Oak Ridge, Tennessee, 232 pp.

Reeves, M., D.S. Ward, N.D. Johns and R.M. Cranwell, 1985. Theory and Implementation for SWIFT II. The Sandia Waste - Isolation Flow and Transport Model for Fractured Media. Release 4.84, NUREG/CR-3328, SAND83-1159.

Sauty, J.P., 1980. An Analysis of Hydrodispersive Transfer in Aquifers. Water Resources Research, Vol. 16, No. 1, pp. 145-158.

Smart, P.L. and I.M.S. Laidlaw, 1977. An Evaluation of Some Flourescent Dyes for Water Tracing. Water Resources Research Vol.13, No.1, pp.15-33.

SENES Consultants Ltd., 1988. Prediction of Future Westner Lake Water Quality. Report prepared for Rio Algom Ltd.

SENES Consultants Ltd., 1986. Estimation of the Limits of Acid Generation by Bacterially Assisted Oxidation in Uranium Mill Tailings. Report prepared for NUTP.

Thiem, G., 1906. Hydrologische Methoden (Hydrologic Methods). J.M. Gebhardt, Leipzig, 56 pp.

Varga, R.S., 1962. Matrix Iterative Analysis. Prentice-Hall, Englewood Cliffs, New Jersey.

Water and Earth Science Associates Ltd., 1987. A Survey of Computer Codes for Flow and Contaminant Transport. Report prepared for AECB.

Yeh, G.T. and D.S. Ward, 1981. FEMWASTE: A Finite Element Model of WASTE Transport through saturated-unsaturated porous media. ORNL-5601. Oak Ridge National Laboratory, Oak Ridge, Tennessee.

Yeh, G.T. and D.S. Ward, 1980. FEMWATER: A Finite-Element Model of WATER Flow through saturated-unsaturated porous media. ORNL-5567. Oak Ridge National Laboratory, Oak Ridge, Tennessee.

# APPENDIX A

## Water Level Data

| NORDIC TAILINGS HEAD SURVEY | | | | | |
|---|---|---|---|---|---|
| INTERVAL NO. | ELEVATION OF TOP OF CENTRE PIPE (mASL) | 26 JUN 89 W.L. DEPTH BELOW CENTRE PIPE (m) | 26 JUN 89 CALCULATED HEAD (mASL) | 12 SEP 89 W.L. DEPTH BELOW CENTRE PIPE (m) | 12 SEP 89 CALCULATED HEAD (mASL) |
| M-1-C | 343.09 | 1.55 | 341.53 | 1.85 | 341.23 |
| M-1-1 | 343.09 | 1.76 | 341.33 | 2.04 | 341.04 |
| M-1-2 | 343.09 | 1.73 | 341.35 | 2.07 | 341.02 |
| M-1-3 | 343.09 | 1.06 | 342.03 | 1.47 | 341.61 |
| M-1-4 | 343.09 | 1.07 | 342.02 | 1.48 | 341.60 |
| M-1-5 | 343.09 | 1.08 | 342.01 | 1.48 | 341.60 |
| M-1-6 | 343.09 | 1.03 | 342.06 | 1.34 | 341.75 |
| M-1-7 | 343.09 | 1.02 | 342.07 | 1.35 | 341.73 |
| M-1-8 | 343.09 | 1.01 | 342.08 | 1.36 | 341.72 |
| M-1-9 | 343.09 | 1.02 | 342.07 | 1.32 D | |
| M-1-10 | 343.09 | 0.81 D | | 0.81 D | |
| M-2-C | 343.01 | 1.43 | 341.58 | 1.78 | 341.23 |
| M-2-1 | 343.01 | 1.47 | 341.54 | 1.79 | 341.22 |
| M-2-2 | 343.01 | 1.53 | 341.48 | 1.77 | 341.24 |
| M-2-3 | 343.01 | 1.71 | 341.30 | 2.00 | 341.01 |
| M-2-4 | 343.01 | 1.73 | 341.28 | 2.02 | 340.99 |
| M-2-5 | 343.01 | 1.73 | 341.28 | 1.79 | 341.22 |
| M-2-6 | 343.01 | 1.72 | 341.29 | 2.01 | 341.00 |
| M-2-7 | 343.01 | 1.57 | 341.44 | 1.37 B | |
| M-2-8 | 343.01 | 1.08 | 341.93 | 1.43 | 341.58 |
| M-2-9 | 343.01 | 1.08 | 341.93 | 1.45 | 341.56 |
| M-2-10 | 343.01 | 1.01 B | | 1.01 B | |
| M-2-11 | 343.01 | 1.08 | 341.93 | | |
| M-2-12 | 343.01 | 1.04 D | | 1.02 D | |
| M-3-C | 342.94 | 1.27 | 341.67 | | |
| M-3-1 | 342.94 | 1.52 | 341.42 | | |
| M-3-2 | 342.94 | 1.36 | 341.58 | | |
| M-3-3 | 342.94 | 1.37 | 341.57 | | |
| M-3-4 | 342.94 | 1.14 | 341.80 | | |
| M-3-5 | 342.94 | 1.07 | 341.87 | | |
| M-3-6 | 342.94 | 1.04 | 341.90 | | |
| M-3-7 | 342.94 | 1.02 | 341.92 | | |
| M-3-8 | 342.94 | 0.91 | 342.03 | | |
| M-3-9 | 342.94 | 0.90 | 342.04 | | |
| M-3-10 | 342.94 | 1.00 | 341.94 | | |
| M-3-11 | 342.94 | 0.98 | 341.96 | | |
| M-3-12 | 342.94 | 1.06 | 341.88 | | |
| M-4-C | 343.09 | 1.51 | 341.58 | | |

B = BLOCKED D = DRY

| | | | | | | |
|---|---|---|---|---|---|---|
| M-4-1 | 343.09 | 1.51 | | 341.58 | | |
| M-4-2 | 343.09 | 1.50 | | 341.59 | | |
| M-4-3 | 343.09 | 1.50 | | 341.59 | | |
| M-4-4 | 343.09 | | B | | | |
| M-4-5 | 343.09 | 1.34 | | 341.75 | | |
| M-4-6 | 343.09 | | B | | | |
| M-4-7 | 343.09 | | B | | | |
| M-4-8 | 343.09 | 1.22 | | 341.87 | | |
| M-4-9 | 343.09 | 1.13 | | 341.96 | | |
| M-4-10 | 343.09 | 1.22 | | 341.87 | | |
| M-4-11 | 343.09 | | B | | | |
| M-4-12 | 343.09 | | B | | | |
| M-5-C | 342.79 | 1.29 | | 341.50 | | |
| M-5-1 | 342.79 | 1.29 | | 341.50 | | |
| M-5-2 | 342.79 | 1.30 | | 341.49 | | |
| M-5-3 | 342.79 | 1.20 | | 341.59 | | |
| M-5-4 | 342.79 | 1.27 | | 341.52 | | |
| M-5-5 | 342.79 | 1.00 | B | | | |
| M-5-6 | 342.79 | 0.99 | | 341.80 | | |
| M-5-7 | 342.79 | 0.98 | | 341.81 | | |
| M-5-8 | 342.79 | 0.98 | | 341.81 | | |
| M-5-9 | 342.79 | 0.83 | B | | | |
| M-5-10 | 342.79 | 0.98 | | 341.81 | | |
| M-5-11 | 342.79 | 0.98 | | 341.81 | | |
| M-5-12 | 342.79 | | B | | | |
| M-6-C | 342.79 | 1.37 | | 341.42 | | |
| M-6-1 | 342.79 | 1.35 | | 341.44 | | |
| M-6-2 | 342.79 | 1.41 | | 341.38 | | |
| M-6-3 | 342.79 | 1.40 | | 341.39 | | |
| M-6-4 | 342.79 | 1.40 | | 341.39 | | |
| M-6-5 | 342.79 | 1.32 | | 341.47 | | |
| M-6-6 | 342.79 | 1.21 | | 341.58 | | |
| M-6-7 | 342.79 | 1.14 | | 341.65 | | |
| M-6-8 | 342.79 | 1.10 | | 341.69 | | |
| M-6-9 | 342.79 | 1.06 | | 341.73 | | |
| M-6-10 | 342.79 | 1.01 | | 341.78 | | |
| M-6-11 | 342.79 | 1.00 | | 341.79 | | |
| M-6-12 | 342.79 | 1.07 | | 341.72 | | |
| M-7-C | 342.63 | 1.27 | | 341.36 | 1.55 | 341.08 |
| M-7-1 | 342.63 | 1.28 | | 341.35 | 1.56 | 341.07 |
| M-7-2 | 342.63 | 1.35 | | 341.28 | 1.54 | 341.09 |
| M-7-3 | 342.63 | 1.35 | | 341.28 | 1.63 | 341.00 |
| M-7-4 | 342.63 | 1.36 | | 341.27 | 1.66 | 340.97 |
| M-7-5 | 342.63 | 1.38 | | 341.25 | 1.67 | 340.96 |
| M-7-6 | 342.63 | 1.35 | | 341.28 | 1.66 | 340.97 |

B = BLOCKED D = DRY

| | | | | | | |
|---|---|---|---|---|---|---|
| M-7-7 | 342.63 | 1.37 | | 341.26 | 1.67 | 340.96 |
| M-7-8 | 342.63 | 1.39 | | 341.24 | 1.67 | 340.96 |
| M-7-9 | 342.63 | 1.38 | | 341.25 | 1.67 | 340.96 |
| M-7-10 | 342.63 | 1.29 | | 341.34 | 1.62 | 341.01 |
| M-7-11 | 342.63 | 1.15 | | 341.48 | 1.58 | 341.05 |
| M-7-12 | 342.63 | 1.03 | | 341.60 | 1.13 | 341.50 |
| M-8-C | 342.78 | 1.41 | | 341.37 | 1.70 | 341.08 |
| M-8-1 | 342.78 | 1.56 | | 341.22 | 1.81 | 340.97 |
| M-8-2 | 342.78 | 1.58 | | 341.20 | 1.83 | 340.95 |
| M-8-3 | 342.78 | 1.60 | | 341.18 | 1.83 | 340.95 |
| M-8-4 | 342.78 | 1.60 | | 341.18 | 1.86 | 340.92 |
| M-8-5 | 342.78 | 1.58 | | 341.20 | 1.85 | 340.93 |
| M-8-6 | 342.78 | 1.57 | | 341.21 | 1.85 | 340.93 |
| M-8-7 | 342.78 | 1.54 | | 341.24 | 1.81 | 340.97 |
| M-8-8 | 342.78 | 1.19 | | 341.59 | 1.49 | 341.29 |
| M-8-9 | 342.78 | 1.15 | | 341.63 | 1.48 | 341.30 |
| M-9-C | 342.76 | 1.65 | | 341.11 | 1.91 | 340.85 |
| M-9-1 | 342.76 | | B | | | |
| M-9-2 | 342.76 | | B | | | |
| M-9-3 | 342.76 | 1.74 | | 341.02 | 1.97 | 340.79 |
| M-9-4 | 342.76 | | B | | | |
| M-9-5 | 342.76 | | B | | | |
| M-9-6 | 342.76 | 1.67 | B | | 1.67 | 341.09 |
| M-9-7 | 342.76 | | B | | | |
| M-9-8 | 342.76 | | B | | | |
| M-9-9 | 342.76 | | B | | | |
| M-9-10 | 342.76 | | B | | | |
| M-9-11 | 342.76 | | B | | | |
| M-10-C | 342.65 | 1.13 | | 341.52 | | |
| M-10-1 | 342.65 | 1.80 | | 340.85 | | |
| M-10-2 | 342.65 | 1.84 | | 340.81 | | |
| M-10-3 | 342.65 | 1.88 | | 340.77 | | |
| M-10-4 | 342.65 | 1.90 | | 340.75 | | |
| M-10-5 | 342.65 | 1.81 | | 340.84 | | |
| M-10-6 | 342.65 | 1.82 | | 340.83 | | |
| M-10-7 | 342.65 | 1.82 | | 340.83 | | |
| M-10-8 | 342.65 | 1.89 | | 340.76 | | |
| M-10-9 | 342.65 | 1.02 | B | | | |
| M-11-C | 342.01 | 1.54 | | 340.47 | | |
| M-11-1 | 342.01 | 1.50 | | 340.51 | | |
| M-11-2 | 342.01 | 1.51 | | 340.50 | | |
| M-11-3 | 342.01 | 1.49 | | 340.52 | | |
| M-11-4 | 342.01 | 1.40 | | 340.61 | | |
| M-11-5 | 342.01 | 1.46 | B | | | |
| M-11-6 | 342.01 | 1.55 | | 340.46 | | |

B = BLOCKED D = DRY

| | | | | | | |
|---|---|---|---|---|---|---|
| M-11-7 | 342.01 | 1.44 | | 340.57 | | |
| M-11-8 | 342.01 | 1.55 | | 340.46 | | |
| M-11-9 | 342.01 | 1.51 | | 340.50 | | |
| M-12 | | | | | | |
| M-13 | | | | | | |
| M-16-C | 342.78 | 1.62 | | 341.16 | 1.87 | 340.91 |
| M-17-C | 342.75 | 1.65 | | 341.10 | 1.87 | 340.88 |
| M-18-1 | 342.78 | 1.57 | | 341.21 | 1.89 | 340.89 |
| M-18-2 | 342.78 | 1.72 | | 341.06 | 1.95 | 340.83 |
| M-18-3 | 342.78 | 1.72 | | 341.06 | 1.97 | 340.81 |
| M-18-4 | 342.78 | 1.72 | | 341.06 | 1.95 | 340.83 |
| M-18-5 | 342.78 | 1.70 | | 341.08 | 1.94 | 340.84 |
| M-19-1 | 342.78 | 1.41 | | 341.37 | 1.52 | 341.26 |
| M-19-2 | 342.78 | 1.74 | | 341.04 | 1.97 | 340.81 |
| M-19-3 | 342.78 | 1.74 | | 341.04 | 1.97 | 340.81 |
| M-20-C | 343.39 | 2.13 | | 341.26 | 2.36 | 341.03 |
| M-20-1 | 343.39 | 2.17 | | 341.22 | 2.22 | 341.17 |
| M-20-2 | 343.39 | 2.18 | | 341.21 | 2.44 | 340.95 |
| M-20-3 | 343.39 | 1.40 | B | | | |
| M-20-4 | 343.39 | 1.40 | | 341.99 | 1.80 | 341.59 |
| M-20-5 | 343.39 | 1.38 | B | | | |
| M-20-6 | 343.39 | 1.39 | | 342.00 | 1.64 | 341.75 |
| M-20-7 | 343.39 | 1.27 | B | | | |
| M-21-C | 343.26 | 2.02 | | 341.24 | 2.30 | 340.96 |
| M-21-1 | 343.26 | 2.02 | | 341.24 | 2.29 | 340.97 |
| M-21-2 | 343.26 | 2.07 | | 341.19 | 2.31 | 340.95 |
| M-21-3 | 343.26 | 2.10 | | 341.16 | 1.88 | 341.38 |
| M-21-4 | 343.26 | 2.09 | | 341.17 | 2.36 | 340.90 |
| M-21-5 | 343.26 | 2.08 | | 341.18 | 2.30 | 340.96 |
| M-21-6 | 343.26 | 2.03 | | 341.23 | 2.33 | 340.93 |
| M-21-7 | 343.26 | 1.99 | | 341.27 | 2.28 | 340.98 |
| M-21-8 | 343.26 | 1.60 | | 341.66 | 1.89 | 341.37 |
| M-21-9 | 343.26 | 1.00 | B | | 0.97 | B |
| M-22-C | 342.35 | 0.97 | | 341.38 | 1.24 | 341.11 |
| M-22-1 | 342.35 | 1.00 | | 341.35 | 1.18 | 341.17 |
| M-22-2 | 342.35 | | B | | | |
| M-22-3 | 342.35 | 1.06 | | 341.29 | 1.34 | 341.01 |
| M-22-4 | 342.35 | 1.08 | | 341.27 | 1.16 | 341.19 |
| M-22-5 | 342.35 | 1.08 | | 341.27 | 1.30 | 341.05 |
| M-22-6 | 342.35 | 1.09 | | 341.26 | 1.24 | 341.11 |
| M-22-7 | 342.35 | 1.10 | | 341.25 | 1.36 | 340.99 |
| M-22-8 | 342.35 | 1.11 | | 341.24 | 1.38 | 340.97 |
| M-22-9 | 342.35 | 0.98 | | 341.37 | 1.26 | 341.09 |
| M-23-C | 342.80 | 1.38 | | 341.42 | | |
| M-23-1 | 342.80 | 1.41 | | 341.39 | | |

B = BLOCKED D = DRY

| | | | | | | | |
|---|---|---|---|---|---|---|---|
| M-23-2 | 342.80 | 1.44 | | 341.36 | | | |
| M-23-3 | 342.80 | 1.45 | | 341.35 | | | |
| M-23-4 | 342.80 | 1.47 | | 341.33 | | | |
| M-23-5 | 342.80 | 1.40 | | 341.40 | | | |
| M-23-6 | 342.80 | 1.34 | | 341.46 | | | |
| M-23-7 | 342.80 | 1.31 | | 341.49 | | | |
| M-23-8 | 342.80 | 1.30 | | 341.50 | | | |
| M-23-9 | 342.80 | 1.25 | | 341.55 | | | |
| M-23-10 | 342.80 | 0.85 | D | | | | |
| M-24-C | 342.54 | 1.32 | | 341.22 | 1.59 | | 340.95 |
| M-24-1 | 342.54 | 1.42 | | 341.12 | 1.62 | | 340.92 |
| M-24-2 | 342.54 | 1.37 | | 341.17 | 1.62 | | 340.92 |
| M-24-3 | 342.54 | 1.39 | | 341.15 | 1.64 | | 340.90 |
| M-24-4 | 342.54 | 1.40 | | 341.14 | 1.66 | | 340.88 |
| M-24-5 | 342.54 | 1.43 | | 341.11 | 1.69 | | 340.85 |
| M-24-6 | 342.54 | 1.19 | | 341.35 | 1.49 | B | 341.05 |
| M-25-C | 342.51 | 1.10 | | 341.41 | | | |
| M-25-1 | 342.51 | 1.34 | | 341.17 | | | |
| M-25-2 | 342.51 | 1.40 | | 341.11 | | | |
| M-25-3 | 342.51 | 1.40 | | 341.11 | | | |
| M-25-4 | 342.51 | 1.37 | | 341.14 | | | |
| M-25-5 | 342.51 | 1.41 | | 341.10 | | | |
| M-25-6 | 342.51 | 1.41 | | 341.10 | | | |
| M-25-7 | 342.51 | 1.42 | | 341.09 | | | |
| M-25-8 | 342.51 | 1.13 | | 341.38 | | | |
| M-25-9 | 342.51 | 0.91 | | 341.60 | | | |
| M-25-10 | 342.51 | 0.54 | D | | | | |
| M-26-C | 342.63 | 1.45 | | 341.18 | | | |
| M-26-1 | 342.63 | 1.47 | | 341.16 | | | |
| M-26-2 | 342.63 | 1.50 | | 341.13 | | | |
| M-26-3 | 342.63 | 1.52 | | 341.11 | | | |
| M-26-4 | 342.63 | 1.52 | | 341.11 | | | |
| M-26-5 | 342.63 | 1.52 | | 341.11 | | | |
| M-26-6 | 342.63 | 1.54 | | 341.09 | | | |
| M-26-7 | 342.63 | 1.54 | | 341.09 | | | |
| M-26-8 | 342.63 | 1.54 | | 341.09 | | | |
| M-26-9 | 342.63 | 1.52 | | 341.11 | | | |
| M-26-10 | 342.63 | 1.05 | D | | | | |
| M-26-11 | 342.63 | 0.39 | D | | | | |
| M-27-C | 342.51 | 1.48 | | 341.03 | 1.73 | | 340.78 |
| M-27-1 | 342.51 | 1.53 | | 340.98 | 1.76 | | 340.75 |
| M-27-2 | 342.51 | 1.57 | | 340.94 | 1.78 | | 340.73 |
| M-27-3 | 342.51 | 1.59 | | 340.92 | 1.80 | | 340.71 |
| M-27-4 | 342.51 | 1.61 | | 340.90 | 1.81 | | 340.70 |
| M-27-5 | 342.51 | 1.60 | | 340.91 | 1.80 | | 340.71 |

B = BLOCKED D = DRY

| | | | | | | |
|---|---|---|---|---|---|---|
| M-27-6 | 342.51 | 1.60 | | 340.91 | 1.69 | 340.82 |
| M-27-7 | 342.51 | 1.61 | | 340.90 | 1.82 | 340.69 |
| M-27-8 | 342.51 | 1.55 | | 340.96 | 1.71 | 340.80 |
| M-27-9 | 342.51 | 0.80 | D | | | D |
| EMR-1 | 342.83 | 1.67 | | 341.16 | 1.95 | 340.88 |
| EMR-A | 342.70 | 1.55 | | 341.15 | 1.82 | 340.88 |
| EMR-B | 342.63 | 1.50 | | 341.13 | 1.75 | 340.88 |
| EMR-C | 342.78 | 1.48 | | 341.30 | 1.81 | 340.97 |
| EMR-D | 342.62 | 1.47 | | 341.15 | 1.74 | 340.88 |
| EMR-E | 342.55 | 1.40 | | 341.15 | 1.66 | 340.89 |
| WW-1 | 342.32 | 1.20 | | 341.12 | 1.45 | 340.87 |
| DP-1 | 342.52 | 1.11 | | 341.41 | 1.10 | 341.42 |
| DP-2 | 342.70 | 1.22 | | 341.48 | 1.44 | 341.26 |

B = BLOCKED D = DRY

# APPENDIX B

## Chemical Analyses and Predictions

Table B.1 : Calculated and Simulated pH Values

| MONITORING INTERVAL | pH DATA 1983 | 1984 | 1989 | CALCULATED VALUES 1983/84 | 1989 PREDICT | 1989 SENS.ANALYSIS |
|---|---|---|---|---|---|---|
| M1-C | 5.7 | - | | 5.995 | 6.007 | 6.014 |
| M1-1 | 5.9 | 6.21 | | 5.990 | 5.988 | 5.980 |
| M1-2 | 5.7 | 6.02 | 5.11 | 5.953 | 5.949 | 5.266 |
| M1-3 | 5.8 | 5.19 | | 5.640 | 5.623 | 4.393 |
| M1-4 | 4.5 | 4.72 | 4.70 | 5.448 | 5.455 | 3.940 |
| M1-5 | 4.6 | 4.71 | | 4.936 | 4.939 | 3.623 |
| M1-6 | 4.4 | 4.69 | 4.56 | 4.936 | 4.939 | 3.623 |
| M1-7 | 4.5 | 4.60 | | 4.409 | 4.410 | 3.379 |
| M1-8 | 4.3 | 4.65 | 4.36 | 4.409 | 4.410 | 3.379 |
| M1-9 | - | 4.04 | 3.96 | 4.171 | 4.171 | 3.283 |
| M1-10 | - | 4.61 | | 4.171 | 4.171 | 3.283 |
| M20-C | 6.1 | - | 6.19 | 5.997 | 5.997 | 5.971 |
| M20-1 | 5.9 | 6.03 | | 5.765 | 5.633 | 5.113 |
| M20-2 | 6.4 | 6.02 | 5.00 | 5.523 | 5.380 | 4.946 |
| M20-3 | 5.5 | 5.96 | | 5.207 | 5.090 | 4.752 |
| M20-4 | 4.9 | 5.81 | 4.79 | 4.876 | 4.805 | 4.530 |
| M20-5 | 4.5 | 5.54 | 4.53 | 4.593 | 4.552 | 4.305 |
| M20-6 | - | 5.02 | | 4.399 | 4.376 | 4.076 |
| M20-7 | - | 6.05 | | 4.372 | 4.354 | 4.061 |
| M8-C | 5.8 | - | | 6.104 | 6.103 | 6.107 |
| M8-1 | 5.8 | 6.11 | 5.83 | 5.991 | 5.979 | 5.833 |
| M8-2 | 5.6 | 5.92 | | 5.949 | 5.804 | 5.367 |
| M8-3 | 5.6 | 5.97 | | 5.482 | 5.239 | 4.987 |
| M8-4 | 5.7 | 5.89 | 5.45 | 5.095 | 4.884 | 4.811 |
| M8-5 | 4.6 | 4.61 | | 4.714 | 4.580 | 4.663 |
| M8-6 | 4.7 | 4.68 | 4.90 | 4.714 | 4.580 | 4.663 |
| M8-7 | 4.5 | 4.58 | | 4.491 | 4.389 | 4.507 |
| M8-8 | 4.4 | 4.46 | 4.54 | 4.491 | 4.389 | 4.507 |
| M8-9 | - | 4.52 | | 4.491 | 4.389 | 4.507 |
| M16-C | 5.8 | - | | 5.931 | 5.706 | 5.341 |
| M16-1 | 5.7 | 5.64 | 4.87 | 5.746 | 5.419 | 5.163 |
| M16-2 | 5.5 | 5.93 | | 5.572 | 5.229 | 5.061 |
| M16-3 | 5.6 | 5.91 | | 5.323 | 5.015 | 4.933 |
| M16-4 | 5.5 | 6.00 | | 5.323 | 5.015 | 4.933 |
| M16-5 | 5.0 | 5.71 | 5.24 | 4.958 | 4.723 | 4.791 |
| M16-6 | 4.6 | 4.75 | 4.57 | 4.958 | 4.723 | 4.791 |
| M16-7 | 4.4 | 4.64 | 4.56 | 4.776 | 4.556 | 4.704 |
| M16-8 | 4.3 | 4.69 | | 4.776 | 4.556 | 4.704 |
| M16-9 | 4.4 | 4.59 | 4.57 | 4.689 | 4.470 | 4.642 |
| M17-C | 5.4 | - | | 5.913 | 5.595 | 5.380 |
| M17-1 | 5.3 | 5.93 | | 5.913 | 5.595 | 5.380 |
| M17-2 | 5.4 | 5.73 | 5.09 | 5.782 | 5.388 | 5.253 |
| M17-3 | 5.7 | 5.69 | 5.05 | 5.565 | 5.167 | 5.104 |
| M17-4 | 5.3 | 5.88 | | 5.226 | 4.874 | 4.925 |
| M17-5 | 5.4 | 5.85 | | 5.226 | 4.874 | 4.925 |
| M17-6 | 4.9 | 4.74 | 4.95 | 5.071 | 4.724 | 4.853 |
| M17-7 | 4.2 | 4.35 | | 5.071 | 4.724 | 4.853 |
| M17-8 | 3.3 | 4.26 | 4.43 | 4.972 | 4.630 | 4.791 |
| M17-9 | - | 4.11 | | 4.972 | 4.630 | 4.791 |
| M18-1 | 5.7 | 5.92 | | 5.970 | 5.734 | 5.601 |
| M18-2 | 5.8 | 5.97 | 4.78 | 5.736 | 5.296 | 5.273 |
| M18-3 | 5.5 | 5.43 | | 5.485 | 5.026 | 5.085 |

| | | | | | | |
|---|---|---|---|---|---|---|
| M18-4 | 4.7 | 4.92 | 4.90 | 5.346 | 4.878 | 5.001 |
| M18-5 | - | 5.36 | | 5.290 | 4.822 | 4.971 |
| M19-1 | 5.4 | 5.50 | | 6.018 | 6.014 | 6.015 |
| M19-2 | 5.2 | 5.60 | 4.83 | 5.970 | 5.967 | 5.967 |
| M19-3 | - | - | 4.78 | 5.627 | 5.056 | 5.191 |
| M9-C | 5.9 | - | 6.36 | 5.978 | 5.973 | 5.973 |
| M9-1 | - | - | | 6.021 | 6.022 | 6.022 |
| M9-2 | - | - | 5.70 | 5.991 | 5.991 | 5.990 |
| M9-3 | - | - | 5.08 | 6.001 | 6.000 | 5.997 |
| M9-4 | - | - | | 5.996 | 5.991 | 5.981 |
| M9-5 | 5.5 | 6.09 | | 5.968 | 5.669 | 5.693 |
| M9-6 | 5.4 | 5.94 | | 5.916 | 5.465 | 5.529 |
| M9-7 | 5.2 | 5.39 | | 5.887 | 5.362 | 5.461 |
| M9-8 | - | - | | 5.887 | 5.362 | 5.461 |
| M9-9 | - | - | | 5.891 | 5.342 | 5.456 |
| M9-10 | - | - | | 5.891 | 5.342 | 5.456 |

Table B.2 : Calculated and simulated Ra 226 Values (pCi/L)

| MONITORING INTERVAL | Ra DATA 1983 | 1984 | 1989 | CALCULATED VALUES 1983/84 | 1989 PREDICT | 1989 SENS.ANALYSIS |
|---|---|---|---|---|---|---|
| M1-C | 4. | | | .04 | .10 | .10 |
| M1-1 | 2. | 2. | | .04 | .10 | .10 |
| M1-2 | 6. | | 6.4 | 10.77 | 13.30 | 13.28 |
| M1-3 | 52. | | | 33.83 | 36.44 | 34.17 |
| M1-4 | 79. | | 49. | 43.62 | 44.82 | 36.70 |
| M1-5 | 75. | | | 62.69 | 63.59 | 45.89 |
| M1-6 | 100. | 79. | 54. | 62.69 | 63.59 | 45.89 |
| M1-7 | 75. | 72. | | 86.41 | 88.00 | 56.31 |
| M1-8 | 54. | | 46. | 86.41 | 88.00 | 56.31 |
| M1-9 | | | 20. | 97.49 | 99.68 | 59.90 |
| M1-10 | | | | 97.49 | 99.68 | 59.90 |
| M20-C | 6. | | 2.4 | .04 | .18 | .18 |
| M20-1 | 4. | | | 13.86 | 20.18 | 20.18 |
| M20-2 | 9. | 8. | 11. | 21.80 | 29.77 | 29.72 |
| M20-3 | 7. | | | 33.08 | 42.34 | 42.10 |
| M20-4 | 49. | | 26. | 50.30 | 58.99 | 58.24 |
| M20-5 | 94. | 44. | 57. | 66.28 | 73.82 | 71.85 |
| M20-6 | | | | 79.75 | 85.47 | 80.98 |
| M20-7 | | | | 76.69 | 81.45 | 76.62 |
| M8-C | 1. | | | .04 | .10 | .10 |
| M8-1 | 2. | | 5.7 | .27 | 1.31 | 1.31 |
| M8-2 | 6. | 6. | | 4.34 | 9.94 | 9.94 |
| M8-3 | 7. | | | 15.80 | 28.11 | 28.10 |
| M8-4 | 7. | | 7.4 | 26.91 | 43.59 | 43.59 |
| M8-5 | 64. | | | 42.92 | 60.12 | 60.05 |
| M8-6 | 61. | 43. | 21. | 42.92 | 60.12 | 60.05 |
| M8-7 | 68. | | | 63.18 | 82.10 | 81.86 |
| M8-8 | 94. | 55. | 59. | 63.18 | 82.10 | 81.86 |
| M8-9 | | | | 63.18 | 82.10 | 81.86 |
| M16-C | 7. | | | 3.45 | 10.70 | 10.70 |
| M16-1 | 8. | | 10. | 6.57 | 17.67 | 17.67 |
| M16-2 | 7. | | | 9.40 | 23.22 | 23.22 |
| M16-3 | 8. | | | 14.96 | 32.13 | 32.13 |
| M16-4 | 6. | 7. | | 14.96 | 32.13 | 32.13 |
| M16-5 | 9. | | 9.6 | 25.15 | 45.65 | 45.64 |
| M16-6 | 45. | 39. | 36. | 25.15 | 45.65 | 45.64 |
| M16-7 | 74. | 34. | 43. | 32.45 | 56.36 | 56.35 |
| M16-8 | 62. | | | 32.45 | 56.36 | 56.35 |
| M16-9 | 81. | 33. | 42. | 37.72 | 65.20 | 65.20 |
| M17-C | 2. | | | 2.03 | 9.54 | 9.54 |
| M17-1 | 3. | 7. | | 2.03 | 9.54 | 9.54 |
| M17-2 | 5. | | 7.2 | 3.46 | 13.80 | 13.80 |
| M17-3 | 5. | 8. | 8.6 | 6.55 | 20.66 | 20.66 |
| M17-4 | 6. | | | 12.98 | 32.75 | 32.75 |
| M17-5 | 8. | | | 12.98 | 32.75 | 32.75 |
| M17-6 | 13. | 20. | 8.5 | 16.19 | 39.28 | 39.28 |
| M17-7 | 11. | | | 16.19 | 39.28 | 39.28 |
| M17-8 | 11. | 12. | 16. | 19.16 | 45.62 | 45.62 |
| M17-9 | | 9. | | 19.16 | 45.62 | 45.62 |
| M18-1 | 2. | | | .50 | 4.52 | 4.52 |
| M18-2 | 3. | 5. | 18. | 2.78 | 13.05 | 13.05 |
| M18-3 | 7. | | | 5.88 | 21.77 | 21.77 |

| | | | | | | |
|---|---|---|---|---|---|---|
| M18-4 | 15. | 15. | 6.3 | 7.67 | 27.09 | 27.09 |
| M18-5 | | | | 8.46 | 29.27 | 29.27 |
| M19-1 | 4. | 6. | | .04 | .10 | .10 |
| M19-2 | 9. | 12. | 8.3 | .04 | .10 | .10 |
| M19-3 | | | 7.3 | 2.96 | 16.58 | 16.58 |
| M9-C | 2. | | | .04 | .10 | .10 |
| M9-1 | | | | .04 | .10 | .10 |
| M9-2 | | | 4.8 | .04 | .10 | .10 |
| M9-3 | | | 7.7 | .04 | .10 | .10 |
| M9-4 | | | | .04 | .10 | .10 |
| M9-5 | 6. | | | .23 | 3.11 | 3.11 |
| M9-6 | 5. | 4. | | .56 | 5.94 | 5.94 |
| M9-7 | 6. | 7. | | .74 | 7.52 | 7.52 |
| M9-8 | | | | .74 | 7.52 | 7.52 |
| M9-10 | | | | .77 | 7.78 | 7.78 |
| M9-11 | | | | .77 | 7.78 | 7.78 |

RIO ALGOM LIMITED

MINING DIVISION

Intera Technologies
Att: Austin Sweezey

PROCESS DEVELOPMENT DEPARTMENT

File

ANALYSIS REPORT

DATE: September 13, 1989.

| LAB NO. | SAMPLE DESCRIPTION | pc/lt Diss Ra | | | | |
|---|---|---|---|---|---|---|
| B-6444 | M-1-2 | 6.4 | | | | |
| 45 | M-1-4 | 49 | | | | |
| 46 | M-1-6 | 44 | | | | |
| 47 | M-1-8 | 46 | | | | |
| 48 | M-1-9 | 20 | | | | |
| 49 | M-1-10 | 64 | | | | |
| 50 | M-8-1 | 5.7 | | | | |
| 51 | M-8-4 | 7.4 | | | | |
| 52 | M-8-6 | 21 | | | | |
| 53 | M-8-8 | 59 | | | | |
| 54 | M-8-10 | 21 | | | | |
| 55 | M-9-2 | 4.8 | | | | |
| 56 | M-16-1 | 10 | | | | |
| 57 | M-16-5 | 9.6 | | | | |
| 58 | M-16-6 | 36 | | | | |
| 59 | M-16-7 | 43 | | | | |

J. Nipius

RIO ALGOM LIMITED

MINING DIVISION

Intera Technologies
Att: Austin Sweezey

PROCESS DEVELOPMENT DEPARTMENT

File

ANALYSIS REPORT

DATE: September 13, 1989.

| LAB NO. | SAMPLE DESCRIPTION | Diss Ra | pc/lt | | | |
|---|---|---|---|---|---|---|
| B-6424 | M-9-3 | 7.1 | | | | |
| B-6424 | M-9-6 | 8.2 | | | | |
| B-6426 | M-16-9 | 42 | | | | |
| B-6427 | M-17-2 | 7.2 | | | | |
| B-6428 | M-17-3 | 8.6 | | | | |
| B-6429 | M-17-6 | 8.5 | | | | |
| B-6430 | M-17-8 | 16 | | | | |
| B-6431 | M-18-2 | 18 | | | | |
| B-6432 | M-18-4 | 6.3 | | | | |
| B-6433 | M-19-2 | 8.3 | | | | |
| B-6434 | M-19-3 | 7.3 | | | | |

J. Nipius

RIO ALGOM LIMITED

MINING DIVISION

Intera Technologies
Att: Austin Sweezey

PROCESS DEVELOPMENT DEPARTMENT

File

ANALYSIS REPORT

DATE: September 13, 1989.

| LAB NO. | SAMPLE DESCRIPTION | pc/lt Diss Ra | | | | |
|---|---|---|---|---|---|---|
| M-6460 | M-20-C | 2.4 | | | | |
| 61 | M-20-2 | 11 | | | | |
| 62 | M-20-4 | 26 | | | | |
| 63 | M-20-5 | 57 | | | | |
| 64 | M-Rinse | 1.7 | | | | |

J.Nipius